รายงานวิจัยฉบับสมบูรณ์

โครงการ ทริสพิราโซลิลบอเรทและทริสเมอร์แคพโทอิมิดา-โซลิลบอเรทไซยาโนเมทัลเลทส์สำหรับเป็นหน่วยการสร้างแม่เหล็กโมเลกุลเดี่ยว

Tris(pyrazolyl)borate and Tris(mercaptoimidazolyl)borate Cyanometallates as Building Blocks for Single-Molecule Magnets

โดย รองศาตราจารย์ ดร. เดวิด เจมส์ ฮาร์ดิง และคณะ

24 มิถุนายน พ.ศ. 2553

สัญญาเลขที่ RMU5080029

รายงานวิจัยฉบับสมบูรณ์

โครงการ Tris(pyrazolyl)borate and Tris(mercapto-imidazolyl)borate Cyanometallates as Building Blocks for Single-Molecule Magnets

คณะผู้วิจัย	สังกัด
1. รศ. ดร. เดวิด เจมส์ ฮาร์ดิง	มหาวิทยาลัยวลัยลักษณ์
2. ผศ. ดร. พิมผกา ฮาร์ดิง	มหาวิทยาลัยวลัยลักษณ์

สนับสนุนโดยสำนักงานคณะกรรมการการอุดมศึกษา และสำนักงานกองทุนสนับสนุนการวิจัย

(ความเห็นในรายงานนี้เป็นของผู้วิจัย สกอ. และ สกว. ไม่จำเป็นต้องเห็นด้วยเสมอไป)

Abstract

The following report details the synthesis and characterization of a wide range of tris(mercaptoimidazolyl)borate complexes [$Tm^{Me}CoX$] (X = OAc, NO_3, NO_2, N_3, NCS, β-dkt). The cyanometallates, [$Tp^{Ph2}Ni(CN)_2$]NEt_4, have also been realized. Reaction of these with a number of $[M(N\text{-}N)_2]^{2+}$ (M = Co, Ni; N-N = diimine ligand) complexes yields in one case $[Co(phen)_3][BF_4]_2$.MeCN which has been crystallographically characterized.

The bipyrimidine cations, $[Tp^{R}Ni(bpym)]^{+}$ (R = Ph,Me; Ph_2) have been prepared. Reaction of these cations with $[M(\beta\text{-dkt})_2(H_2O)_2]$ (M = Co, Ni) yields [$Tp^{R}M$(β-dkt)] rather than the expected dimer due to migration of the β-diketonate ligand. The β-diketonate complexes [$Tp^{Ph2}Ni$(β-dkt)] have also been prepared by the reaction of [$Tp^{Ph2}NiBr$] with the appropriate β-diketone.

The reaction of Nadtc (dtc = dithiocarbamate) with [$Tp^{Ph2}MBr$] (M = Co, Ni) gives the complexes, [$Tp^{Ph2}M$(dtc)]. The compounds undergo reversible or quasi-reversible oxidation to M^{III}. Oxidation of [$Tp^{Ph2}Co$(dtc)] reveals that the oxidation is irreversible on the synthetic timescale yielding instead $[Co(dtc)_3]$. Computational studies suggest that the HOMO is strongly M-S σ* antibonding rationalizing the unusually low oxidation potential in these compounds.

The reaction of [$Tp^{R}CoBr$] (R = Ph,Me; Ph_2) with BHBQ or CA in the presence of DBU yields the [$Tp^{R}Co(\mu\text{-L})CoTp^{R}$] dimers. [$Tp^{Ph,Me}Co(\mu\text{-CA})CoTp^{Ph,Me}$] has been characterized by X-ray crystallography showing two independent molecules in which the cobalt metal centres are five and six coordinate. Nickel analogues have also been prepared and appear identical to their cobalt counterparts.

บทคัดย่อ

ในรายงานฉบับสมบูรณ์นี้จะกล่าวถึงการสังเคราะห์และพิสูจน์เอกลักษณ์ของสารประกอบเชิงซ้อนทริสเมอร์แคพโทอิมิดาโซลิลบอเรท $[Tm^{Me}CoX]$ (X = OAc, NO_3, NO_2, N_3, NCS, β-dkt) และสารประกอบเชิงซ้อนไซยาโนเมทัลเลท $[Tp^{Ph2}Ni(CN)_2]NEt_4$ การศึกษาปฏิกิริยาระหว่างสารประกอบเหล่านี้กับสารประกอบ $[M(N\text{-}N)_2]^{2+}$ (M = Co, Ni; N-N = diimine ligand) ในกรณีศึกษาหนึ่งพบว่าจะได้ผลิตภัณฑ์คือ $[Co(phen)_3][BF_4]_2.MeCN$ ซึ่งพิสูจน์เอกลักษณ์ทางโครงสร้างด้วยเทคนิคคริสทัลโลกราฟฟี

สารประกอบไอออนบวกไบพิริมิดิน $[Tp^RNi(bpym)]^+$ (R = Ph,Me; Ph_2) ถูกสังเคราะห์ขึ้นมา และเมื่อนำมาทำปฏิกิริยากับ $[M(β\text{-}dkt)_2(H_2O)_2]$ (M = Co, Ni) จะได้สารประกอบเชิงซ้อน $[Tp^RM(β\text{-}dkt)]$ แทนที่จะได้เป็นสารประกอบไดเมอร์ดังที่คาดการณ์ไว้ สาเหตุเนื่องจากเกิดไมเกรชั่นของลิแกนด์เบต้าไดคีโตเนท นอกจากนี้สารประกอบเบต้าไดคีโตเนท $[Tp^{Ph2}Ni(β\text{-}dkt)]$ ยังสามารถเตรียมได้จากการทำปฏิกิริยาระหว่าง $[Tp^{Ph2}NiBr]$ กับเบต้าไดคีโตเนทลิแกนด์ที่เหมาะสม

ปฏิกิริยาระหว่าง Nadtc (dtc = dithiocarbamate) กับ $[Tp^{Ph2}MBr]$ (M = Co, Ni) จะได้สารประกอบเชิงซ้อน $[Tp^{Ph2}M(dtc)]$ โดยสารประกอบจะเกิดออกซิเดชันแบบย้อนกลับได้หรือย้อนกลับได้แบบบางส่วนได้สารประกอบ M^{III} ส่วนการเกิดออกซิเดชันของ $[Tp^{Ph2}Co(dtc)]$ บ่งชี้ให้เห็นว่ากระบวนการออกซิเดชันของสารประกอบนี้จะเป็นแบบไม่ย้อนกลับในช่วงเวลาของการสังเคราะห์ทำให้เกิด $[Co(dtc)_3]$ แทน การศึกษาทางคอมพิวเตอร์ระบุให้ทราบว่า HOMO ของสารประกอบจะประกอบด้วย M-S σ* antibonding เป็นหลักทั้งนี้เนื่องมาจากการที่สารประกอบมีศักย์ไฟฟ้าออกซิเดชันที่ต่ำกว่าปกติ

ปฏิกิริยาระหว่าง $[Tp^RCoBr]$ (R = Ph,Me; Ph_2) และ BHBQ หรือ CA ในระบบที่มี DBU จะได้สารประกอบไดเมอร์ $[Tp^RCo(μ\text{-}L)CoTp^R]$ และจากการศึกษาโครงสร้างของสารประกอบ $[Tp^{Ph,Me}Co(μ\text{-}CA)CoTp^{Ph,Me}]$ พบว่าจะมีสองโมเลกุลที่เป็นอิสระต่อกันโดยโคบอล์จะมีโคออร์ดิเนทแบบ 5 และ 6 ส่วนสารประกอบนิกเกิลได้มีการสังเคราะห์ด้วยวิธีการเดียวกันและแสดงสมบัติเหมือนกับสารประกอบโคบอลต์

Acknowledgements

I would like to acknowledge at this point the various people who have helped during this project. A number of students have worked on this project during the last three years and their help and determination is gratefully acknowledged.

A large number of crystal structures have also been determined in the course of this project by our research collaborator Harry Adams at the University of Sheffield. I also wish to acknowledge Professor Keith Murray at Monash University who has undertaken SQUID magnetometry measurements on some of the compounds presented in this report.

A further thank you must also go to Associate Professor Dr Vudhichai Parasuk at Chulalongkorn and Dr Supapporn Dokmaisrijan at Walailak University who have undertaken computational studies on several of the tris(pyrazolyl)borate complexes synthesized in this work.

Finally, I wish to acknowledge the help and support of Assistant Professor Dr Phimphaka Harding for useful discussions and advice during the course of this project. There is no doubt that this project could not have completed without her assistance.

Table of Contents

1. Executive Summary

The cobalt tris(mercaptoimidazolyl)borate complexes, $[Tm^{Me}CoX]$ (X = OAc, NO_3) have been prepared by the reaction between CoX_2 and $NaTm^{Me}$. Additional compounds have been made by reacting $Tm^{Me}CoCl$ with $NaNO_2$, NaN_3 and KNCS to give tetrahedral Tm^{Me} complexes $[Tm^{Me}CoX]$ (X = NO_2, N_3, NCS).

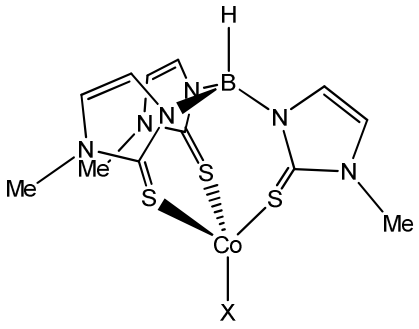

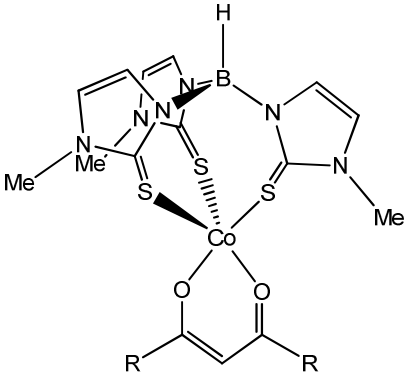

Further studies have also shown that β-diketonate ligands may be introduced by the reaction of β-Hdkt with $[Tm^{Me}Co(OAc)]$ in the presence of NaOMe. Electrochemical studies reveal irreversible oxidation to Co^{III} which may be coupled to a change in spin state.

The reaction of $[Tp^{Ph2}Ni(CN)_2]NEt_4$ with $[Co(NCMe)_6][BF_4]_2$ in the presence of phenanthroline yields $[Co(phen)_3][BF_4]_2$ rather than the anticipated cyano bridged metal cluster. The structure exhibits extensive C-H···π and π···π interactions forming discrete dimers.

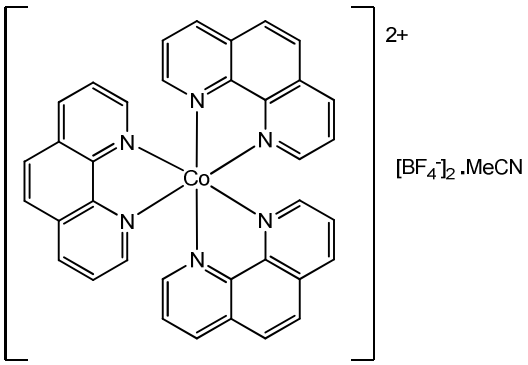

The bipyrimidine cations, $[Tp^{R}Ni(bpym)]^{+}$ (R = Ph,Me; Ph_2) have been synthesized by the reaction of $[Tp^{R}NiBr]$ with bipyrimidine in the presence of KPF_6. Electrochemical studies reveal irreversible one-electron reduction presumably to Ni^{I}. X-ray crystallography shows a square pyramidal coordination geometry with the potentially bridging bipyrimidine exhibiting a chelating bonding mode.

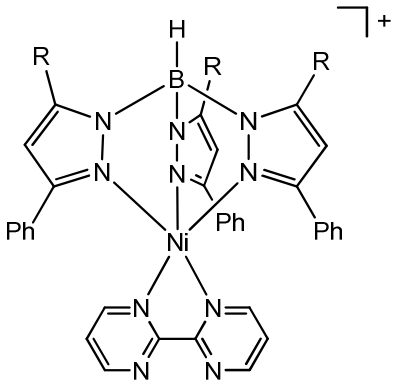

Attempts to prepare dimers with the bipyrimidine cations resulted in the isolation of [Tp^{Ph2}Ni(dbm)] in one instance. Further computational studies suggest that smaller co-ligands or metals with a lower coordination number may be required to realize the proposed dimers.

The addition of a β-diketone to [Tp^{Ph2}NiBr] and subsequent addition of NEt_3 gives range of β-diketonate nickel complexes [Tp^{Ph2}Ni(β-dkt)] {β-dkt = 1,3-diphenylpropane-dionate (dbm), 2,2,6,6-tetramethylheptanedionate (tmhd), hexafluoroacetylacetonate (hfac), 1-phenylbutanedionate (pbd)}.

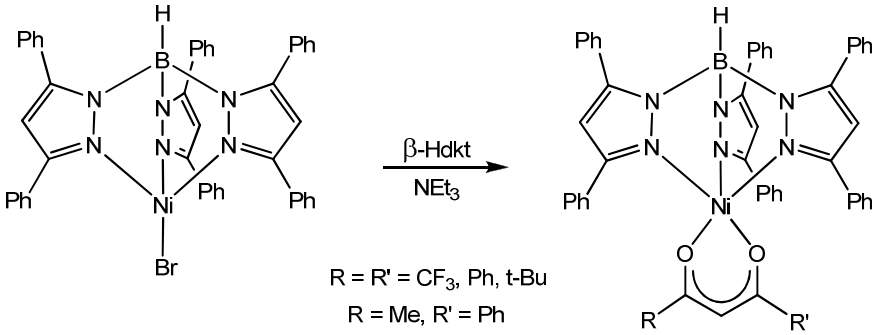

The reaction of Nadtc (dtc = dithiocarbamate) with [Tp^{Ph2}MBr] (M = Co, Ni) yields the complexes, [Tp^{Ph2}M(S_2CNR_2)] (M = Co, Ni; R = Et, Bz) and [Tp^{Ph2}M(S_2Cpyr)] (M = Co, Ni). Crystallographic results show five coordinate metals in all cases with asymmetrically coordinated dtc ligands and a geometry intermediate between trigonal bipyramidal and square pyramidal.

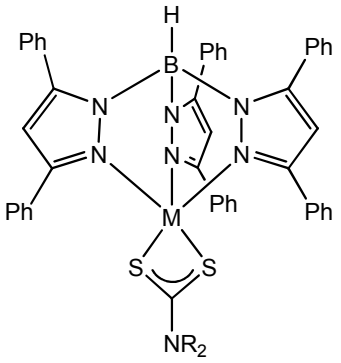

Cyclic voltammetric studies suggest that the metals are reversibly oxidized to Co^{III} or Ni^{III} while SQUID magnetometry is consistent with high spin Co^{II} with no evidence of spin crossover even at low temperatures. Computational studies show that the HOMO consists of a strong M-S σ^* antibonding interaction explaining the ease with which the compounds are oxidized.

The crystal structure of [Tp^{Ph2}NiBr] has also been determined revealing a rare example of a complex with a tris(pyrazolyl)borate ligand that possesses a crystallographic C_3 axis. The crystal packing in the structure contains several C-H$\cdots\pi$ interactions between the phenyl rings of neighbouring Tp^{Ph2} ligands.

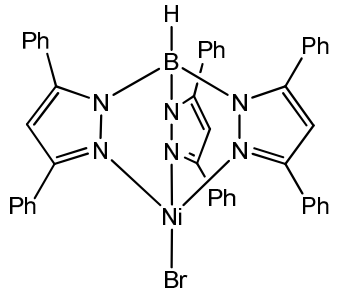

The reaction of [Tp^{R}CoBr] (R = Ph,Me; Ph_2) with BHBQ or CA in the presence of the weak base DBU yields the [Tp^{R}Co(μ-L)CoTp^{R}] dimers. Structural studies reveal the presence of two cobalt centres bridged by a dianionic semiquinone ligand. Interestingly, two independent molecules with five and six coordinate cobalt centres are found in the same crystal lattice.

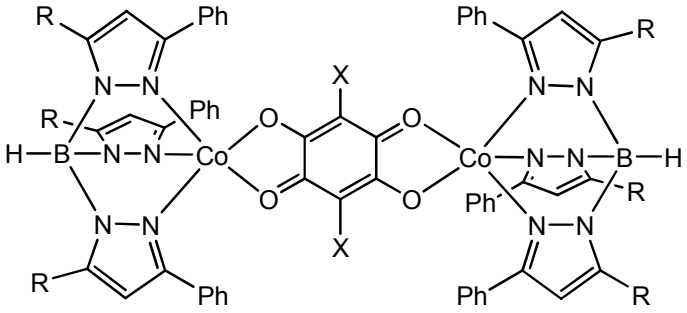

1.1. Objectives

1.1.1. Proposed Objectives for the Project

1. To synthesize cyanometallate $[MTp^{R}(CN)_3]^-$ (R = Me_3, Ph_2; M = Fe, Co) and $[MTp^{R}(CN)_2]^-$ (R = Me_3, Ph_2; M = Co, Ni) complexes as precursors for magnetic materials.
2. To prepare molecular magnets of the general formula $[MTp^{R}(CN)_3M'L_n]_m$ (M = Fe; R = Me_3, Ph_2; M′ = Mn, Fe, Co, Ni, Cu; m =1, 2, 3, 4; L = solvent, chelating ligand, tripodal ligand) and investigate their electrochemical and magnetic properties.
3. To synthesize molecular magnets of the general formula $[MTp^{R}(CN)_3M'L_n]_m$ (M = Fe; R = Me_3, Ph_2; M′ = Tb, Gd, Nd, Eu and Dy; m =1, 2, 3, 4; L = solvent, chelating ligand) and investigate their electrochemical, optical and magnetic properties.
4. To synthesize and characterize $[MTm^{R}X]$ (M = Fe, Co, Ni; R = Me, Ph, *t*-Bu, X = N_3^-, SCN^-, NO_2^-, NO_3^-, OAc^-, $acac^-$) or $[MTm^{R}(L)]^+$ (M = Fe, Co, Ni; R = Me, Ph, *t*-Bu; L = pyridine, pyrazine, bipy, phen, en, dppm, dppe).
5. To prepare and characterize novel cyanometallates $[MTm^{R}(CN)_3]^-$ (M = Fe, Co; R = Me, Ph, *t*-Bu) and $[MTm^{R}(CN)_2]^-$ (M = Co, Ni; R = Me, Ph, *t*-Bu).
6. To explore the chemistry of magnetic clusters of the general formula $[MTm^{R}(CN)_3M'L_n]_m$ (M = Fe; R = Me, Ph, *t*-Bu; M′ = Mn, Fe, Co, Ni, Cu; L = solvent, chelating ligand, tripodal ligand) and investigate their electrochemical and magnetic properties.
7. To train a new generation of Thai researchers in nanotechnology.
8. To publish 2 or 3 international research papers based upon this research.

1.1.2 Achieved Objectives

The following objectives have been achieved. Details are provided in the results section below.

1. We have synthesized and characterized $[CoTm^{Me}X]$ (X = N_3^-, SCN^-, NO_2^-, NO_3^-, OAc^-, $acac^-$, $hfac^-$, dbm^-, $tmhd^-$).
2. We have synthesized and characterized $[Tp^{R}Ni(bpym)]^+$ (R = PhMe, Ph_2). Structural and electrochemical studies have been undertaken.

3. Preparation and characterization of [Tp^{Ph2}M(dtc)] (M = Co, Ni; dtc = dithiocarbamate) by spectroscopic, electrochemical, structural, magnetic and computational methods.
4. We have prepared and characterized [Tp^{R}Co(μ-L)CoTp^{R}] (R = PhMe, Ph_2; L = chlorinate, dihydroxybenzoquinonate).
5. We have trained four students in this type of research, three summer training students and a graduate researcher. The latter of these has now been awarded a scholarship to study nanotechnology in the United States.
6. Three international research papers have been published based upon this research.
7. '*Best Research Scholar Award*' awarded by Walailak University to Assoc. Prof. Dr. David J. Harding

2. Literature Review

The following review is intended to highlight the key areas of iron, cobalt, and nickel tris(pyrazolyl)borate and tris(mercaptoimidazolyl)borate chemistry to put the proposal in context. The review begins with a short discussion of the ligands and their syntheses before describing the chemistry of their iron, cobalt and nickel complexes with specific reference to cyanometallates.

Ligands

The tris(pyrazolyl)borate anions ($Tp^{R,R'}$) are facially capping, monoanionic, six-electron donors. They are strong σ-donors and are readily derivatized by altering the substituents on the pyrazole rings.[1] This allows the preparation of a range of ligands with different steric and electronic properties. The preparation of tris(pyrazolyl)borates is achieved by reacting the free pyrazole with M[BH_4] (M = Na or K) under heating.

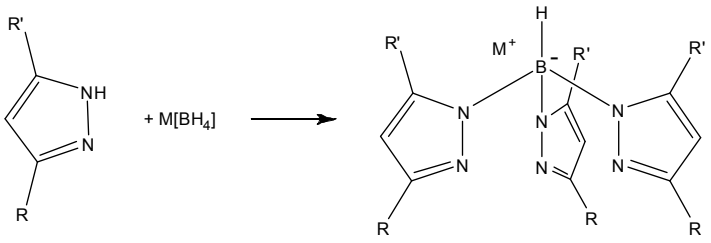

Scheme 1 Preparation of tris(pyrazolyl)borate anions.

[1] S. Trofimenko, *Scorpionates: The Coordination Chemistry of Polypyrazolylborate Ligands*, Imperial College Press: London, 1999.

A vast number of Tp ligands are now known but for the purpose of this proposal the most important are Tp (R = R′ = H), Tp* (R = R′ = Me), $Tp^{i\text{-}Pr}$ (R = *i*-Pr, R′ = H), Tp^{Ph} (R = Ph, R′ = H) and $Tp^{t\text{-}Bu}$ (R = *t*-Bu, R′ = H).

Table 1 Cone and wedge angles for several Tp ligands.

Ligand	Cone angle (θ)	Wedge angle (ω)
Tp	199	91
Tp*	236	75
Tp^{Ph}	242	-
$Tp^{i\text{-}Pr}$	262	36
$Tp^{t\text{-}Bu}$	265	35

The steric bulk of tris(pyrazolyl)borates is determined by their cone and wedge angles (see table above). The cone angle is defined as the apex angle of a cylindrical cone which originates from the bound metal and just touches the van der Waals radii of the outermost atoms of the ligand. The wedge angle is a measure of the open wedgelike spaces *between* pyrazolyl rings.[2]

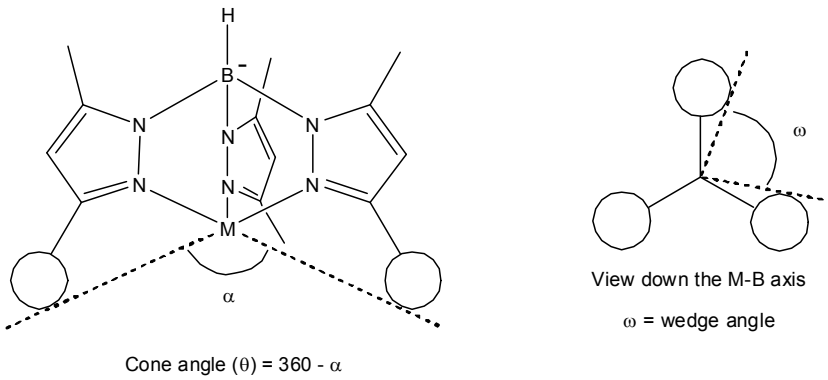

Figure 1 Cone and wedge angle of Tp ligands.

The electronic properties of tris(pyrazolyl)borate ligands have been determined by the comparison of tris(pyrazolyl)borate complexes which differ only in their pyrazolyl ring substituents.[2] This has led to an order of ligand electron-releasing ability:

[2] N. Kitajima and W. B. Tolman, *Prog. Inorg. Chem.*, 1995, **43**, 419.

$$Tp^* > Tp^{i\text{-}Pr} \sim Tp^{t\text{-}Bu} > Tp > Tp^{Ph}$$

Tp and Tp* were the first tris(pyrazolyl)borates prepared and with first row transition metals tend to form octahedral ML_2 complexes {L = tris(pyrazolyl)borate}. $Tp^{t\text{-}Bu}$ has a very large cone angle forming $MXTp^{t\text{-}Bu}$ instead of ML_2 complexes. $Tp^{i\text{-}Pr}$ and Tp^{Ph} are of intermediate steric bulk allowing the formation of four- and five-coordinate species. Once again, the formation of chemically inactive sandwich complexes is avoided.

In the above complexes we have assumed that the tris(pyrazolyl)borate ligand binds to the metal through all three nitrogen donors. However, in some cases the bonding (κ) of the Tp ligand is κ^2 not κ^3 (Figure 2). This is particularly true for second and third row *d*-block transition metals with a d^8 electron configuration.[1] These two bonding modes are readily distinguished from each other by the $\nu_{B\text{-}H}$ stretching frequency.[3] As a rule of thumb, κ^2 $\nu_{B\text{-}H}$ = 2300 - 2450 cm^{-1} and κ^3 $\nu_{B\text{-}H}$ = 2500 - 2650 cm^{-1}.

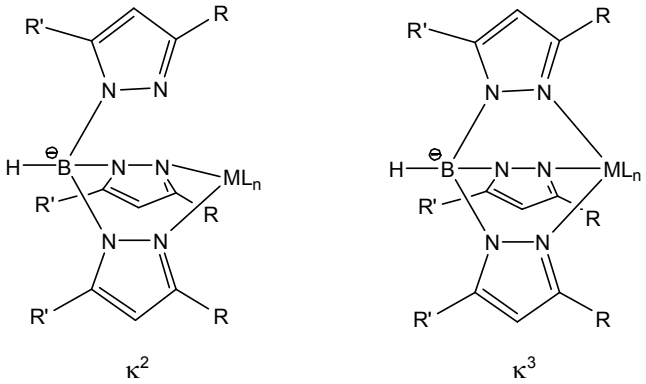

Figure 2 The κ^2 and κ^3 binding modes of Tp complexes.

Tris(mercaptoimidazolyl)borate ligands (Tm^R) are soft tripodal analogues of the more familiar Tp ligands and were first prepared in 1996.[4] They are synthesized by reacting mercaptoimidazole with sodium or potassium borohydride in a melt at elevated temperature.[4,5]

[3] M. Akita, K. Ohta, Y. Takahashi, S. Hikichi and Y. Moro-oka, *Organometallics*, 1997, **16**, 4121.
[4] M. Garner, A. R. Kennedy, J. Reglinski and M. D. Spicer, *J. Chem. Soc., Chem. Commun.*, 1996, 1975.
[5] J. Reglinski, M. Garner, I. D. Cassidy, P. A. Slavin and M. D. Spicer, *J. Chem. Soc., Dalton Trans.*, 1999, 2119.

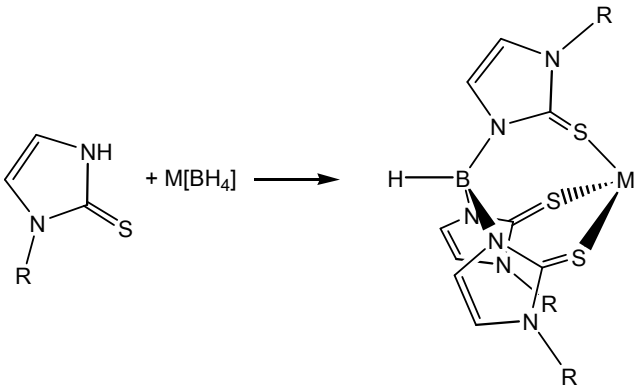

Scheme 2 Preparation of tris(mercaptoimidazolyl)borate ligands.

As with Tp^R ligands, Tm^R ligands can have their steric and electronic properties modified by substitution at the nitrogen atom. To date only nine Tm^R ligands have been prepared in which R = Me, Et,[6] Ph,[7] Mes,[7] *t*-Bu,[8] Cumyl,[8] Xylyl,[9] Bz[9] and *p*-tolyl.[9] While Tp is a hard tripodal ligand, Tm ligands are soft tripodal ligands coordinating the metal with three S-donors. In addition, Tm ligands form eight membered chelate rings when bound to the metal such that the individual rings adopt a propeller conformation. A further departure from Tp chemistry is the greater participation of the B-H bond in coordination to metal centres. In certain circumstances this can lead to oxidative addition and formation of metallaboratrane species (see Figure 3).

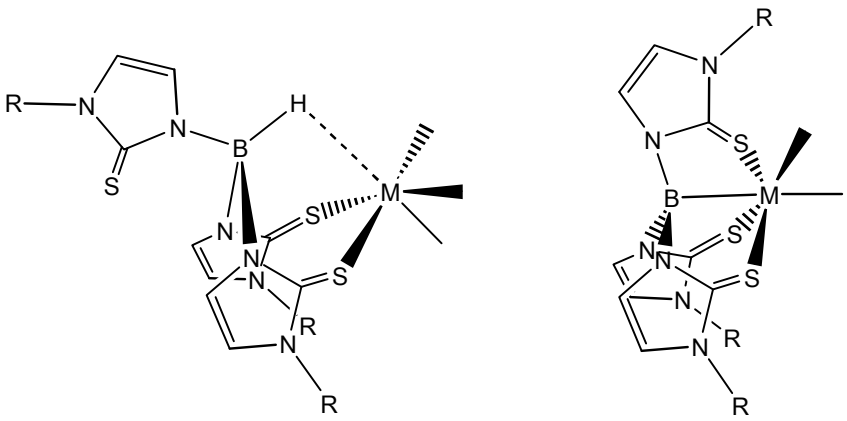

Figure 3 κ^3-S,S,H coordination mode and metallaboratranes.

[6] P. J. Bailey, A. Dawson, C. McCormack, S. A. Moggach, I. D. H. Oswald, S. Parsons, D. W. H. Rankin and A. Turner, *Inorg. Chem.*, 2005, **44**, 8884.
[7] C. Kimblin, B. M. Bridgewater, D. G. Churchill and G. Parkin, *J. Chem. Soc., Chem. Commun.*, 1999, 2301.
[8] M. Tesmer, M. Shu and H. Vahrenkamp, *Inorg. Chem.*, 2001, **40**, 4022.
[9] M. M. Ibrahim, J. Seebacher, G. Steinfeld and H. Vahrenkamp, *Inorg. Chem.*, 2005, **44**, 8531.

Comparisons between Tm, Tp and Cp suggest that the ligands are more electron donating in the order

Tm > Tp > Cp

This is thought to be due to partial delocalization of the negative charge onto the thione sulfur thereby increasing donation to the metal centre. As such Tm ligands are best thought of as σ-donor/π-donors.[10]

Tp Cyanometallates

The use of scorpionates as facially capping ligands in magnetic materials chemistry has been pioneered by Holmes and co-workers. The scorpionate cyanometallates, $[Tp^*Fe(CN)_3]^-$,[11] $[pzTpFe(CN)_3]^-$,[12] $[Tp^*V(CN)_3]^-$,[13] and $[Tp^*V(O)(CN)_2]$[13] have proved to be excellent building blocks for constructing magnetic molecules.

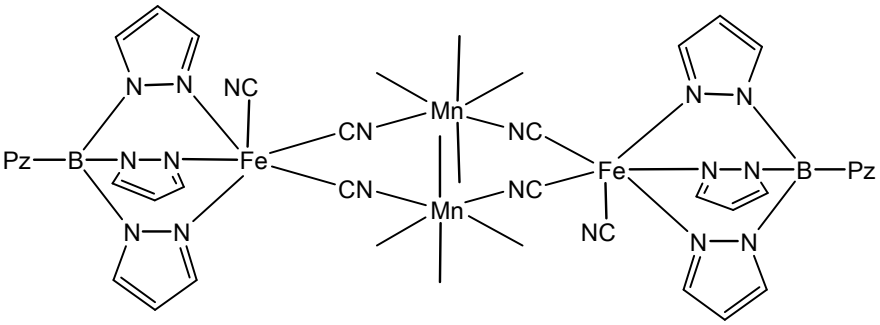

Figure 4 Structure of $\{[Tp^*Fe(CN)(\mu\text{-}CN)_2Mn(DMF)_4]_2\}^{2+}$.

Thus, the reaction of $[Tp^*Fe(CN)_3]^-$ with $Mn(OTf)_2$ in DMF affords a rectangular cluster $\{[Tp^*Fe(CN)(\mu\text{-}CN)_2Mn(DMF)_4]_2\}^{2+}$, while $Mn(OTs)_2$ yields a 1D polymer, $[Tp^*Fe(CN)(\mu\text{-}OTs)(\mu\text{-}CN)_2Mn(DMF)_2]_n$ (Figure 4).[11] Only the former exhibits magnetic coupling albeit antiferromagnetic.

In a similar manner the rectangular cluster $\{[Tp^*V(O)(CN)_2]_2[Mn(bpy)_2]_2\}^{2+}$ can been made, as before the metal centres are antiferromagnetically coupled.[13] However, single-molecule magnets have been realized in the case of the cubic cluster $[pzTpFe(CN)_3]_4[Ni(L)]_4$ {L = tris(pyrazolyl)ethanol} and trinuclear complex $[pzTpFe(CN)_3]_2[Ni(bpy)_2]$ which are

[10] C. A. Dodds, M.-A. Lehmann, J. F. Ojo, J. Reglinski and M. D. Spicer, *Inorg, Chem.*, 2004, **43**, 4927.
[11] D. Li, S. Parkin, G. Wang, G. T. Yee and S. M. Holmes, *Inorg. Chem.*, 2006**, 45**, 1951.
[12] D. Li, S. Parkin, G. Wang, G. T. Yee, A. V. Prosvirin and S. M. Holmes, *Inorg. Chem.*, 2005**, 44**, 4903.
[13] D. Li, S. Parkin, G. Wang, G. T. Yee and S. M. Holmes, *Inorg. Chem.*, 2006**, 45**, 2773.

prepared from $[pzTpFe(CN)_3]^-$ and $[Ni(L)(H_2O)_3]^{2+}$,[14] and $[pzTpFe(CN)_3]^-$ and $[Ni(bpy)_2(H_2O)_2]^{2+}$,[15] respectively (Figure 5). Both exhibit ferromagnetic coupling at low temperature and show hysteresis loops.

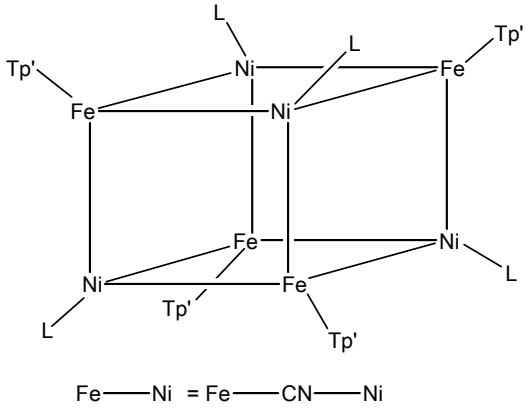

Figure 5 Structure of $[pzTpFe(CN)_3]_4[Ni(L)]_4$ {L = tris(pyrazolyl)ethanol}.

Functionalization of the ancillary ligands can also be achieved allowing preparation of molecule-based electronic devices through binding of the metallic clusters to an appropriate surface (*e.g.* gold, metal oxides *etc*, Figure 6).

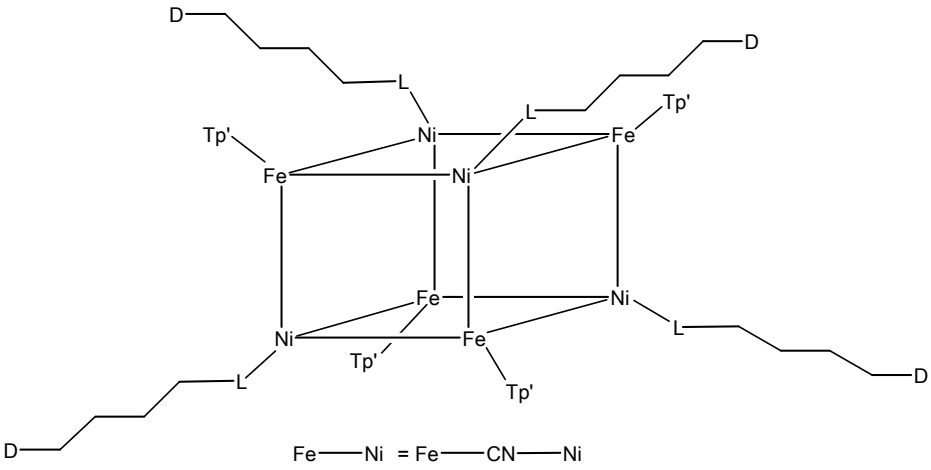

Figure 6 Structure of $[pzTpFe(CN)_3]_4[Ni(tpzmSAc)]_4$ (L = facially capping ligand and D = donor arm).

An example of such a cluster is $[pzTpFe(CN)_3]_4[Ni(L)]_4$ in which L is 1-S(acetyl)-tris(pyrazolyl)alkanes $\{(pz)_3C(CH_2)_nSAc$, tpzmSAc$\}$.[16]

[14] D. Li, S. Parkin, G. Wang, G. T. Yee, R. Clérac, W. Wernsdorfer and S. M. Holmes, *J. Am. Chem. Soc.*, 2006, **128**, 4214.
[15] D. Li, R. Clérac, S. Parkin, G. Wang, G. T. Yee and S. M. Holmes, *Inorg. Chem.*, 2006**, 45**, 5251.
[16] D. Li, S. Parkin, R. Clérac and S. M. Holmes, *Inorg. Chem.*, 2006**, 45**, 7569.

Further work by Zuo *et al* has produced two new SMM, namely a face-centred cubic cluster $[(Tp)_8(H_2O)_6Cu_6Fe_8(CN)_{24}]^{4+}$[17] and a pentanuclear cluster, $[(Tp)_2(Me_3tacn)_3Cu_3Fe_2(CN)_6]^{2+}$.[18] The reaction of $[TpFe(CN)_3]^-$ with $[TpCu(H_2O)_2]^+$, $[(bpca)Cu(H_2O)_2]^+$ {bpca = bis(pyridylcarbonyl)amide}, $[(tren)Ni(ClO_4)_2]$ and $[(bipy)_2Ni(ClO_4)_2]$ yields the molecular squares $[TpFe(CN)_3CuTp]_2$, $[TpFe(CN)_3Cu(bpca)]_2$, $[TpFe(CN)_3Ni(tren)]_2[ClO_4]_2$ and $[TpFe(CN)_3Ni(bipy)_2]_2[TpFe(CN)_3]_2$, respectively (Figure 7).[19] The complexes all exhibit ferromagnetic interactions and $[TpFe(CN)_3Ni(tren)]_2[ClO_4]_2$ shows SMM behaviour.

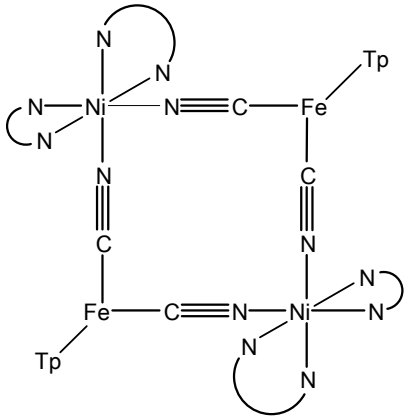

Figure 7 Structure of $[TpFe(CN)_3Ni(bipy)_2]_2^{2+}$.

Pentanuclear clusters, $[(Tp)_3(tpzm^*)_2Fe_3M_2(CN)_9]X$ (M = Fe, X = BF_4; M = Co, Ni, X = ClO_4) in which the metal centres are arranged in a trigonal bipyramidal geometry have been prepared by addition of $[M(tpzm^*)(H_2O)_3]^{2+}$ {M = Fe, Co, Ni; tpzm* = tris(3,5-dimethylpyrazolyl)methane} to $[TpFe(CN)_3]^-$.[20] The Fe^{III} metal centres are in the equatorial positions with the remaining two metals capped by tpzm* ligands occupying the axial positions (Figure 8). Magnetic studies of these complexes reveal ferromagnetic coupling for the Fe_3Co_2 and Fe_3Ni_2 clusters and antiferromagnetic coupling for the $(Fe^{III})_3(Fe^{II})_2$ cluster.

[17] S. Wang, J.-L. Zuo, H.-C. Zhou, H. J. Choi, X. Y. Ke, J. R. Long and X.-Z. You, *Angew. Chem. Int. Ed.*, 2004, **43**, 5940.
[18] C.-F. Wang, J.-L. Zuo, B. M. Bartlett, Y. Song, J. R. Long and X.-Z. You, *J. Am. Chem. Soc.*, 2006, **128**, 7162.
[19] W. Liu, C.-F. Wang, Y.-Z. Li, J.-L. Zuo and X.-Z. You, *Inorg. Chem.*, 2006, **45**, 10058.
[20] Z.-G. Gu, Q.-F. Yang, W. Liu, Y.-Z. Li, J.-L. Zuo and X.-Z. You, *Inorg. Chem.*, 2006, **45**, 8895.

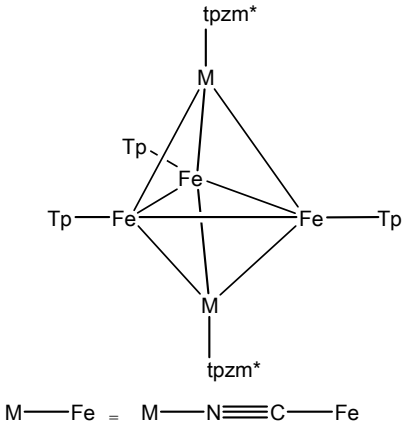

Figure 8 Structure of $[(Tp)_3(tpzm^*)_2Fe_3M_2(CN)_9]^+$.

Cyano-bridged heterobimetallic chains have been made by the reaction of $[TpFe(CN)_3]^-$ with fully solvated Cu^{II}, Co^{II} and Ni^{II} cations in MeOH or DMF giving $[(Tp)_2Fe_2(CN)_6Cu(CH_3OH)\cdot 2CH_3OH]_n$, $[(Tp)_2Fe_2(CN)_6Cu(DMF)\cdot DMF]_n$ and $[(Tp)_2Fe_2(CN)_6M(CH_3OH)_2\cdot 2CH_3OH]_n$ (M = Co, Ni).[21] The 1D polymers are formed by a continuous chain of squares. Magnetic studies reveal that the two FeCu polymers exhibit intrachain ferromagnetic coupling and single-chain magnetic behaviour. However, the FeCo and FeNi chains show metamagnetic behaviour with ferromagnetic intrachain coupling and interchain π-π stacking interactions leading to antiferromagnetic coupling.

In the last few weeks Holmes *et al* have also reported the synthesis of three new cyanometallates $[Tp^*M(CN)_2][NEt_4]$ (M = Cr, Co and Ni). The Cr and Co complexes have S = 2 and ½ respectively. In contrast, the corresponding Ni complex is diamagnetic.[22]

Tm Complexes

The relative newness of the Tm^R ligands has meant that their chemistry still remains largely undeveloped. In the case of Fe the most common type of complex are tetrahedral half-sandwich complexes $[Tm^RFeX]$ {R = Ph, *t*-Bu, Ar (2,6-$^i Pr_2C_6H_3$); X = Cl, I}.[23] The sandwich compounds $[(Tm^{Me})_2Fe]$[24] and $[(Tm^{Ph})_2Fe]$[25] are prepared by reaction of $NaTm^R$ with

[21] H.-R. Wen, C.-F. Wang, Y. Song, S. Gao, J.-L. Zuo and X.-Z. You, *Inorg. Chem.*, 2006, **45**, 8942.
[22] D. Li, C. Ruschman, S. Parkin, R. Clérac and S. M. Holmes, *Chem. Commun.*, 2006, 4036.
[23] S. Senda, Y. Ohki, T. Hirayama, D. Toda, J.-L. Chen, T. Matsumoto, H. Kawaguchi and K. Tatsumi, *Inorg. Chem.*, 2006, **45**, 9914.
[24] M. Garner, K. Lewinski, A. Pattek-Janczyk, J. Reglinski, B. Sieklucka, M. D. Spicer and M. Szaleniec, *Dalton Trans.*, 2003, 1181.
[25] C. Kimblin, D. G. Churchill, B. M. Bridgewater, J. N. Girard, D. A. Quarless and G. Parkin, *Polyhedron*, 2001, **20**, 1891.

anhydrous $FeCl_2$. Interestingly, in $[(Tm^{Me})_2Fe]$ the Tm ligand is κ^3-S_3 coordinated while in $[(Tm^{Ph})_2Fe]$ it is κ^3-S,S,H coordinated. Furthermore, $[(Tm^{Ph})_2Fe]$ undergoes oxidation to give $[(Tm^{Ph})_2Fe]^+$ while $[(Tm^{Me})_2Fe]$ does not. The oxidation is also accompanied by a change in coordination mode to κ^3-S_3. These results clearly indicate that the substituent on the Tm ligand can have a significant effect on the chemistry of the system.

Cobalt Tm^R complexes are synthesized by reaction of excess metal dihalides with thallium or sodium tris(mercaptoimidazolyl)borate.

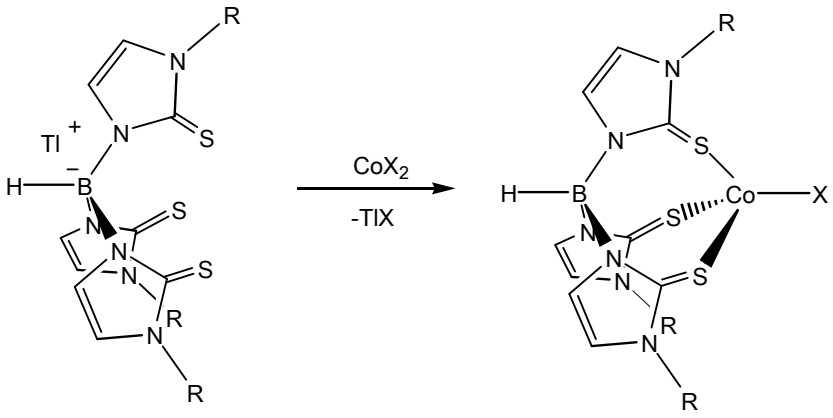

Scheme 3 Preparation of $[Tm^RCoX]$.

This results in formation of a wide range of tetrahedral complexes, $[Tm^RCoX]$ (R = Me, X = Cl, Br, I; R = Ph, *t*-Bu and Ar, X = Cl, I).[23] In attempting to crystallize one of these complexes Reglinski *et al* isolated a Co^{III} compound $[Co(Tm^{Me})_2]BF_4$.[10] The complex is low spin and has an S_6 donor set. A related sandwich compound $[Co(Tm^{Ph})_2]$ has also been prepared but unlike $[Co(Tm^{Me})_2]$ does not appear to oxidize to the trivalent state. Mixed sandwich complexes have also been realized by the reaction of $[Cp^{Me}Co(CO)I_2]$ with $NaTm^{Me}$ to give $[CoCp^{Me}Tm^{Me}]I$.[10]

Reaction of $NaTm^R$ with nickel(II) halides yields dimeric compounds with five coordinate nickel metal centres.[23]

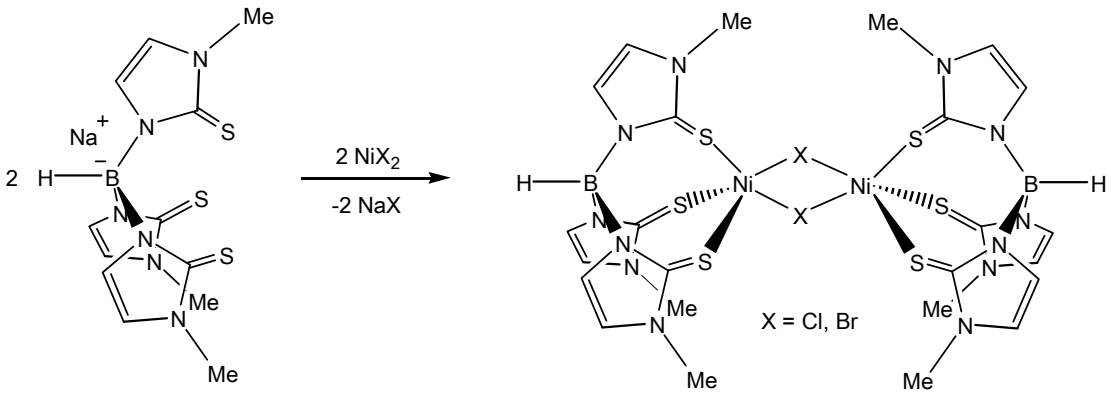

Scheme 4 Preparation of $[Tm^{Me}NiX]_2$.

Increasing the size of the substituents on the Tm ligands results in formation of simple tetrahedral compounds, $[Tm^{R}NiX]$ (R = Ph, *t*-Bu and Ar, X = Cl, I) analogous to the Fe and Co complexes described previously.[23] The sandwich complex $[Ni(Tm^{Me})_2]$ has also been prepared and has an S_6 donor set. Interestingly, an unusual Ni^{III} complex has been characterized namely, $[Ni(Tm^{Me})_2]Br$ indicating the ability of Tm ligands to stabilize a wide range of metals in different oxidation states.[24]

A final series of Ni Tm^{R} complexes are given by $[Tm^{R}Ni(dppe)]X$ (R = Me, *p*-tolyl, *t*-Bu; X = Cl, Br) which are prepared by the reaction of $[NiX_2(dppe)]$ (X = Cl, Br) and $TlTm^{R}$ (R = Me, *p*-tolyl, *t*-Bu).[26] In these complexes the Tm^{R} ligands exhibit a κ^3-S,S,H coordination mode.

Copper complexes unlike those of Fe, Co and Ni are rather scarce owing to decomposition of the $Cu^{II}Tm^{R}$ compounds. However, Cu^{I} compounds are readily synthesized by reaction of Cu(I) halides with sodium or thallium Tm^{R}. This yields $[CuTm^{Et}(PPh_3)]$[6] or $[Cu(PhTm^{Me})(PPh_3)]$[27] if a phosphine is added to the reaction mixture. If no donor ligands are added then a dimer such as $[Cu(PhTm^{Me})]_2$ is formed in which all three S atoms are bound to the Cu metal and one is involved in bridging between the two metal centres.[27]

[26] H. M. Alvarez, J. M. Tanski and D. Rabinovich, *Polyhedron*, 2004, **23**, 395.
[27] C. A. Dodds, M. Garner, J. Reglinski and M. D. Spicer, *Inorg. Chem.*, 2006, **45**, 2733.

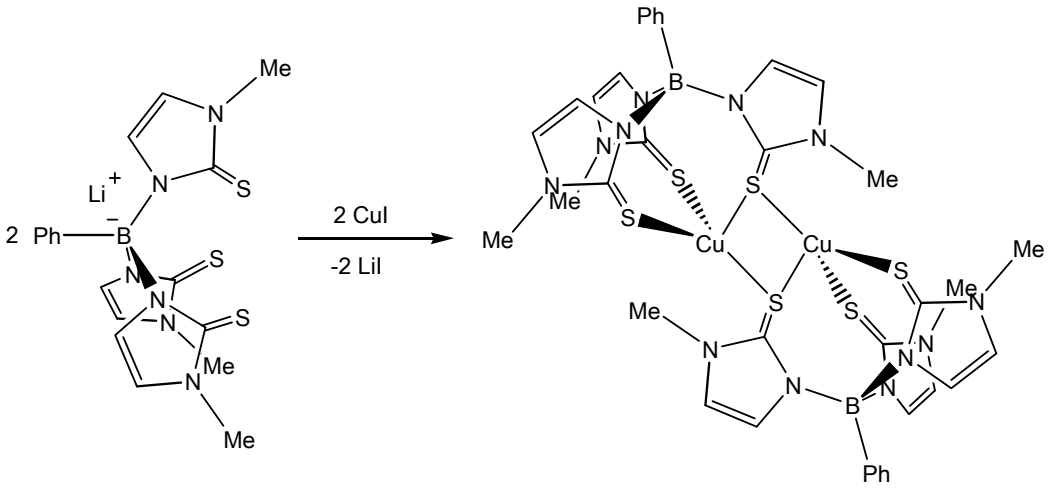

Scheme 5 Preparation of $[PhTm^{Me}Cu]_2$.

3. Results and Discussion

Experimental

In this section we report only the synthesis of novel complexes that have been isolated and fully characterized. The preparation of incompletely characterized complexes is included in the text below.

All reagents and solvents were purchased from commercial sources and were used as received unless otherwise noted. Preparation and handling of air-sensitive materials were carried out in an inert atmosphere using standard Schlenk line techniques. The ligands KTp^{Ph2}, KTp^{PhMe}, $NaTm^{Me}$, were prepared as previously reported.

Synthesis of $[Tm^{Me}Co(OAc)]$

$Co(OAc)_2.4H_2O$ (150 mg, 0.6 mmol) was dissolved in MeOH (20 ml) to give a purple solution. $NaTm^{Me}$ (74 mg, 0.2 mmol) was added in a suspension in CH_2Cl_2 (30 ml) resulting in a gradual colour change to deep green. The solution was stirred for 4 hr and then the solvent removed on a rotary evapourator to give a brown-green solid. The solid was redissolved in CH_2Cl_2 (10 ml) and filtered through celite to give a green solution. Addition of hexane (20 ml) resulted in precipitation of an olive green solid (46 mg, 50%).

Synthesis of $[Tm^{Me}Co(NO_3)]$

$Co(NO_3)_2.6H_2O$ (175 mg, 0.6 mmol) was dissolved in MeOH (10 ml) to give a pink-red solution. $NaTm^{Me}$ (74 mg, 0.2 mmol) was added as a suspension in CH_2Cl_2 (20 ml) resulting in

a gradual colour change to green. The solution was stirred for 3 hr and then the solvent removed on a rotary evapourator to give a green solid. The solid was redissolved in CH_2Cl_2 (10 ml) and filtered through celite to give a green solution. Addition of hexane (20 ml) resulted in precipitation of a green solid (50 mg, 53%).

Synthesis of [$Tm^{Me}Co(NO_2)$]

$Tm^{Me}CoCl$ (59 mg, 0.13 mmol) was dissolved in THF (10 ml) to give an olive green solution. $NaNO_2$ (9 mg, 0.13 mmol) was dissolved in MeOH (2 ml):H_2O (1 ml) and added to the solution which was stirred for 4 hr resulting in a red-brown solution. The solvent was removed on a rotary evapourator to give a red solid and then redissolved in CH_2Cl_2 (10 ml) and filtered through celite to give an orange solution. Hexane (10 ml) was added and the solution was left to evapourate giving orange-red crystals (10 mg, 16%).

Synthesis of [$Tm^{Me}Co(N_3)$]

$Tm^{Me}CoCl$ (50 mg, 0.11 mmol) was dissolved in THF (10 ml) to give an olive green solution. NaN_3 (8 mg, 0.11 mmol) was added resulting in a gradual colour change to orange brown. The solution was stirred for 3 hr and then filtered to give a copper-brown solid. The solid was washed with H_2O, MeOH and Et_2O to give a copper-brown solid (28 mg, 55%).

Synthesis of [$Tm^{Me}Co(NCS)$]

$Tm^{Me}CoCl$ (49 mg, 0.11 mmol) was dissolved in THF (10 ml) to give an olive green solution. KNCS (11 mg, 0.11 mmol) was added resulting in a gradual change to brown over 3 hrs. The solvent was removed on a rotary evapourator to give a dark red-brown solid. The solid was redissolved in CH_2Cl_2 (5 ml) and filtered through celite to give a red-brown solution. Hexane (10 ml) was added and the solution was left to evapourate giving orange-red crystals (10 mg, 20%).

Synthesis of [$Tm^{Me}Co(acac)$]

$Tm^{Me}Co(OAc)$ (50 mg, 0.1 mmol) was dissolved in CH_2Cl_2 (5 ml) to give a green solution. Hacac (11 μl, 0.1 mmol) was added resulting in a colour change to red. NaOMe (6 mg, 0.1 mmol) was added to the solution which was stirred for 12 hr. The solvent was reduced on a

rotary evapourator to *ca*. 1 ml. Addition of Et_2O (20 ml) resulted in precipitation of a dark green solid. Filtration and drying in air gave a dark green solid (30 mg, 55%).

Synthesis of [Tm^{Me}Co(hfac)]

Tm^{Me}Co(OAc) (50 mg, 0.1 mmol) was dissolved in CH_2Cl_2 (10 ml) to give a green solution. Hhfac (14 μl, 0.1 mmol) was added resulting in a colour change to yellow-green. NaOMe (6 mg, 0.1 mmol) was added to the solution which was stirred for 12 hr. The solvent was reduced on a rotary evapourator to *ca*. 1 ml. Addition of Et_2O (20 ml) resulted in precipitation of a green solid. Filtration and drying in air gave a green solid (48 mg, 74%).

Synthesis of [Tm^{Me}Co(dbm)]

Tm^{Me}Co(OAc) (50 mg, 0.1 mmol) was dissolved in CH_2Cl_2 (10 ml) to give a green solution. Hdbm (20 mg, 0.1 mmol) was added resulting in a colour change to brown-green. NaOMe (6 mg, 0.1 mmol) was added to the solution which was stirred for 1 hr. The solvent was reduced on a rotary evapourator to *ca*. 1 ml. Addition of Et_2O (20 ml) resulted in precipitation of a green solid. Filtration and drying in air gave a green solid (46 mg, 67%).

Synthesis of [Tm^{Me}Co(tmhd)]

Tm^{Me}Co(OAc) (50 mg, 0.1 mmol) was dissolved in CH_2Cl_2 (10 ml) to give a green solution. Htmhd (21 μl, 0.1 mmol) was added resulting in a colour change to green. NaOMe (6 mg, 0.1 mmol) was added to the solution which was stirred for 1 hr. The solvent was reduced on a rotary evapourator to *ca*. 1 ml. Addition of Et_2O (20 ml) resulted in precipitation of a brown-green solid. Filtration and drying in air gave a brown-green solid (51 mg, 81%).

Synthesis of [$Tp^{Ph2}Co(CN)_2$][NEt_4]

[Tp^{Ph2}Co(OAc)] (237 mg, 0.3 mmol) was dissolved in acetonitrile (15 ml) to give a purple solution. [NEt_4][CN] (95 mg, 0.6 mmol) was added to the solution resulting in a rapid colour change to orange. The solution was stirred for 1 hr and then the volume was reduced to ca. 5 ml *in vacuo*. Et_2O (40 ml) was layered on top of the solution which was left for 2 days giving orange rod crystals. The crystals were isolated by filtration and then dried *in vacuo* (172 mg, 63 %).

Synthesis of $[Tp^{Me3}Co(CN)_2][NEt_4]$

$[Tp^{Me3}Co(OAc)]$ (100 mg, 0.2 mmol) was dissolved in acetonitrile (15 ml) to give a purple solution. $[NEt_4][CN]$ (63 mg, 0.4 mmol) was added to the solution resulting in a rapid colour change to orange. The solution was stirred for 1 hr and then the volume was reduced to ca. 5 ml *in vacuo*. Et_2O (40 ml) was layered on top of the solution which was left for 2 days giving orange rod crystals. The crystals were isolated by filtration and then dried *in vacuo* (48 mg, 41 %).

Synthesis of $[Tp^{Ph2}Ni(CN)_2][NEt_4]$

$[Tp^{Ph2}Ni(OAc)]$ (236 mg, 0.3 mmol) was dissolved in acetonitrile (15 ml) to give a green solution. $[NEt_4][CN]$ (94 mg, 0.6 mmol) was added to the solution resulting in a rapid colour change to yellow. The solution was stirred for 1 hr and then the volume was reduced to ca. 5 ml *in vacuo*. Et_2O (40 ml) was layered on top of the solution which was left for 2 days giving orange rod crystals. The crystals were isolated by filtration and then dried *in vacuo* (143 mg, 54 %).

Synthesis of $[Tp^{Me3}Ni(CN)_2][NEt_4]$

$[Tp^{Me3}Ni(OAc)(NCMe)]$ (199 mg, 0.4 mmol) was dissolved in acetonitrile (10 ml) to give a green solution. $[NEt_4][CN]$ (125 mg, 0.8 mmol) was added to the solution resulting in a rapid colour change to yellow. The solution was stirred for 2 hr and then the volume was reduced to ca. 5 ml *in vacuo*. Et_2O (40 ml) was layered on top of the solution which was left for 2 days giving orange rod crystals. The crystals were isolated by filtration and then dried *in vacuo* (61 mg, 29 %).

Synthesis of $[Co(phen)_3][BF_4]_2$.MeCN

Cobalt(II) chloride (130 mg, 1 mmol) was suspended in MeCN (20 ml). $AgBF_4$ (389 mg, 2 mmol) was then added resulting in precipitation of a white solid. The solution was filtered through celite to remove AgCl and phenanthroline (541 mg, 3 mmol) was added giving an orange solution. The volume of the solution was reduced *in vacuo* to *ca*. 10 ml and then layered with Et_2O (60 ml). After two days yellow crystals formed (602 mg, 74%).

Synthesis of [Tp^{Ph2}Ni(bpym)]PF_6

[Tp^{Ph2}NiBr] (242 mg, 0.3 mmol) was dissolved in CH_2Cl_2 (10 ml) giving a purple-pink solution. Bpym (48 mg, 0.3 mmol) was added resulting in a change to emerald green. The solution was stirred for 30 min. KPF_6 (57 mg, 0.31 mmol) was then added and the solution stirred for 2 hrs resulting in an emerald green solution. The solution was filtered through celite and reduced to dryness *in vacuo*. The solid was redissolved in CH_2Cl_2 (4 ml) and layered with hexane (15 ml). After 2 days dark green crystals formed which were washed with Et_2O (2 x 5 ml) and air dried (278 mg, 90%).

Synthesis of [$Tp^{Ph,Me}$Ni(bpym)]PF_6

To a stirred pink suspension of [$Tp^{Ph,Me}$NiBr] (62 mg, 0.1 mmol) in CH_2Cl_2 (10 ml) was added bpym (16 mg, 0.1 mmol) to give a green solution. The solution was stirred at room temperature for 1 hr. KPF_6 (18 mg, 0.1 mmol) was added and the solution stirred overnight. The solution was filtered through celite and hexane (15 ml) was added. The solvent was reduced to a small volume on a rotary evapourator giving a green solid which was isolated by decantation (63 mg, 75%).

Synthesis of [Tp^{Ph2}Co(S_2CNEt_2)]

[Tp^{Ph2}CoBr] (81 mg, 0.1 mmol) was suspended in CH_2Cl_2 (10 ml) giving a turquoise suspension. NaS_2CNEt_2 (24 mg, 0.1 mmol) was added resulting in a colour change to brown. The solution was stirred for 5 hrs and reduced to dryness *in vacuo*. The solid was redissolved in CH_2Cl_2 (2 ml) and layered with hexanes (15 ml). After 2 days purple-brown crystals formed which were washed with Et_2O (2 x 5 ml) and air dried (56 mg, 63%).

Synthesis of [Tp^{Ph2}Co(S_2CNBz_2)]

[Tp^{Ph2}CoBr] (245 mg, 0.3 mmol) was suspended in CH_2Cl_2 (10 ml) giving a turquoise suspension. NaS_2CNBz_2 (95 mg, 0.3 mmol) was added resulting in a colour change to brown. The solution was stirred for 5 hrs and reduced to dryness *in vacuo*. The solid was redissolved in CH_2Cl_2 (3 ml) and layered with hexanes (15 ml). After 2 days purple-brown crystals formed which were washed with Et_2O (2 x 5 ml) and air dried (208 mg, 69%).

Synthesis of [$Tp^{Ph2}Co(S_2CN(CH_2)_4)$]

[Tp^{Ph2}CoBr] (164 mg, 0.2 mmol) was suspended in CH_2Cl_2 (10 ml) giving a turquoise suspension. NaS_2Cpyr (35 mg, 0.2 mmol) was added resulting in a colour change to brown. The solution was stirred for 5 hrs and reduced to dryness *in vacuo*. The solid was redissolved in CH_2Cl_2 (2 ml) and layered with hexanes (15 ml). After 2 days purple crystals formed which were washed with Et_2O (2 x 5 ml) and air dried (111 mg, 64%).

Synthesis of [$Tp^{Ph2}Ni(S_2CNEt_2)$]

[Tp^{Ph2}NiBr] (81 mg, 0.1 mmol) was dissolved in CH_2Cl_2 (10 ml) giving a deep pink solution. NaS_2CNEt_2 (23 mg, 0.1 mmol) was added resulting in a colour change to green. The solution was stirred for 5 hrs and reduced to dryness *in vacuo*. The solid was redissolved in CH_2Cl_2 (4 ml) and layered with hexanes (15 ml). After 2 days dark green crystals formed which were washed with Et_2O (2 x 5 ml) and air dried (75 mg, 85%).

Synthesis of [$Tp^{Ph2}Ni(S_2CNBz_2)$]

[Tp^{Ph2}NiBr] (81 mg, 0.1 mmol) was dissolved in CH_2Cl_2 (10 ml) giving a deep pink solution. NaS_2CNBz_2 (30 mg, 0.1 mmol) was added resulting in a colour change to green. The solution was stirred for 5 hrs and reduced to dryness *in vacuo*. The solid was redissolved in CH_2Cl_2 (4 ml) and layered with hexanes (15 ml). After 2 days dark green crystals formed which were washed with Et_2O (2 x 5 ml) and air dried (84 mg, 84%).

Synthesis of [$Tp^{Ph2}Ni(S_2CN(CH_2)_4)$]

[Tp^{Ph2}NiBr] (162 mg, 0.2 mmol) was dissolved in CH_2Cl_2 (10 ml) giving a deep pink solution. NaS_2Cpyr (35 mg, 0.2 mmol) was added resulting in a colour change to green. The solution was stirred for 5 hrs and reduced to dryness *in vacuo*. The solid was redissolved in CH_2Cl_2 (2 ml) and layered with hexanes (15 ml). After 2 days green crystals formed which were washed with Et_2O (2 x 5 ml) and air dried (135 mg, 77%).

Synthesis of [$Tp^{Ph2}Co(\mu$-DHBQ)$CoTp^{Ph2}$]

[Tp^{Ph2}CoBr] (81 mg, 0.1 mmol) was suspended in CH_2Cl_2 (5 ml) giving a turquoise suspension. DHBQ (7 mg, 0.05 mmol) was added giving a dark green solution. DBU (16 μl, 0.1 mmol) was then added resulting in a brown solution and a small amount of brown solid. The solution

was stirred for 3 hrs and then filtered through celite giving a brown solution which was layered with hexanes (15 ml). After one day a brown solid had formed which was washed with Et_2O (2 x 5 ml) and air dried (41 mg, 52%).

Synthesis of [Tp^{Ph2}Co(μ-CA)CoTp^{Ph2}]

[Tp^{Ph2}CoBr] (81 mg, 0.1 mmol) was suspended in CH_2Cl_2 (5 ml) giving a turquoise suspension. CA (11 mg, 0.05 mmol) was added giving a dark green solution. DBU (16 μl, 0.1 mmol) was then added resulting in a brown solution and a small amount of brown solid. The solution was stirred for 3 hrs and then filtered through celite giving a brown solution which was layered with hexanes (15 ml). After one day a brown solid had formed which was washed with Et_2O (2 x 5 ml) and air dried (39 mg, 47%).

Synthesis of [$Tp^{Ph,Me}$Co(μ-DHBQ)Co$Tp^{Ph,Me}$]

[$Tp^{Ph,Me}$CoBr] (125 mg, 0.2 mmol) was dissolved in CH_2Cl_2 (7 ml) giving a blue solution. DHBQ (14 mg, 0.1 mmol) was added giving a dark green solution. DBU (31 μl, 0.2 mmol) was then added resulting in a brown solution and a small amount of brown solid. The solution was stirred for 5 hrs and then filtered through celite giving a brown solution which was layered with hexanes (15 ml). After one day a brown solid had formed which was washed with Et_2O (2 x 5 ml) and air dried (96 mg, 78%).

Synthesis of [$Tp^{Ph,Me}$Co(μ-CA)Co$Tp^{Ph,Me}$]

[$Tp^{Ph,Me}$CoBr] (156 mg, 0.25 mmol) was suspended in CH_2Cl_2 (10 ml) giving a blue suspension. CA (26 mg, 0.13 mmol) was added giving a dark green solution. DBU (38 μl, 0.25 mmol) was then added resulting in a brown solution and a small amount of brown solid. The solution was stirred for 3 hrs and then filtered through celite giving a brown solution which was layered with hexanes (15 ml). After one day a brown solid had formed which was washed with Et_2O (2 x 5 ml) and air dried (88 mg, 55%).

Synthesis of [Tm^{Me}CoX] Complexes

The reaction of NaTm^{Me} with CoX_2 readily affords the half-sandwich complexes, [Tm^{Me}CoX] (X = N_3^- **1**, SCN^- **2**, NO_2^- **3**, NO_3^- **4**, OAc^- **5**, $acac^-$ **6**, $hfac^-$ **7**, dbm^- **8**, $tmhd^-$ **9**), which have been characterized by IR and UV-Vis spectroscopy with B-H stretches indicative of κ^3 coordinated Tm^{Me} ligands. The electronic spectra suggest four- or five-coordinate cobalt centres (Table 2). The synthesis of the β-diketonate complexes has been improved using NaOMe as a base rather than NEt_3. This gives higher yields of the complexes and also gives cleaner products.

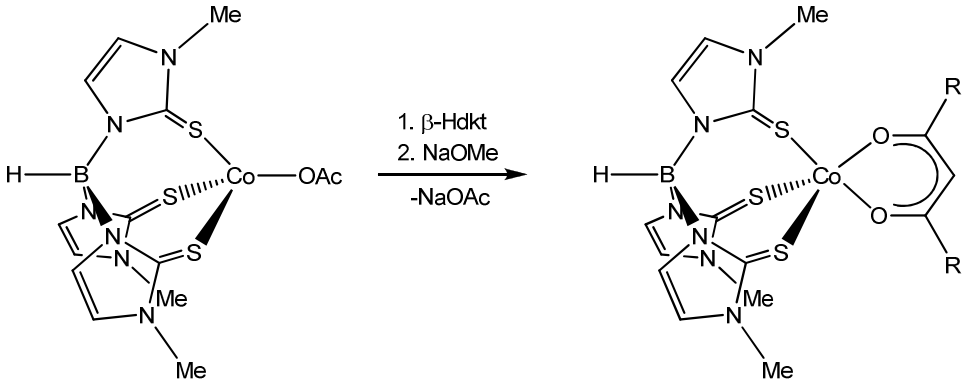

However, the [Tm^{Me}CoX] complexes are difficult to crystallize and to date we have been unable to obtain an X-ray crystal structure. The complexes also present a further problem: despite repeated attempts we have been unable to obtain satisfactory elemental analysis and mass spectrometric data for the compounds. Similar problems have been observed by other researchers in the case Tm^{Me} compounds.

Table 2 Physical and IR spectroscopic data for [Tm^{Me}CoX].

Compound X	Yield (%)	Colour	IR (cm^{-1})	
			ν_{B-H}	$\nu_{X\equiv N}$
1 OAc	50	Olive green	2403	
2 NO_3	53	Green	2427	
3 NO_2	16	Orange-red	2436	
4 N_3	55	Copper-brown	2415	2057
5 NCS	20	Orange-red	2435	2066
6 acac	55	Dark green	2449	

7 hfac	74	Green	2401
8 dbm	67	Green	2452
9 tmhd	81	Brown-green	2457

Synthesis of $[Tp^{R}M(CN)_2][NEt_4]$

The reaction of $[Tp^{R}M(OAc)]$ (R = Ph_2 or Me_3) with two equivalents $[NEt_4]CN$ results in an almost instant colour change from purple to orange in the case of cobalt and green to yellow in the case of nickel. Subsequent addition of Et_2O yields the novel cyanometallates $[Tp^{R}M(CN)_2][NEt_4]$ (M = Co, R = Ph_2 **10** or Me_3 **11**; M = Ni, R = Ph_2 **12** or Me_3 **13**) as orange or yellow solids (Table 3). It is interesting to note that in both cases the yield for complexes **10** and **12** is significantly higher than that of **11** and **13**. This is due to the lower solubility and higher crystallinity of the Tp^{Ph2} derivatives.

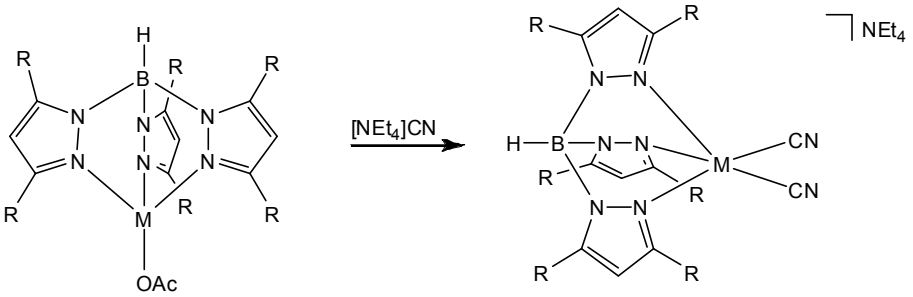

Table 3 Physical and IR spectroscopic data of $[Tp^{R}M(CN)_2][NEt_4]$.

Compound	Yield (%)	Colour	IR (cm^{-1})	
			ν(B-H)	**ν(C≡N)**
10	63	Orange	2592	2103
11	41	Orange	2504	2092
12	54	Orange	2603	2128
13	29	Orange	2509	2119

IR spectroscopy shows a single cyanide band for all compounds between 2092 and 2128 cm^{-1}. Compounds **11** and **13** show bands at slightly higher wavenumbers than those found for $[Tp^*M(CN)_2][NEt_4]$ 2091 (Co) and 2114 (Ni) cm^{-1} respectively suggesting that the Tp^{Me3} ligand is unexpectedly a poorer electron donor than Tp*. Moreover, we observe that complexes **10** and **12** are more electron poor than complexes **11** and **13** suggesting that the

Tp^{Ph2} ligand is a poorer *net* donor than the Tp^{Me3} as one would expect. The B-H stretches are in a range typical for κ^3 coordinated Tp ligands with the Tp^{Ph2} ligand *ca*. 100 cm^{-1} higher than the Tp^{Me3} ligand. Similar values have been reported for the structurally characterized $[Tp^*M(CN)_2][NEt_4]$ in which the metal centre is five-coordinate. In addition, there is a difference of approximately 25 cm^{-1} between the cobalt and nickel complexes consistent with a more electron rich cobalt centre.

Electrochemical studies of the nickel compounds **12** and **13** show irreversible oxidation to Ni^{III} as shown in Figure 9. The two oxidations are observed at 0.80 and 0.61 V for complexes **12** and **13** respectively. This is in accord with the IR data and confirms that the Tp^{Me3} ligand is considerably more electron donating that Tp^{Ph2}. In addition, there is a further quasi-reversible oxidation at 1.24 V which is coupled to the first oxidation suggesting that the decomposition species is also redox-active. Chemical oxidation of $[Tp^{Ph2}Ni(CN)_2][NEt_4]$ will be attempted in the hope of providing further insight into this interesting redox behaviour.

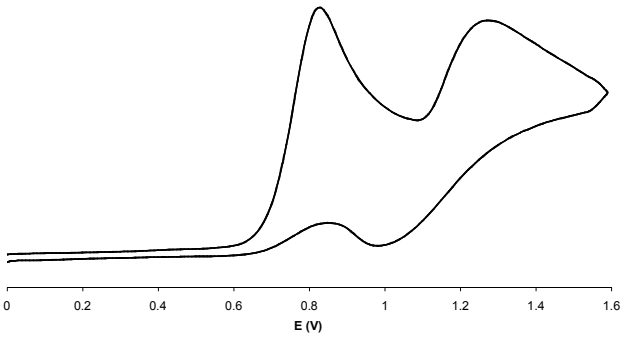

(a)

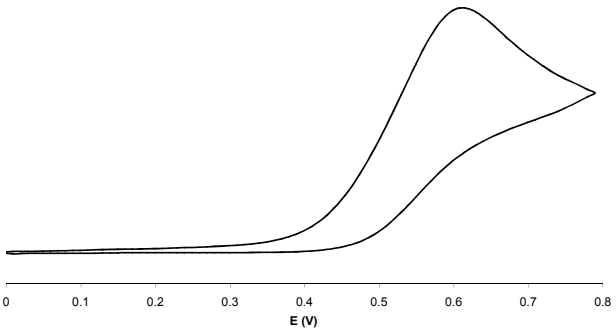

(b)

Figure 9 Cyclic voltammogram of (a) $[Tp^{Ph2}Ni(CN)_2]^-$ **12** and (b) $[Tp^{Me3}Ni(CN)_2]^-$ **13**.

Attempts to study the related cobalt complexes have thus far proved unsuccessful as the cobalt analogues are extremely air-sensitive.

Reactions of $[Tp^{Ph2}Ni(CN)_2][NEt_4]$

Reactions have been attempted using $[Tp^{Ph2}Ni(CN)_2][NEt_4]$ as a building block to prepare small clusters. Thus, $[Tp^{Ph2}Ni(CN)_2][NEt_4]$ has been reacted with $MnCl_2$, $FeCl_2$, $Co(BF_4)_2$ and $Ni(BF_4)_2$ in the presence of bidentate ligands such as bipyridine (bipy) and phenanthroline (phen).

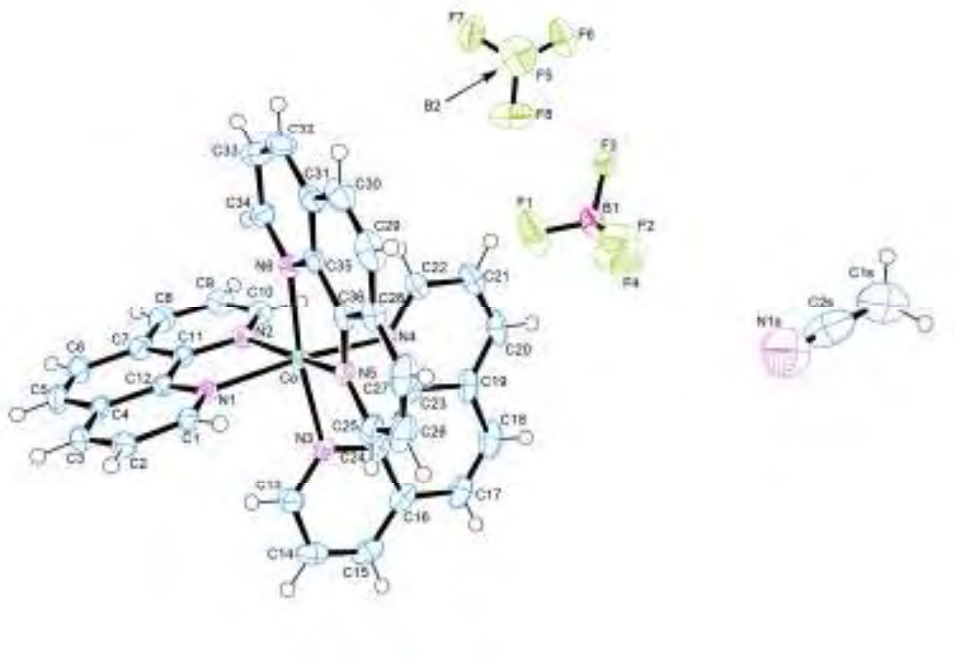

Figure 10 Molecular structure of $[Co(phen)_3][BF_4]_2$.MeCN **14**.

Numerous crystallizations have been undertaken and in the case of Co and phen, small orange crystals formed after a few days. Sadly, X-ray crystallographic analysis showed these to be $[Co(phen)_3][BF_4]_2$.MeCN **14** which although a known compound is a new crystal structure (see Figure 10).

Table 4 Selected bond distances and angles for **14**.

Bond lengths (Å)		Bond angles (°)	
Co-N1	2.131 (4)	N1-Co-N2	78.55 (14)
Co-N2	2.129 (4)	N1-Co-N3	93.21 (13)
Co-N3	2.124 (4)	N1-Co-N5	93.34 (14)
Co-N4	2.123 (4)	N3-Co-N4	78.43 (14)
Co-N5	2.133 (4)	N5-Co-N6	78.11 (14)
Co-N6	2.129 (4)		

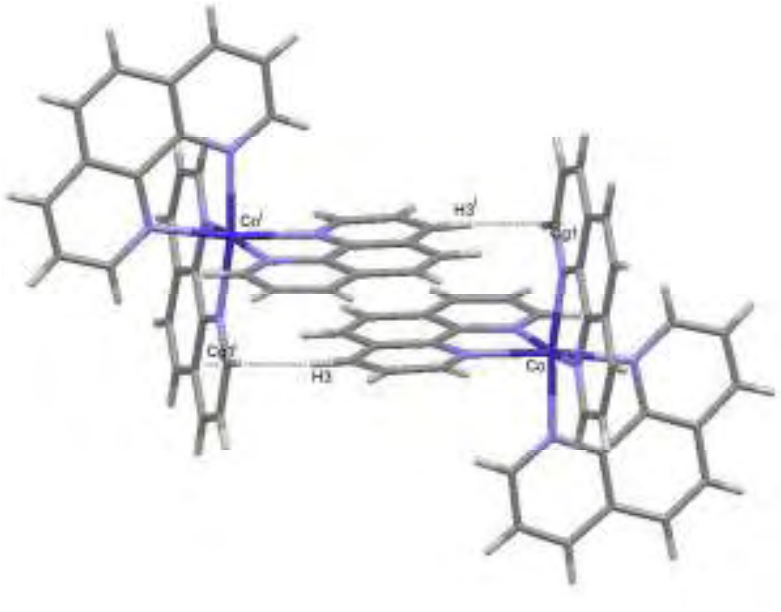

Figure 11 The molecular packing in **14** showing the P4AE interaction. Only selected hydrogen atoms are shown for clarity.

The cobalt metal centre is octahedral with typical Co-N bond lengths for Co^{II} (Table 4). The crystal lattice of **14** contains dimers of $[Co(phen)_3]^{2+}$ cations in which there is a P4AE (Parallel Fourfold Aryl Embrace) motif involving one $\pi\cdots\pi$ (centroid$\cdots$centroid 3.542 (4) Å) and two CH$\cdots\pi$ interactions between the phenanthroline ligands as shown in Figure 11 (Cg1 is the centroid of the ring C31-C35). The offset between the central aryl ring of the two phenanthroline ligands is 6.443(3) Å and indicative of overlap of a single aryl ring. The dimers found in **14** are isolated from each other unlike in the structure of $[Co(phen)_3][BF_4]_2.H_2O.EtOH$ where a further P4AE interaction results in formation of a zigzag

chain. A further difference is that the anions are not found in hydrophilic channels between chains of the cations but rather in aryl boxes formed from six phenanthroline ligands. This difference is presumably the result of a lack of suitable hydrogen bonding solvent in the current structure. Further studies and attempts to prepare the metal clusters are still in progress.

Synthesis of [Tp^{Ph2}MX] Complexes

[Tp^{Ph2}FeCl$_2$] **15** has been prepared as a yellow solid from the reaction of KTp^{Ph2} with $FeCl_3$ in MeOH and THF. Attempts to convert this to the iron(III) [Tp^{Ph2}Fe(CN)$_3$][NEt$_3$] complex results in a complex mixture of products, one of which is [(Tp^{Ph2})$_2$Fe]$^+$.

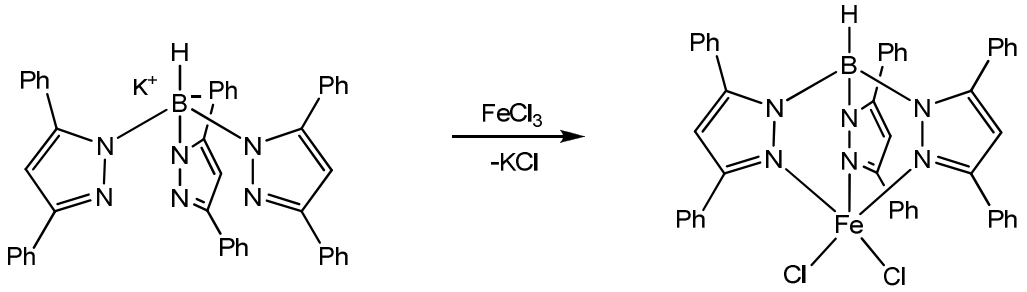

The reaction of [Tp^{Ph2}NiBr] with bipyrimidine in CH_2Cl_2 in the presence of KPF_6 yields the cationic complex [Tp^{Ph2}Ni(bpym)]PF$_6$ **16** as a dark green solid. A similar reaction between [Tp^{Ph,Me}NiBr], bpym and KPF_6 also gives [Tp^{Ph,Me}Ni(bpym)]PF$_6$ **17**. IR and UV-Vis spectroscopic data for the compounds are shown in Table 5.

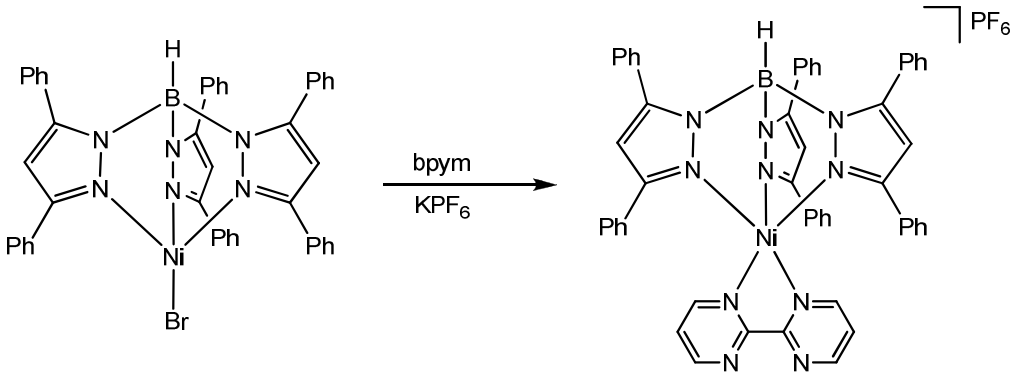

Table 5 Physical, IR and UV-Vis spectroscopic data for $[Tp^{R}Ni(bpym)]^{+}$.

Complex	Colour	Yield (%)	IR ν_{BH} (cm^{-1})	IR $\nu_{C=N}$ (cm^{-1})	λ_{max}, ε ($M^{-1}cm^{-1}$)
16	Emerald green	90	2634	1578	340sh (2,200), 593 (51), 810 (34)
17	Green	75	2545	1577	408sh (354), 598 (102), 812 (89)

In addition, there is strong band at *ca*. 1580 cm^{-1} assigned to a C=N stretch of the bipyrimidine ligand. The coordination mode of the bipyrimidine ligand cannot unfortunately be determined by IR spectroscopy as the band at *ca*. 1565 cm^{-1} typically used for this purpose is masked by bands due to the Tp^{R} ligands. Further bands are also observed at 845, 558 and 847, 558 cm^{-1} for **16** and **17**, respectively, consistent with the presence of PF_6^- counter anions.

The UV-Vis spectra of **16** and **17** reveal two bands at 810, 593 (ε = 34, 51 $dm^3mol^{-1}cm^{-1}$) and 812, 598 nm (ε = 89, 102 $dm^3mol^{-1}cm^{-1}$) respectively consistent with d-d transitions and similar to those reported for other five-coordinate nickel Tp^{R} complexes. A further more intense band (ε = 2200 and 354 $dm^3mol^{-1}cm^{-1}$ for **16** and **17** respectively) at lower wavelengths is also observed for both complexes and is tentatively assigned to an MLCT band.

The ^1H NMR spectra of both complexes reveal appropriately shifted resonances due to the paramagnetic nickel centre with the borohydride resonances are found at -10.82 and -9.77 ppm for **16** and **17**, respectively. The presence of a single pyrazolyl hydrogen peak at 71.14 and 70.83 ppm for **16** and **17**, respectively and a single methyl resonance for **17** indicate fast rotation of the Tp^{R} ligand. Such fluxional behaviour and relatively sharp NMR are frequently observed in four- and five-coordinate first row transition tris(pyrazolyl)borate metal compounds such as $[Tp^{R}Ni(OAc)]$ (R = Me_3; Me_2; Me_2,Br), $[Tp^{Ph,Me}Ni(SR)]$ (R = aryl) [26] and $[Tp^{Ph,Me}Ni(S_2CNR_2)]$ (R = Et, Ph). Interestingly, we were unable to locate two of the protons on the bipyrimidine ligand which are presumably lost due to their close proximity to the paramagnetic nickel centre. Magnetic susceptibilities of 3.57 and 3.35 μ_B were observed for **16** and **17** respectively and are consistent with two unpaired electrons for both complexes and further support fluxionality in these systems as complexes with the square-

based pyramidal geometry observed in the crystal structure (*vide infra*) would be expected to be diamagnetic.

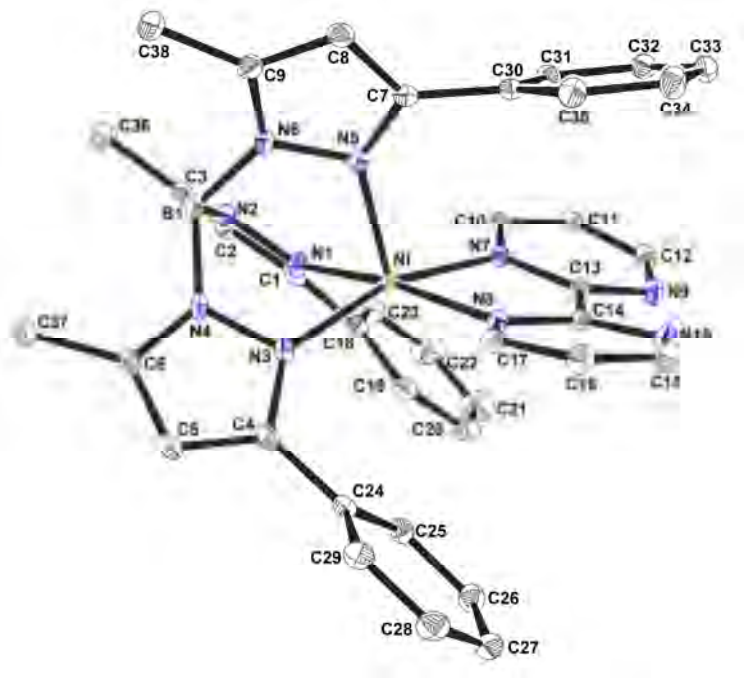

Figure 12 Molecular structure of $[Tp^{Ph,Me}Ni(bpym)]^+$ **17**. The PF_6^- anion, CH_2Cl_2 molecule and hydrogen atoms have been removed for clarity.

Crystals of **17** were grown by diffusion of hexanes into a concentrated solution of the complex in CH_2Cl_2. The compound crystallizes in the triclinic $P\bar{1}$ space group with two independent molecules in the lattice and a molecule of CH_2Cl_2. The molecular structure of one of the independent molecules is shown in Figure 12 with bond lengths and angles given in Table 6. The two independent molecules show five-coordinate nickel metal centres with a κ^3 coordinated $Tp^{Ph,Me}$ ligand, consistent with the above IR data. The coordination geometry is best described as square pyramidal with trigonality indices of 0.12 and 0.07 for the two independent molecules and similar to that reported for the related bipyridine complex $[Tp^{Ph,Me}Ni(bipy)]OTf$ (τ = 0.06). As expected, the bipyrimidine ligand adopts a bidentate chelating coordination mode but is significantly twisted about the C13-C14 bond and thus contains non-coplanar pyrimidine rings. This is particularly evident in the case of molecule 1 where the torsion angle is 8.14° (N7-C13-C14-N8) compared with 2.68° (N7a-C13a-C14a-N8a) for molecule 2. The Ni-N bond lengths for the tris(pyrazolyl)borate ligand are in accord with those reported for other nickel $Tp^{Ph,Me}$ complexes and reveal symmetric coordination

of the $Tp^{Ph,Me}$ ligand. The Ni-N bond lengths for the bipyrimidine ligand are similar to those found in $[(H_2O)_4Ni(\mu\text{-bpym})Ni(H_2O)_4]^{4+}$ despite the difference in coordination number (2.092 and 2.097 Å). The chelate angle for the bipyrimidine ligand is typical for coordinated diimine ligands.

Table 6 Selected bond lengths and angles for **17**.

Bond lengths (Å)		**Bond angles (°)**	
Molecule 1			
Ni-N1	2.051 (3)	N1-Ni-N3	85.42 (9)
Ni-N3	2.048 (2)	N1-Ni-N5	94.09 (9)
Ni-N5	2.018 (2)	N3-Ni-N5	92.11 (9)
Ni-N7	2.070 (2)	N7-Ni-N8	78.34 (8)
Ni-N8	2.066 (2)	τ	0.12
Molecule 2			
Ni-N1a	1.987 (2)	N1a-Ni-N3a	91.01 (8)
Ni-N3a	2.038 (2)	N1a-Ni-N5a	93.92 (8)
Ni-N5a	2.068 (3)	N3a-Ni-N5a	86.46 (8)
Ni-N7a	2.063 (2)	N7a-Ni-N8a	78.10 (8)
Ni-N8a	2.074 (3)	τ	0.07

The structure contains extensive intermolecular interactions (Figure 13). There are three CH···π interactions between the two independent molecules involving the hydrogen atom of one of the Tp phenyl rings and one of the pyrimidine rings of the bpym ligand and the pyrazole rings of the neighbouring $Tp^{Ph,Me}$ ligand (C5···H10a = 2.879(3) Å, C2···H22a = 2.790(4) Å). The final interaction is between the pyrazole hydrogen atom and an adjacent pyrazole ring (C8a···H5 = 2.790(3) Å). Each set of independent molecules is then linked to neighbouring sets by a hydrogen bonding interaction (H17a···N10 = 2.737(3) Å) and a further CH···π interaction (H15···N4a-C6aπ = 2.608(3) Å) forming a linear chain.

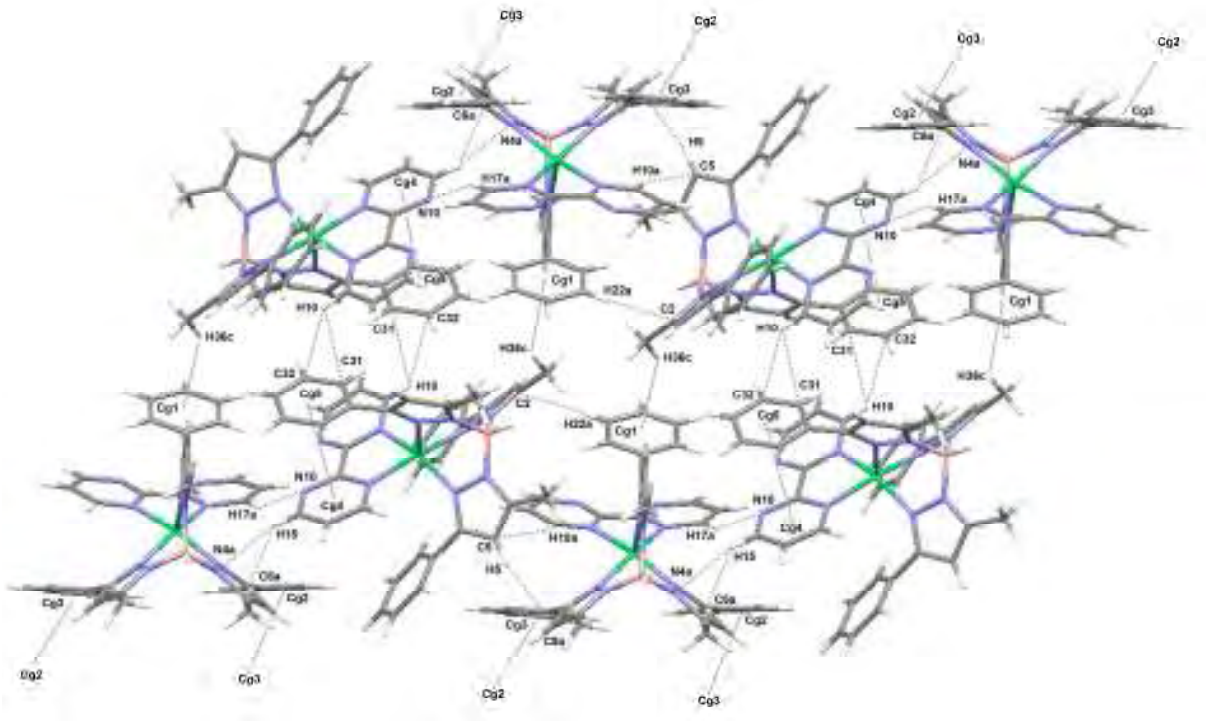

Figure 13 Mercury plot of $[Tp^{Ph,Me}Ni(bpym)]^+$ **17** showing the intramolecular and intermolecular interactions between the molecules. The PF_6^- counter anion and CH_2Cl_2 molecule have been omitted for clarity.

This chain is then connected to another chain through two CH···π interactions one between one of the hydrogen atoms on the bpym ligand and a neighbouring Tp phenyl ring and the other between a methyl hydrogen and the centroid of another Tp phenyl ring (H10···C31-C32π = 2.775(3) Å, H36c···Cg1 = 2.834(2) Å where Cg1 is the centroid of the ring described by C18a-C23a). Further π···π interactions connect these two chains to further sets of chains completing the structure (Cg2···Cg3 = 4.388(2) Å, Cg2 and Cg3 are the centroids of the rings described by C24a-C29a and C30a-C35a, respectively). Finally, an intramolecular interaction between the phenyl ring of the $Tp^{Ph,Me}$ ligand that lies directly above the bipyrimidine ligand is oriented to provide preferential overlap with one of the aromatic rings suggesting π···π interactions (Cg4···Cg5 = 3.687(2) Å where Cg4 and Cg5 are the centroids of the rings described by N8-C14-N10-C15-C17 and C30-C35, respectively).

Cyclic voltammetric studies of the two compounds reveal irreversible one-electron reduction. Interestingly, the degree of reversibility is dependent on the type of Tp^R ligand used with the Tp^{Ph2} ligand showing the most reversibility (Figure 14). This seems to suggest

that the larger Tp^{Ph2} ligand is better able to stabilize the product formed upon reduction, albeit only on the CV timescale.

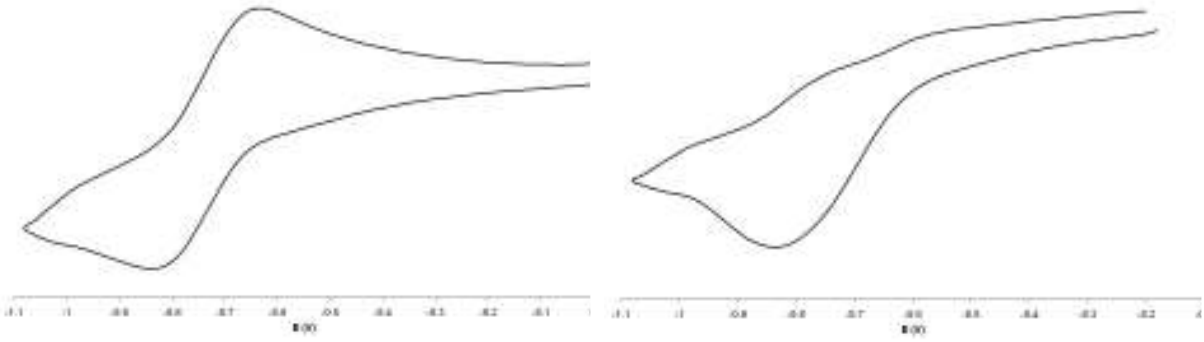

a) b)

Figure 14 Cyclic voltammograms of a) $[Tp^{Ph2}Ni(bpym)]^+$ and b) $[Tp^{Ph,Me}Ni(bpym)]^+$.

Reactions have been attempted with the aim of preparing asymmetric dimers, one of the principal aims of this research. Thus the reaction of metal β-diketonates with **16** or **17** is designed to give $[Tp^{R}Ni(\mu\text{-bpym})M(\beta\text{-dkt})_2]^+$ {M = Co, Ni; R = Ph_2; Ph,Me; β-dkt = 2,2,6,6-tetramethylheptane-3,5-dionate (tmhd), 1,3-diphenylpropane-1,3-dionate (dbm); see below}.

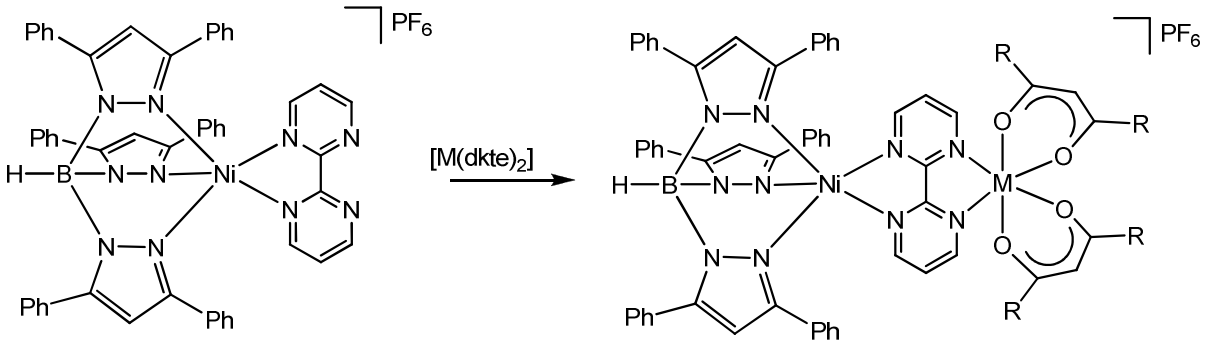

Numerous reactions have been undertaken with cobalt and nickel starting materials and although the reaction appears to proceed smoothly recrystallization of the crude solids produces at least two crystalline substances in most cases. The identity of these remains unknown although all have been characterized by IR spectroscopy. In one case the reaction of $[Tp^{Ph2}Ni(\mu\text{-bpym})]OTf$ and $[Co(dbm)_2(H_2O)_2]$ did yield crystals suitable for a structural study. These proved to $[Tp^{Ph2}Ni(dbm)]$ **18** rather than the anticipated dimer revealing that the dbm ligand has migrated from the cobalt metal to the nickel centre displacing the neutral bipyrimidine ligand.

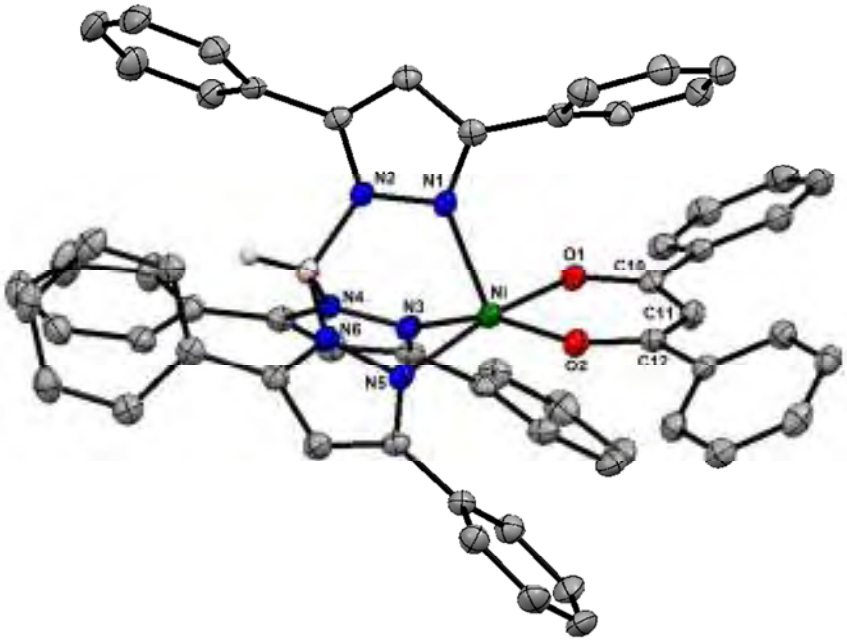

Figure 15 Molecular structure of [Tp^{Ph2}Ni(dbm)] **18**.

The nickel metal centre is five coordinate with a κ^3 coordinated Tp^{Ph2} ligand (see Figure 15). The structure exhibits a slightly distorted square pyramidal coordination geometry and is very similar to the structure of the cobalt analogue [Tp^{Ph2}Co(dbm)] previously reported by us. The six membered dbm chelate ring is almost planar although there is a slight titling of the ligand relative to the nickel centre ($\beta = 9.71^{o}$).

Table 7 Selected bond lengths and angles for **18**.

Bond lengths (Å)		**Bond angles (°)**	
Ni-N1	2.040 (2)	N1-Ni-N3	94.17 (7)
Ni-N3	2.060 (1)	N1-Ni-N5	91.58 (7)
Ni-N5	2.089 (2)	N3-Ni-N5	85.66 (7)
Ni-O1	1.976 (2)	O1-Ni-O2	90.89 (6)
Ni-O2	1.976 (2)	τ	0.13
		β	9.71

The dbm ligand is symmetric indicating that the negative charge is distributed over the β-diketonate fragment. The Ni-O bond lengths are again similar to those reported for

[Tp^{Ph2}Co(dbm)] being shorter by *ca*. 0.01 Å and consistent with the slightly smaller atomic radius of nickel. As observed for **17** the phenyl rings are twisted with respect to the pyrazole rings to accommodate the planar dbm ligand.

The fact that the proposed dimer isn't formed in any of the above reactions may be due to the steric bulk of the Tp^R ligands. This is most clearly seen in the spacefill diagram of **13** shown in Figure 16.

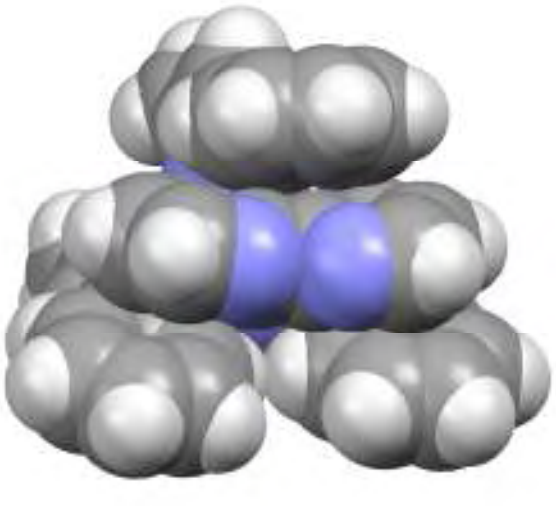

Figure 16 Spacefill diagram of **17** showing the close proximity of the $Tp^{Ph,Me}$ phenyl rings and bipyrimidine ligand.

As can be seen the upper phenyl ring of the $Tp^{Ph,Me}$ ligand lies directly above the bipyrimidine ligand and may result in steric clashes between this ring and any ligand in the axial position. It follows that we may require smaller ligands to realize the proposed dimers. Thus reactions were attempted between $[Tp^RNi(bpym)]^+$ and $[PdCl_2bipy]$ in the presence of KPF_6 and $Na_2[PdCl_4]$. In both cases recrystallization of the products yielded a yellow solid and a green solid indicating that no reaction had taken place. The reactions were also attempted at higher temperatures with the same result. It therefore appears as though the $[Tp^RNi(bpym)]^+$ unit is a poor acceptor for use in the construction of coordination networks.

As noted in the first year report the analogous cobalt complexes have proved surprisingly elusive. The use of different solvents also did not yield $[Tp^RCo(bpym)]PF_6$. Even changing the anion perhaps to BPh_4^- gave the same result. The reason why the cobalt Tp^{Ph2} complexes should be so difficult to prepare remains unclear.

Synthesis of [Tp^{Ph2}Ni(β-dkt)] Complexes

Following the successful crystallization of [Tp^{Ph2}Ni(dbm)] **18** we undertook the synthesis of a range of β-diketonate nickel complexes [Tp^{Ph2}Ni(β-dkt)] {β-dkt = 1,3-diphenyl-propanedionate (dbm) **18**, 2,2,6,6-tetramethylheptanedionate (tmhd) **19**, hexafluoroacetyl-acetonate (hfac) **20**, 1-phenylbutanedionate (pbd) **21**} by reacting [Tp^{Ph2}NiBr] with β-diketone in the presence of a weak base NEt_3. The complexes are isolated as green solids in good yields.

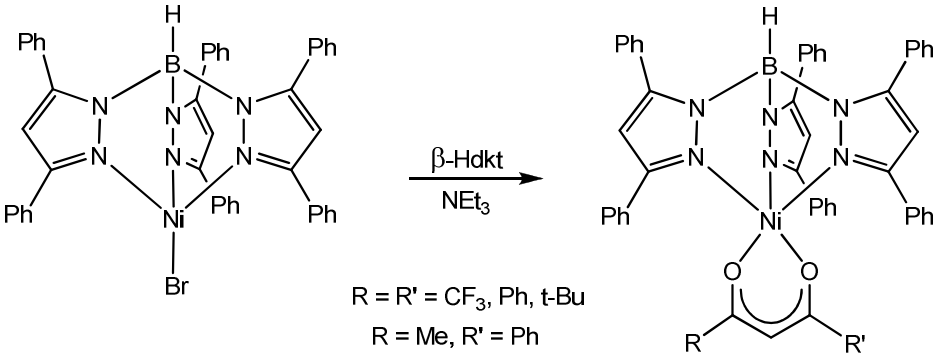

IR spectroscopy reveals B-H stretches between 2620-2631 cm^{-1} and characteristic of a κ^3 coordinated Tp^{Ph2} ligand. There are also C-O stretches ascribed to the β-diketonate ligands between 1645-1594 cm^{-1}.

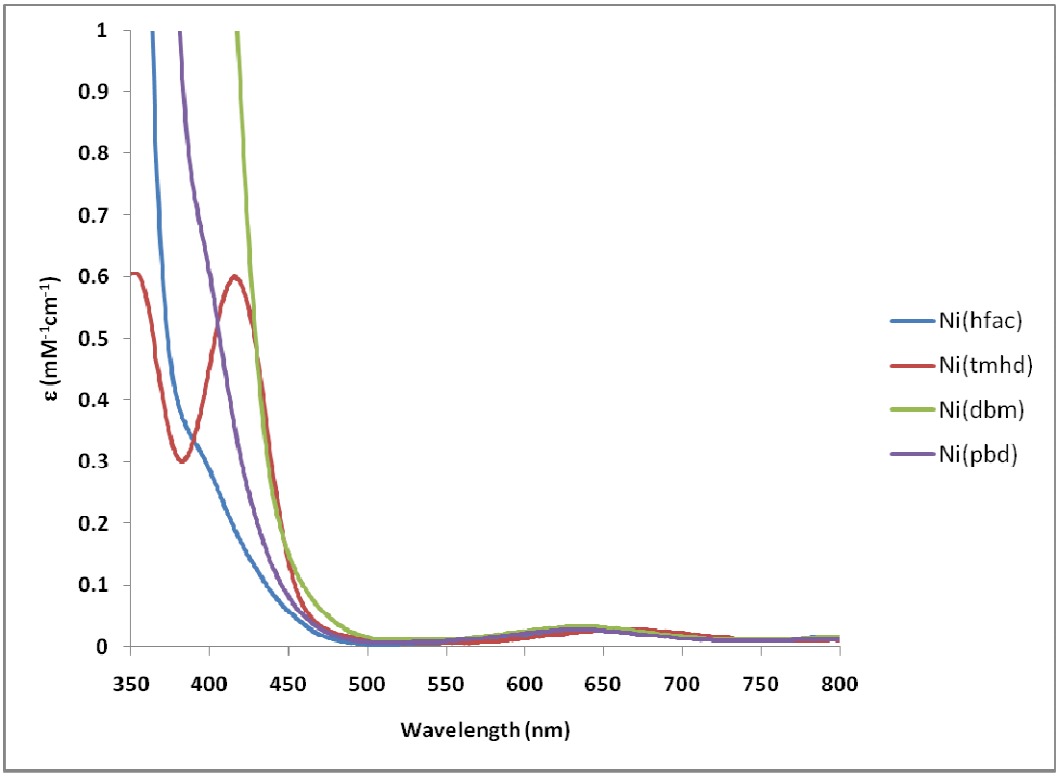

Figure 17 UV-Vis spectra of [Tp^{Ph2}M(β-dkt)].

The UV-Vis spectra of **18**-**21** reveal a single band between 633-663 cm^{-1} (ε = 56-66 $dm^3mol^{-1}cm^{-1}$) consistent with d-d transitions and similar to those reported for other five-coordinate nickel Tp^R complexes. A series of more intense bands are observed at lower wavelengths and are assigned to ligand π to π^* transitions.

The complexes have also been characterized by ^1H NMR spectroscopy with resonances similar to those found for the cation bipyrimidine complexes, **16** and **17**.

Electronic Structure of [Tp^{Ph2}Co(β-dkt)] Compounds

Recent successes in this group have included the isolation of a range of [Tp^{Ph2}Co(X)] complexes (X = Cl^-, Br^-, NO_3^-, N_3^-, NCS^-, NO_2^-, OAc^-(Hpz^{Ph2}), $acac^-$, $hfac^-$, dbm^-, $tmhd^-$). Several of these complexes are vital in the synthesis of the clusters which are the goal of this research. Furthermore, the β-diketonate complexes (with the exception of $hfac^-$) are redox-active *oxidizing*, albeit irreversibly, to Co^{III}. Such compounds are comparatively rare in Tp chemistry and we have now undertaken computational studies to better understand the electronic structure of these compounds. It is hoped that these studies will allow us to better design our system to achieve molecular magnets.

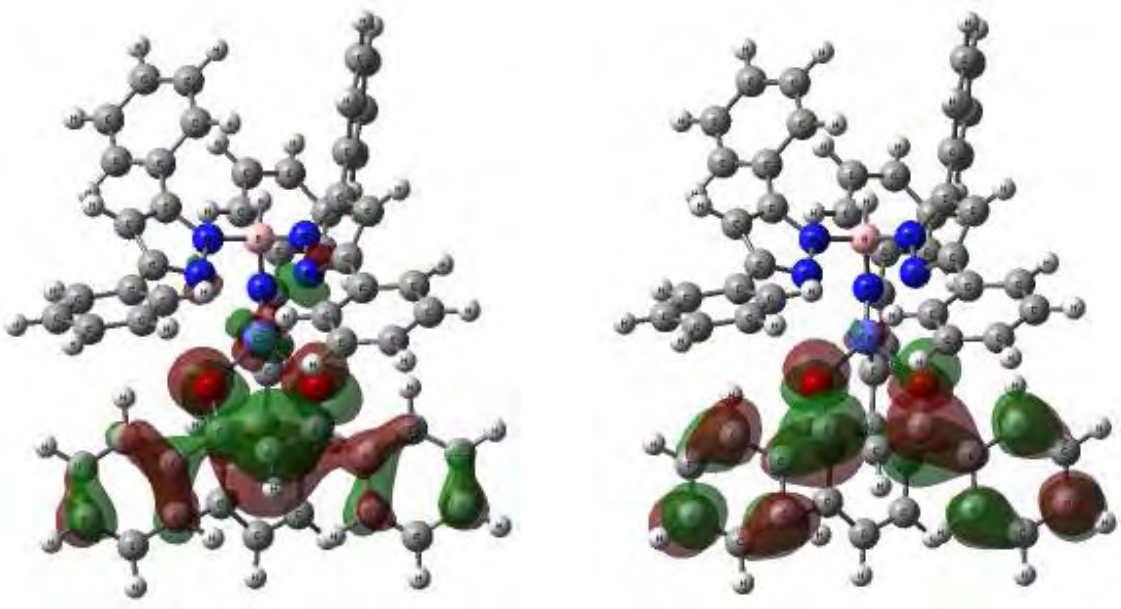

Figure 18 HOMO and LUMO of [Tp^{Ph2}Co(dbm)].

The computational analysis reveals that the HOMO is strongly influenced by the supporting ligand X with a Co-β-diketonate π^* antibonding interaction. In the case of the β-diketonates through their delocalized network they are able to *push* electron density onto

the metal thereby making oxidation easier. Simple halides cannot do this and thus the complex reduces instead. The analysis also confirms that the oxidation occurs at the metal centre and not at either of the ligands. The [Tp^{Ph2}Co(hfac)] complex, however, has a totally different electronic structure with the HOMO almost exclusively located on the Tp^{Ph2} ligand explaining the lack of redox-activity seen in this case. In contrast, the LUMO is dominated by the β-diketonate ligand with little or no electron density on the metal and thus no metal-based reductions.

Synthesis of [Tp^{Ph2}M(dtc)]

Given the importance of the anion in determining the stability of the Co^{III} oxidation state as detailed in the previous section attempts were made to lower the oxidation potential by using sulfur donors instead of oxygen. Thus, addition of NaS_2CNR_2 (R = Et, Bz) and NaS_2Cpyr (pyr = pyrrolidene) to a suspension of [Tp^{Ph2}MBr] (M = Co, Ni) yields the dithiocarbamate (dtc) complexes, [Tp^{Ph2}M(S_2CNR_2)] (M = Co, R = Et **22**, Bz **23**, $(CH_2)_2$ **24**; M = Ni, R = Et **25**, Bz **26**, $(CH_2)_2$ **27**) in good yields as purple-brown (M = Co) or green (M = Ni) solids.

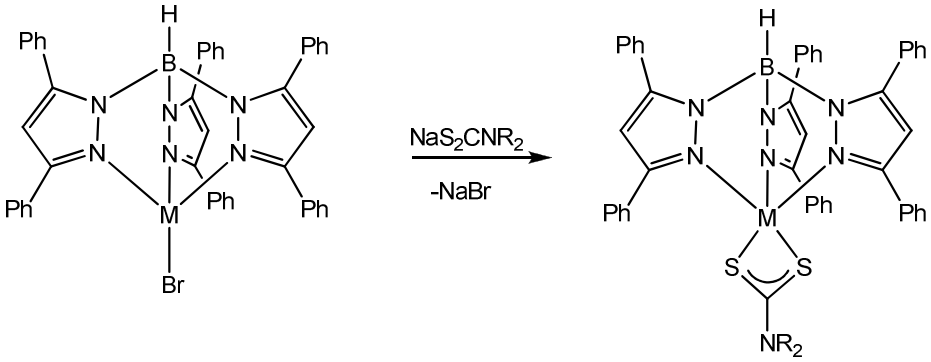

The compounds are soluble in polar organic solvents such as CH_2Cl_2 and acetone. Succesful synthesis of the cobalt complexes requires longer reaction times than the corresponding nickel complexes, typically 5-6 hours compared with 2 hours, as [Tp^{Ph2}CoBr] is only sparingly soluble in CH_2Cl_2 while [Tp^{Ph2}NiBr] dissolves readily. The synthesis of the air-stable cobalt(II) dithiocarbamate complexes, **22**-**24**, is particularly notable as cobalt(II) dithiocarbamate complexes are comparitively rare and usually highly susceptible to oxidation. Moreover, while **22**-**24** are readily synthesized attempts to prepare the $Tp^{Ph,Me}$ analogues under the same conditions led to a complex mixture of products including the cobalt(III) tris(dithiocarbamate) complexes, [$Co(dtc)_3$], suggesting

that the electron poor Tp^{Ph2} ligand is vital to the successful synthesis of stable Co(II) dithiocarbamate compounds.

Table 8 Physical, spectroscopic and electrochemical data for $[Tp^{Ph2}M(dtc)]$.

Complex	Colour	Yield (%)	IR ν_{BH} (cm^{-1})	$E^{o'}$ (V)	λ_{max}/nm ($\varepsilon/M^{-1}cm^{-1}$)
22	Purple-brown	63	2623	0.49	408 (859), 536 (63)
23	Purple-brown	69	2613	0.56	404 (974), 535 (72)
24	Purple	64	2626	0.54	402 (1,071), 505 (73)
25	Dark green	85	2624	0.57	372sh (1,460), 426 (1,190), 654 (95)
26	Dark green	84	2610	0.64	365sh (1,860), 426 (1,187), 655 (103)
27	Green	77	2626	0.62	372sh, (1,360), 429 (1,011), 658 (95)

IR spectroscopy reveals B-H stretches between 2610 and 2626 cm^{-1} indicative of κ^3 coordinated Tp^{Ph2} ligands (Table 8). There are also very strong C-N streches between 1479 and 1471 cm^{-1} confirming the presence of a dithiocarbamate ligand in the metal coordination sphere.

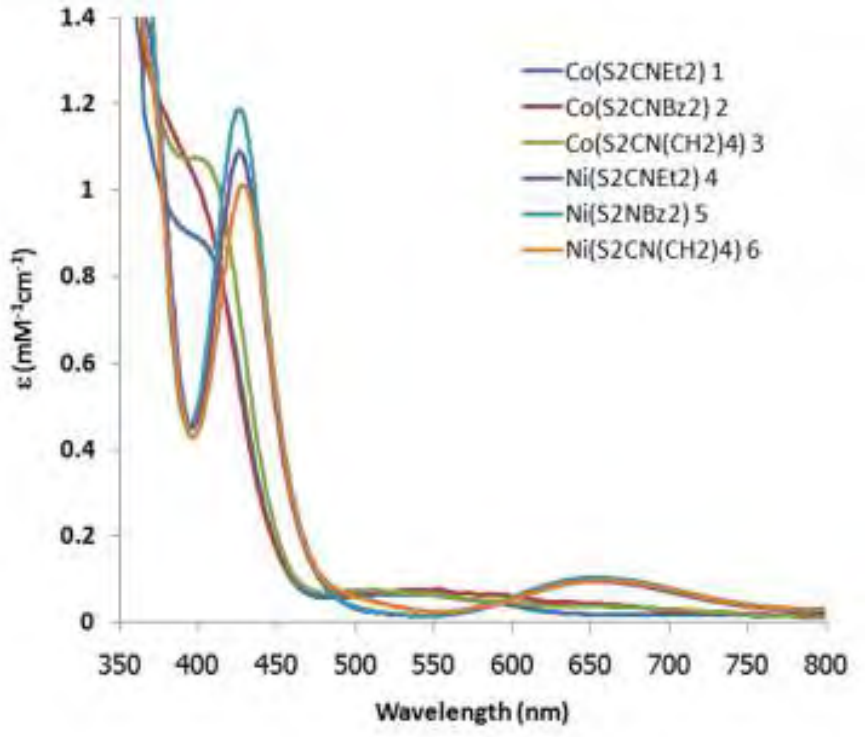

Figure 19 UV-Vis spectra of $[Tp^{Ph2}M(dtc)]$.

The corresponding C-S streches are weak bands observed between 1011 and 1009 cm^{-1}. Similar stretches are observed in the closely related [Tp*Ni(dtc)] complexes.

Solution spectra of **22**-**27** were recorded in CH_2Cl_2 and are shown in Figure 19. In the case of the cobalt complexes there are two main features in the spectra one at *ca*. 400 nm and another between 505 and 535 nm. The former of these bands has a large molar extinction coefficient and by comparison with the analogous complex [$Tp^{Ph,Me}$Co(thiomaltolate)] which has a similar band at 391 nm is assigned as a sulfur-to-Co(II) LMCT band. The other band is assigned to a d-d transition as the related five-coordinate complex [$Tp^{i\text{-}Pr2}$Co(SMeIm)] (SMeIm = 2-mercapto-1-methylimidazolate) has a band at 563 nm. The analogous nickel complexes, **25**-**27** have two features a shoulder at *ca*. 370 nm and further band between 426 and 429 nm indicative of sulfur-to-Ni(II) LMCT bands. For comparison, the recently reported [$Tp^{Ph,Me}$Ni(dtc)] (dtc = S_2CNEt_2, S_2CNPh_2) complexes also exhibit bands at 420 and 428 nm, respectively and in the case of [$Tp^{Ph,Me}$Ni(S_2CNEt_2)] a shoulder at 380 nm. The CT bands at *ca*. 370 nm are thought to correspond to the S-Ni σ bond while the lower energy bands are caused by the S-metal π bond in accordance with the assignments made by Fujisawa *et al* in the cobalt and nickel complexes [$Tp^{i\text{-}Pr2}$M(SMeIm)].

Interestingly, while the cobalt complexes reveal a weak blue shift in going from **22** to **24** an opposite trend is observed for **25**-**27** where the band is red-shifted with decreasing *S*,*S*'-chelate donor strength. Furthermore, the sulfur-to-metal(II) CT bands of the cobalt series are found on average 22 nm lower than their nickel counterparts. A comparable albeit larger shift is observed in [Tp*M(CysEt)] (M = Co, Ni, CysEt = *l*-cysteine ethyl ester) where the difference is 48 nm. In addition to the above charge transfer bands there is also a d-d transition between 654 and 658 nm. Once again similar bands are observed in previously reported [Tp^{R}Ni(dtc)] complexes. Overall, the spectra are consistent with five-coordinate, high spin M(II) complexes.

^{1}H NMR spectra of **22**-**27** were recorded in $CDCl_3$ and have been assigned by comparison with the previously reported [$Tp^{Ph,Me}$Ni(dtc)] (dtc = S_2CNEt_2, S_2CNPh_2) complexes and in the case of **22**-**24** with [$Tp^{Ph,Me}$Co(O-S)] (O-S = thiomaltolate, 1,2-hydroxypyridinethionate, 3,4-hydroxypyridinethionate), [Tp^{Ph}Co(lactate)] and [Bp^{Ph2}Co{HB(3,5-pz^{Ph2})(pz^{Me2})$_2$}]. The ^{1}H NMR spectra reveal paramagnetically shifted

resonances (Table 9) with the cobalt compounds exhibiting particularly large shifts over a range of 200 ppm (Figure 20).

Table 9 ^{1}H NMR spectroscopic data for [Tp^{Ph2}M(dtc)] **22**-**27**.

	Tp^{Ph2} ligand								**Dithiocarbamate ligand**	
	5Ph (*o*)	5Ph (*m*)	5Ph (*p*)	3Ph (*o*)	3Ph (*m*)	3Ph (*p*)	4H	BH	N-CH_2	R
22	36.7	22.4	18.2	-73.5	3.7	3.8	49.0	119.1	101.6	32.4 (Me)
23	35.9	22.0	17.8	-71.2	3.2	3.9	49.8	115.6	93.3	36.9 (*o*-Ph), 15.2 (*m*-Ph), 13.8 (*p*-Ph)
24	36.6	22.3	18.1	-73.6	2.9	3.7	49.1	118.6	102.4	28.2 (CH_2)
25	7.7	7.0	7.4	4.8	6.9	7.2	59.3	-11.1	39.0	1.1 (Me)
26	7.8	7.1	7.4	4.7	6.7	7.1	61.0	-11.3	30.7	8.4 (*o*-Ph), 7.6 (*m*-Ph), 8.0 (*p*-Ph)
27	7.8	7.1	7.4	4.8	6.9	7.3	59.9	-10.9	38.8	4.9 (CH_2)

The borohydride resonances are very broad and for **22**-**24** and **25**-**27** are found between 116 and 119 ppm and *ca*. -11 ppm, respectively. In both sets of complexes there is a single peak for the pyrazolyl protons indicative of fast rotation of the Tp^{Ph2} ligand. Such fluxional behaviour is well documented in first row transition metal Tp^{R} complexes. For **22**-**24** the hydrogen atoms of the 3-phenyl ring are observed between -74 and -71 ppm, 2.9 and 3.7 ppm and 3.7 and 3.9 ppm for the *ortho*, *meta* and *para* protons respectively. In contrast, the 5-phenyl ring protons are strongly deshielded and found between 17.8 and 36.7 ppm.

The nickel complexes exhibit similar resonances between 4.7 and 7.3 ppm and 7.1 and 7.8 ppm for the 3-phenyl and 5-phenyl protons respectively. As with **22**-**24** the *ortho*-hydrogens of the 3-phenyl substituents are broad and shifted upfield of the other aromatic protons for the Tp^{Ph2} ligand. The dithiocarbamate ligand has sharp resonances for the N-CH_2R protons between 102 and 93 ppm and 39 and 31 ppm for **22**-**24** and **25**-**27** respectively. Interestingly, in the case of the benzyl dithiocarbamate ligand the resonance is always *ca*. 9 ppm upfield of the other dithiocarbamates. The other protons for the dithiocarbamate ligands are readily identified and assigned based on their position and integration intensity, although the CH_2 protons for the pyrrolidene ring in **27** are found to overlap with *ortho* protons of the Tp^{Ph2} ligand.

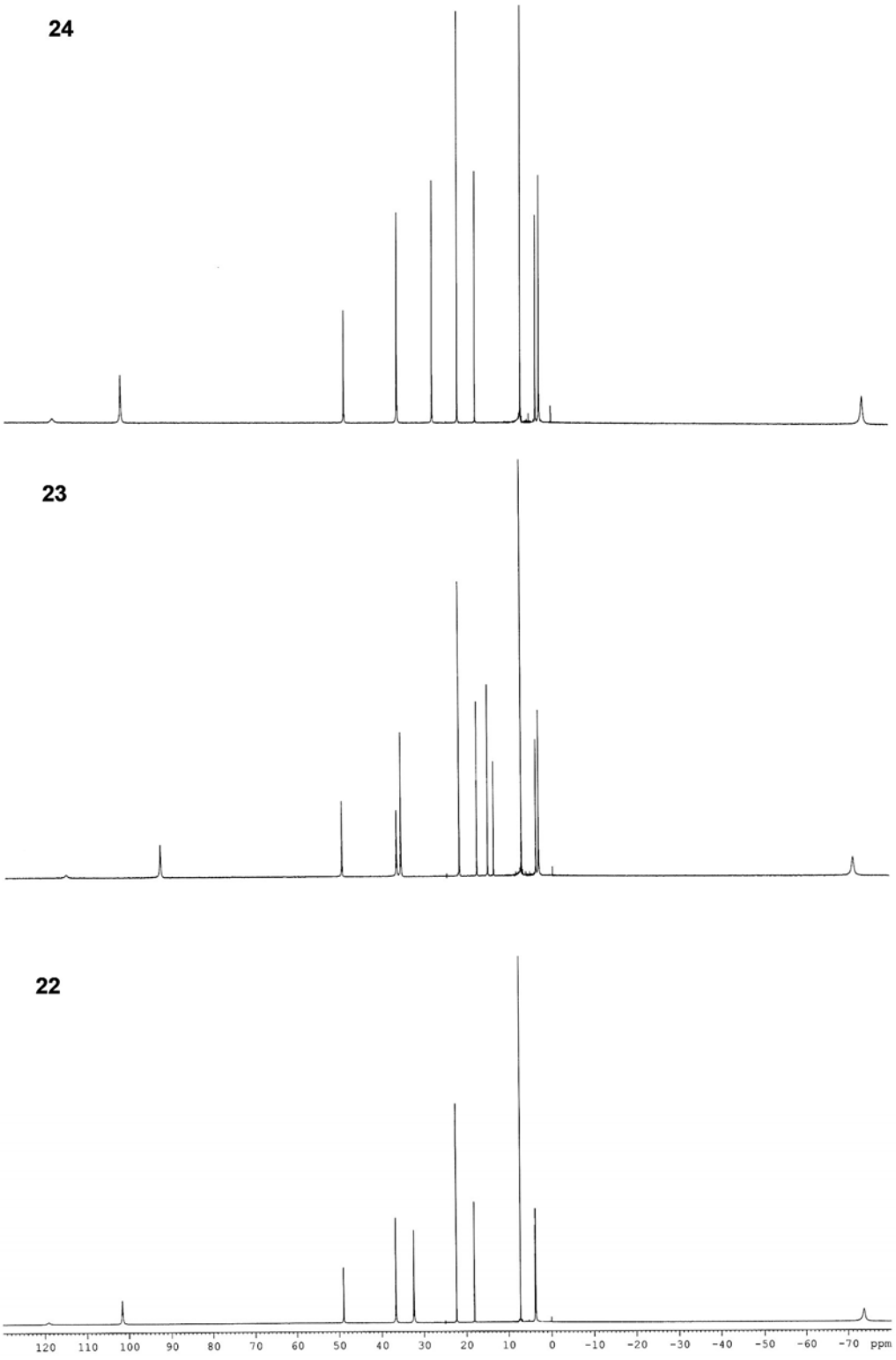

Figure 20 ^{1}H NMR spectra of [Tp^{Ph2}Co(dtc)] **22**-**24**.

The molecular structures of [Tp^{Ph2}Co(S_2CNEt_2)] **22**, [Tp^{Ph2}Co($S_2CN(CH_2)_4$)] **24** and [Tp^{Ph2}Ni($S_2CN(CH_2)_4$)] **27** have been determined by X-ray crystallography.

Crystallographic data are presented in Table 10 while the structures are shown in Figures 21 and 22. In the case of **24** and **27** two of the carbons in the pyrrolidene ring of the dithiocarbamate ligand are crystallographically disorded over two positions. All complexes show five-coordinate metal centres with κ^3 coordinated Tp^{Ph2} ligands and a geometry intermediate between square pyramidal and trigonal bipyramidal being slightly closer to the former. In contrast, the related $[Tp^{Ph,Me}Ni(dtc)]$ (dtc = S_2CNEt_2, S_2CNPh_2) complexes are four-coordinate and square planar in the solid state, although a five-coordinate geometry exists in solution. However, $[Tp^*Ni(S_2CNEt_2)]$[24] and the xanthate complex $[Tp^{Ph,Me}Ni(S_2COEt)]$ are five-coordinate. In this instance it would appear that the more electron poor Tp^{Ph2} ligand leads to coordination of the apical nitrogen in both the solid state and in solution while the more electron rich $Tp^{Ph,Me}$ ligand is able to stabilize a four- rather than five-coordinate species. The importance of steric effects is highlighted by $[Tp^*Ni(S_2CNEt_2)]$ which although more electron rich than both Tp^{Ph2} and $Tp^{Ph,Me}$ still results in a five-coordinate complex presumably due to the smaller steric bulk of Tp*. It is clear that a subtle combination of both steric and electronic effects influences the prefered coordinating mode of the Tp^R ligands in such dithiocarbamate complexes.

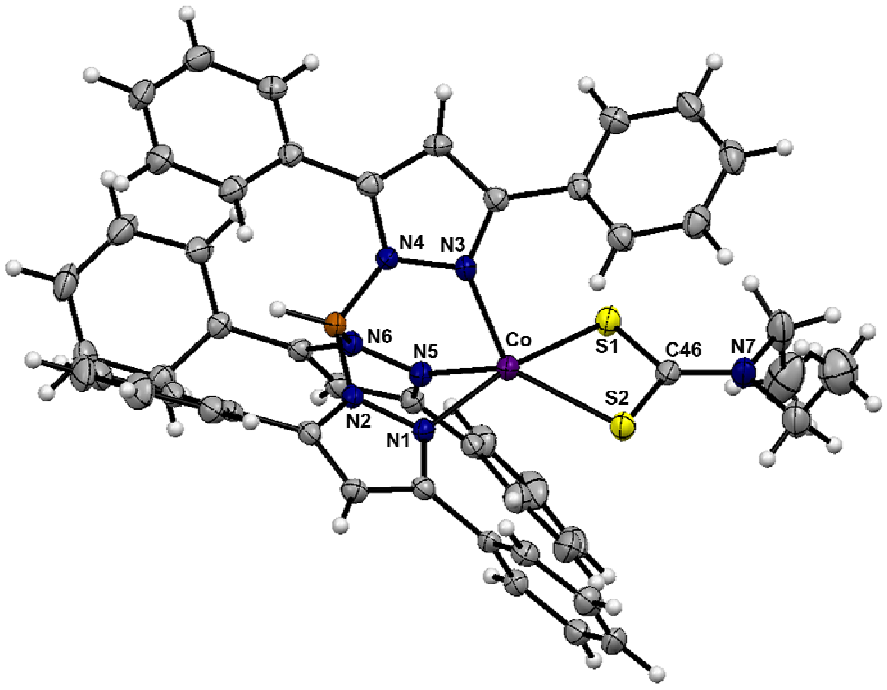

a)

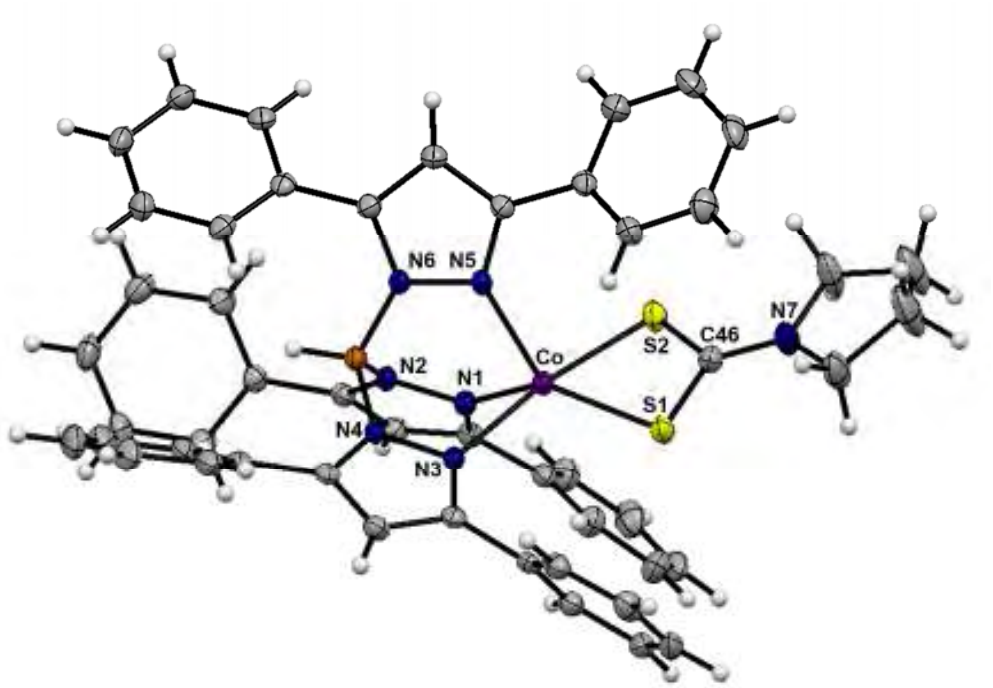

b)

Figure 21 Molecular structures of a) [$Tp^{Ph2}Co(S_2CNEt_2)$] **22** and b) [$Tp^{Ph2}Co(S_2Cpyr)$] **24**.

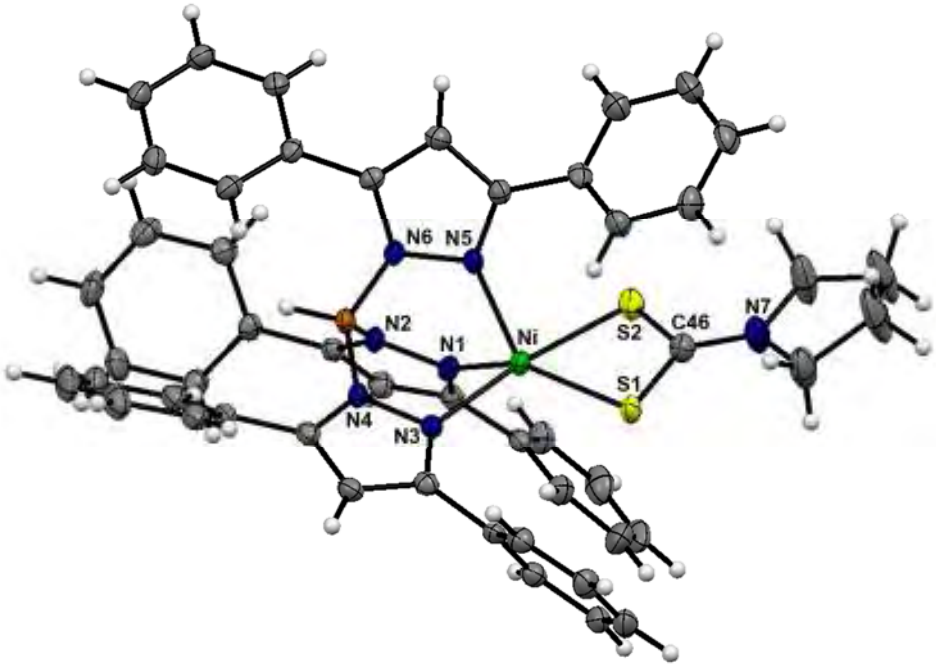

Figure 22 Molecular structure of [$Tp^{Ph2}Ni(S_2Cpyr)$] **27**.

The Ni-N_{pz} and Ni-S bond lengths in **27** are very similar to those found in [Tp*Ni(S_2CNEt_2)] and [Tp^{PhMe}Ni(S_2COEt)] where the bond lengths are Ni-N_{pz} 2.042-2.078(2) Å; Ni-S1 2.399(1), Ni-S2 2.379(1) Å and Ni-N_{pz} 2.027-2.065(2) Å and Ni-S1

2.4099(7), Ni-S2 2.3747(8) Å, respectively and consistent with a paramagnetic Ni(II) centre. On average the cobalt-nitrogen bond lengths are *ca*. 0.05 Å longer than in **27** and consistent with the different ionic radii of Co(II) and Ni(II). A further difference between the cobalt and nickel complexes is that while the Tp^{Ph2} ligand is symmetrically coordinated in **27** one of the pyrazole arms of the Tp^{Ph2} ligand is elongated by between *ca*. 0.06-0.08 Å in **22** and **24** (see Table 10). Such asymmetric binding of the Tp^{Ph2} ligand has previously been observed in the structure of $[Tp^{Ph2}Co(OAc)(Hpz^{Ph2})]$. Furthermore, in all the complexes asymmetric binding of the dithiocarbamate is observed although the degree of asymmetry is dependent on the particular dithiocarbamate present. Thus ΔM-S = 0.038(1) Å for **22** and 0.079(1) and 0.085(1) Å for **24** and **27** respectively. Interestingly, for $[Tp^*Ni(S_2CNEt_2)]$ ΔM-S = 0.035(1) Å suggesting that the constrained pyrrolidene dithiocarbamate ligand may cause asymmetric binding in Tp^R dithiocarbamate complexes. The dithiocarbamate ligands display small bite angles between 74.4 and 75.1^o and similar with those reported for $[Tp^*Ni(S_2CNEt_2)]$ (73.99(3)^o) and $[Tp^{Ph,Me}Ni(S_2COEt)]$ (74.75(2)^o). The carbon-nitrogen and carbon-sulfur bond lengths are typical for bound dithiocarbamate ligands with values intermediate between those expected for carbon-element single and double bonds.

Table 10 Selected bond lengths and angles for **22**, **24** and **27** (Å, ^{o}).

	22	**24**	**27**	**$Tp^*Ni(S_2CNEt_2)$**
Bond Lengths/Å				
M-N1	2.164(2)	2.0876(17)	2.049(2)	2.063(2)
M-N3	2.080(2)	2.1674(17)	2.085(2)	2.065(2)
M-N5	2.106(2)	2.0709(17)	2.051(2)	2.027(2)
M-S1	2.4267(8)	2.3676(10)	2.3510(9)	2.3747(8)
M-S2	2.3891(8)	2.4461(10)	2.4357(10)	2.4099(7)
C46-S1	1.716(3)	1.726(2)	1.696(3)	1.710(3)
C46-S2	1.735(3)	1.716(2)	1.715(3)	1.707(3)
C46-N7	1.335(3)	1.318(3)	1.322(4)	1.329(4)

Bond Angles/^{o}				
N1-M-N3	87.83(8)	81.47(6)	84.23(10)	88.39(8)
N1-M-N5	81.16(8)	95.75(7)	95.31(9)	93.47(9)
N3-M-N5	94.39(8)	87.56(7)	89.64(9)	88.68(8)
N3-M-S2	121.32(6)	171.78(4)	173.04(7)	171.95(6)
N5-M-S2	144.24(6)	100.51(5)	97.12(7)	98.19(6)
N1-M-S2	100.36(6)	99.13(5)	96.71(7)	95.33(6)
N3-M-S1	103.01(6)	99.57(5)	101.29(7)	99.59(6)
N5-M-S1	97.25(6)	119.97(5)	115.12(7)	112.05(7)
N1-M-S1	169.15(6)	144.27(5)	148.92(7)	153.27(7)
S1-M-S2	74.61(3)	75.11(2)	74.38(3)	73.99(3)
N7-C46-S1	122.0(2)	121.07(16)	121.7(3)	122.7(2)
N7-C46-S2	122.4(2)	121.90(16)	122.2(3)	122.4(2)
S1-C46-S2	115.54(15)	117.02(12)	116.11(19)	114.8(1)
τ	0.42	0.46	0.40	0.31

In addition, we have also inadvertently determined the structure of the [Tp^{Ph2}NiBr] **28**. Crystals were grown by allowing hexanes to diffuse into a concentrated solution of the complex in CH_2Cl_2. The compound crystallizes in the trigonal, *R3* space group and is a rare example of a metal Tp complex with a crystallographic C_3 axis. The structure is shown in Figure 23. The geometry around the nickel centre is best described as distorted tetrahedral {N1-Ni-N1^{i} = 92.46(10)^{o}, N1-Ni-Br = 123.50(7)^{o}}. The Ni-N bond lengths are very slightly longer by 0.01 Å than those found in [Tp^{Ph2}NiCl]. A similar difference is observed in the structures of [Tp*NiCl] and [Tp*NiBr]. The Ni-Br distance is 2.3627(7) Å, *ca.* 0.16 Å longer than the corresponding Ni-Cl distance in [Tp^{Ph2}NiCl], and consistent with the difference in the bromine and chlorine covalent radii (0.15 Å). Interestingly, the Ni-Br bond length in **28** is significantly longer than that observed for [Tp*NiBr] {2.291(2) Å}. A similar increase, albeit not so marked, is also found between [Tp^{Ph2}NiCl] and [Tp*NiCl] (ΔNi-Cl = 0.03 Å) suggesting that the larger Tp^{Ph2} ligand may be responsible for the longer nickel-halide bond distances.

The crystal packing in the structure of **28** contains several C-H···π interactions between the phenyl rings of neighbouring Tp^{Ph2} ligands. The hydrogen atoms H6 and H11 are directed at the π bonds between C1-N1 and C4-C5, respectively {(C1-N1)π···H6 2.646(3)

Å; (C4-C5)π···H11 2.828(5) Å} while H5 interacts with a phenyl ring (Cg1···H5 2.743(3) Å; Cg1 is the centroid of ring C10-C15). Similar interactions occur on all three faces of the Tp^{Ph2} ligand creating a network of triangular columns such that all the [Tp^{Ph2}NiBr] molecules point in the same direction and the phenyl rings adopt a propeller configuration.

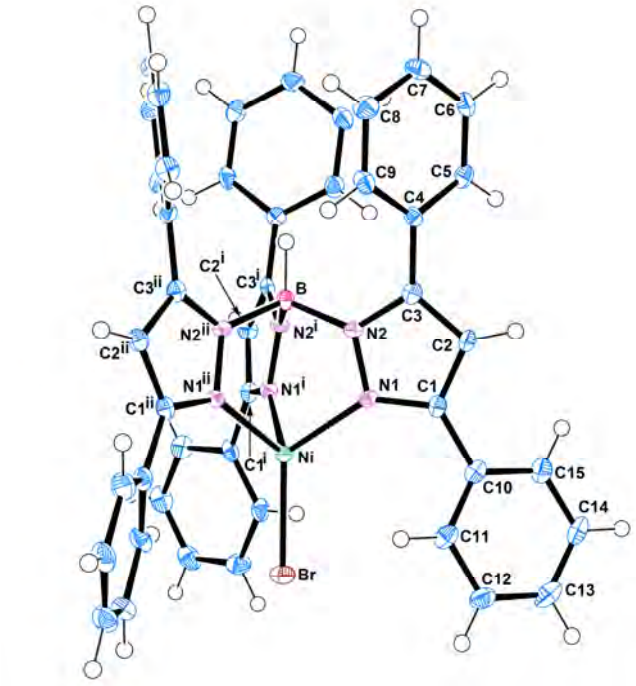

Figure 23 The molecular structure of [Tp^{Ph2}NiBr] **28**.

Electrochemical studies reveal that both the Co and Ni complexes undergo *quasi-reversible* oxidation to Co(III) and Ni(III) respectively. The Co series are shown in Figure 24 as representative examples. The quasi-reversibilty of the redox couples of **25**-**27** matches those of the previously reported [Tp^{R}Ni(dtc)] (R = Ph,Me; Me_2) compounds. It is noteworthy that the reduction of [$Co(dtc)_3$] to [$Co(dtc)_3$]$^-$ is also quasi-reversible. The cobalt complexes are *ca*. 80 mV more easily oxidized than the corresponding nickel compounds reflecting the greater stability of the Co(III) oxidation state (see Table 8).

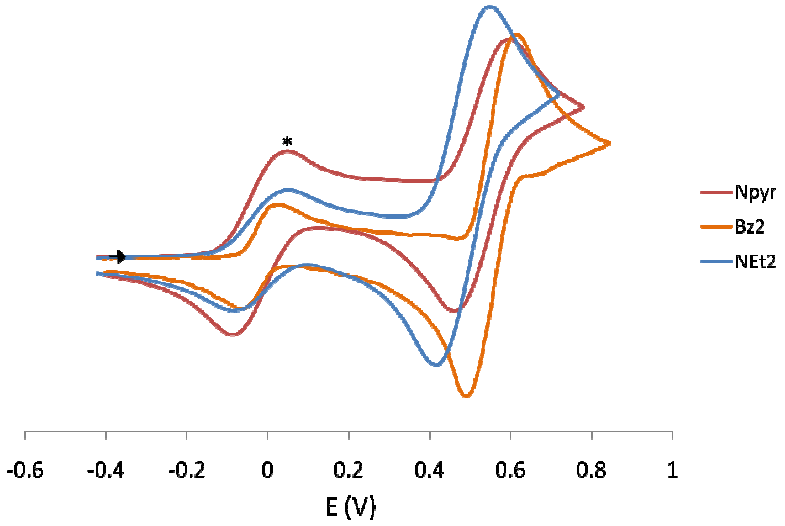

Figure 24 Cyclic voltammogram of the [Tp^{Ph2}Co(dtc)] complexes (* = decamethylferrocene).

Surprisingly, the [Tp^{Ph2}Co(dtc)] complexes are more easily oxidized than the [Tp^{Ph2}Co(β-diketonate)] complexes by on average 750 mV. This is extraordinary given that the only difference is the exchange of a β-diketonate ligand for a dithiocarbamate ligand. [Tp^{Ph2}Ni(S_2CNEt_2)] is found to be 130 mV more difficult to oxidize [$Tp^{Ph,Me}$Ni(S_2CNEt_2)] indicating that substituents on the Tp^R ligand are able to influence the redox potential more than the dithiocarbamate ligands. It may also explain the difficulty encountered in successfully synthesizing the [$Tp^{Ph,Me}$Co(dtc)] complexes noted earlier as these would be expected to more easily oxidized than their Tp^{Ph2} counterparts. complexes are oxidized in the order Et < pyr < Bz over a range of 70 mV suggesting that the substituent groups are also able to influence the oxidation potential and reflect the relative donor strength of the different dithiocarbamate ligands. The difference between the pyrrolidene and ethyl substituted dithiocarbamates is particularly interesting given that the ligands are so similar. This suggests that ring strain in the dithiocarbamate ligand may favour the dithiocarbamate resonance form over the thioureide form thereby reducing electron density at the metal (Figure 25). A decrease in the reduction potential of [Fe($S_2CNC_4H_4$)$_3$] has also been ascribed to a decrease in the thioureide resonance form.

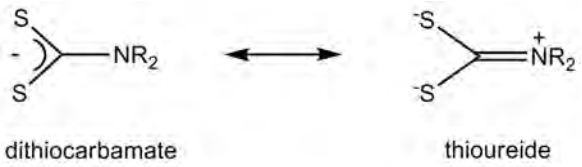

Figure 25 Dithiocarbamate and thioureide resonance forms.

The oxidation potentials of **22**-**24** suggested that oxidation could be achieved using mild oxidizing agents. We therefore attempted the oxidation of [Tp^{Ph2}Co(dtc)] with acetyl ferrocenium, [$FeCpCp^{COMe}$]BF_4.

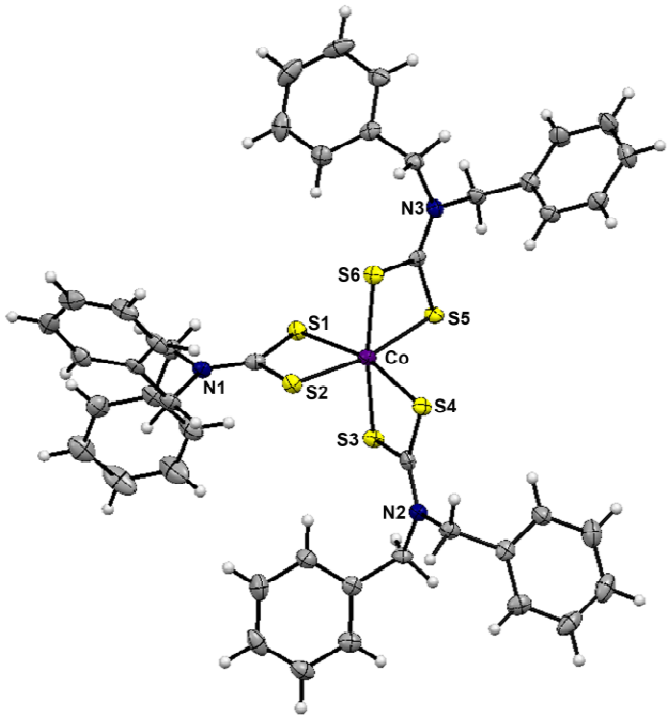

Figure 26 ORTEP diagram of [$Co(S_2CNBz_2)_3$] drawn with 50% ellipsoids.

The reaction proved to be not as simple as expected and after crystallization three products were evident. The first of these were colourless needles which proved to be Hpz^{Ph2} on the basis of IR and ^{1}H NMR spectroscopy. The other products were green and pink crystals. In the case of **23** we were able to structurally characterize one of these products. The crystals proved to be [$Co(S_2CNBz_2)_3$] with two molecules in the asymmetric unit (Figure 26). The structure has previously been reported and the bond lengths and angles found in our structure are essentially identical. The presence of free pyrazole in the reaction mixture suggests that the final product may be [$Tp^{Ph2}CoBp^{Ph2}$]BF_4. A five-coordinate mixed pyrazole

Tp^{R} and Bp^{Ph2} cobalt complex, $[HB(pz^{Me2})_2(pz^{Ph2})CoBp^{Ph2}]$ has previously been prepared by Wołoweic *et al* lending support to this hypothesis.

In an attempt to better understand the remarkably low oxidation potential of the $[Tp^{Ph2}M(dtc)]$ complexes and the instability of the $[Tp^{Ph2}M(dtc)]^{+}$ cations we have undertaken DFT calculations of the redox pairs $[Tp^{Ph2}M(dtc)]^{0/+}$. All calculations were performed using the Gaussian 03 software package with the B3LYP functional.

Table 11 Computed and X-ray crystallographically determined bond lengths for $[Tp^{Ph2}M(dtc)]$ **22**, **24** and **27**.

	22	**22**[a]	**24**	**24**[a]	**27**	**27**[a]
Bond Lengths/Å						
M-N1	2.164	2.171	2.0876	2.109	2.049	2.051
M-N3	2.080	2.077	2.1674	2.170	2.085	2.115
M-N5	2.106	2.110	2.0709	2.075	2.051	2.048
M-S1	2.4267	2.542	2.3676	2.462	2.3510	2.450
M-S2	2.3891	2.457	2.4461	2.548	2.4357	2.536
C46-S1	1.716	1.764	1.726	1.790	1.696	1.788
C46-S2	1.735	1.792	1.716	1.760	1.715	1.756
C46-N7	1.335	1.353	1.318	1.344	1.322	1.346

[a]Computed value.

The M-N and M-S bond lengths and the metal bond angles are close to those found in the structurally characterized compounds indicating that the models are accurate representations of $[Tp^{Ph2}M(dtc)]$ (Table 11). Spin unrestricted calculations on the compounds reveal that the both the Co and Ni dithiocarbamate complexes are high spin being more stable than the corresponding low spin state by between 43.7-43.5 and 87.8-78.1 $kJmol^{-1}$ for the Co and Ni series, respectively. In the case of the $[Tp^{Ph2}M(dtc)]^{+}$ cations a singlet state is found for Ni indicating that it is low spin while for Co surprisingly a triplet state is found although it must be stated that B3LYP often overestimates the energy of different spin states.

The eight principal orbitals that dithiocarbamate ligands possess in C_{2v} symmetry and which may be used in metal-ligand bonding have previously been described by Bitterwolf and are shown in Figure 27. Metal-dithiocarbamte bonding is thus described by a combination of these orbitals with suitable metal orbitals. In the present compounds the molecular orbitals concerning M-S interactions are shown in Figure 28 for **22** as a representative example.

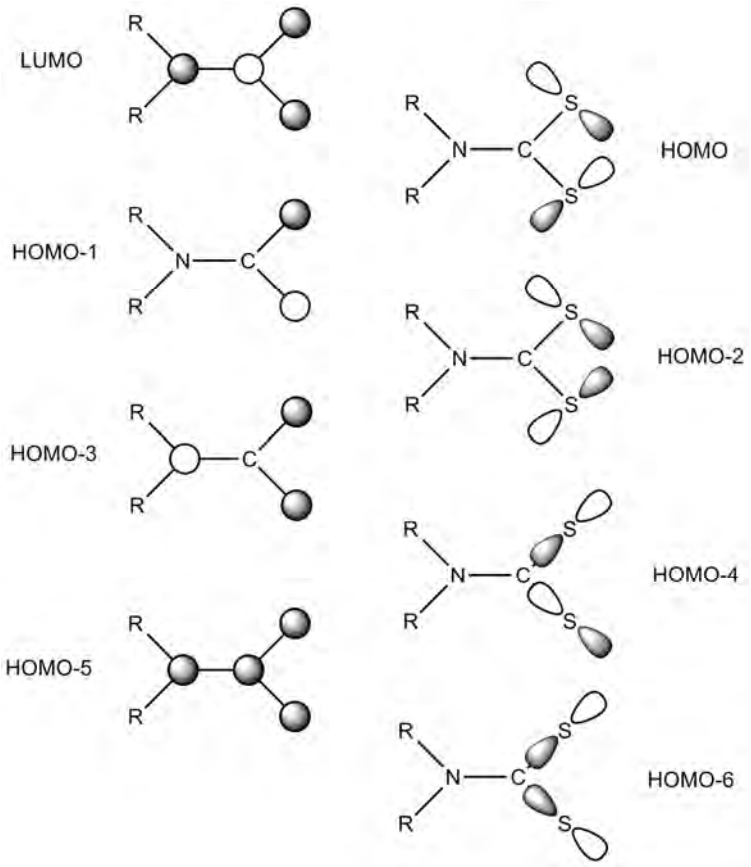

Figure 27 Simplified dithiocarbamate molecular orbitals.

The HOMO of all the complexes is found to be a strong M-S σ^* interaction involving a metal d_{x2-y2} and an asymmetric combination of the sulfur p_x and p_y orbitals (dtc HOMO in Figure 27). The strong antibonding character of the orbital results in the HOMO being destablised and therefore at high energy making oxidation comparitively easy. As expected, the benzyl substituted dithiocarbamate complexes **23** and **26** are found to be stabilised relative to the ethyl and pyrrolidene substituted dithiocarbamate compounds consistent with the higher redox potential observed in the electrochemical studies. Interestingly, no significant difference in the energy of the HOMO is observed between the ethyl and pyrrolidene substituted dithiocarbamate compounds despite

there being a 50 mV difference in redox potential. The orbital immediately below the HOMO is composed of an asymmetric combination of the sulfur p_z orbitals (dtc HOMO-1) and a metal d_{xz} orbital resulting in a M-S π^* interaction. The HOMO-2 also contains a M-S π^* antibonding interaction constructed from a symmetric combination of the sulfur p_z orbitals (dtc HOMO-3) and a metal d_{yz} orbital. A weaker but almost indentical M-S π^* antibonding interaction, differing only in the inclusion of a strong M-Tp interaction, is found in the HOMO-3 orbital.

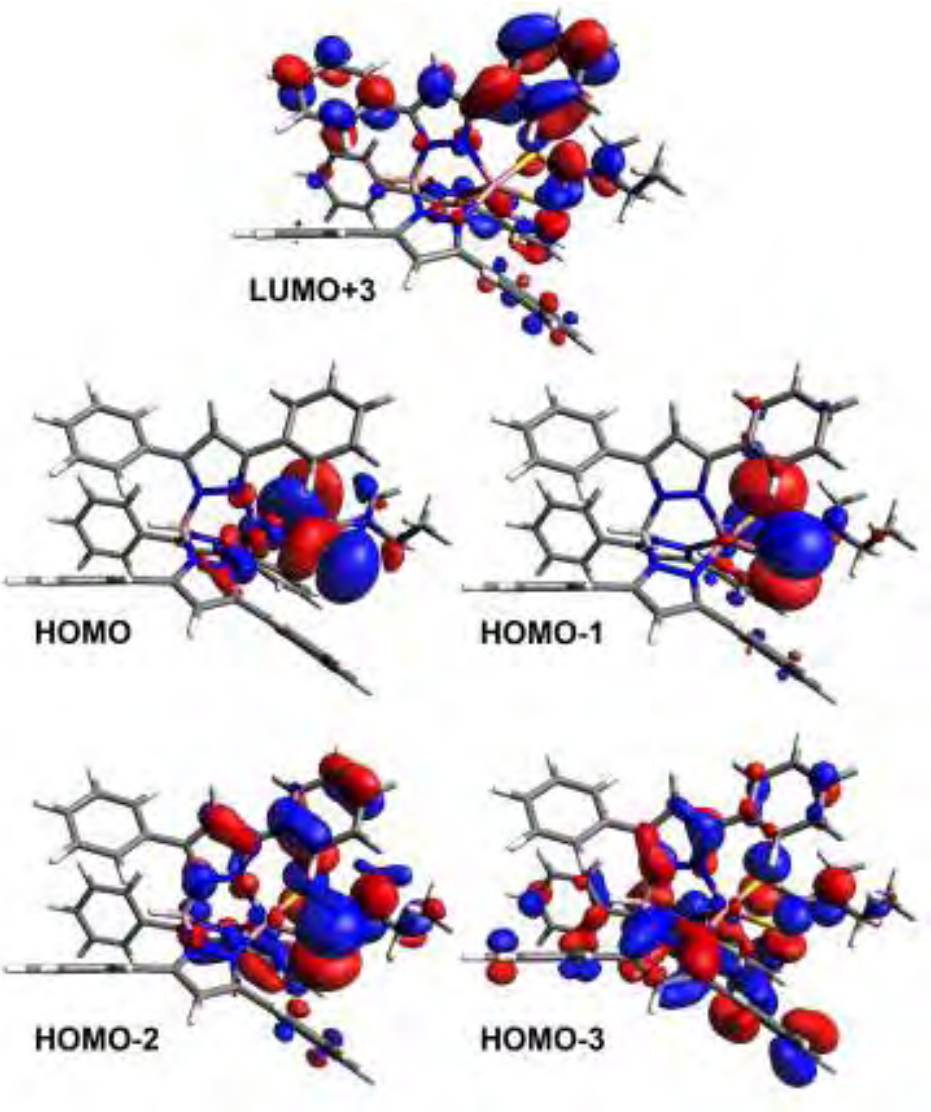

Figure 28 Selected molecular orbitals of [$Tp^{Ph2}Co(S_2CNEt_2)$] **22** showing the M-S interactions

The antibonding nature of all of the above interactions is consistent with the findings of Bitterwolf for [$M(dtc)_2$] (M = Ni, Cu, Zn) where the first three M-S ineractions were all antibonding although the highest of these is empty in the case of the 16-electron Ni

complex. In addition, the metal d_{z2} orbital is found in the HOMO-4 orbital and as with $[Ni(dtc)_2]$ is non-bonding with respect to the dithiocarbamate ligand. The dithiocarbamate LUMO is located in the LUMO+3 orbital and is essentially a ligand π^* orbital with no significant electron density on the metal. Once again a similar interaction is also observed in $[Ni(dtc)_2]$. These combined M-S interactions complete the picture of M-S bonding in the $[Tp^{Ph2}M(dtc)]$ complexes.

In contrast to the M-S dominated HOMOs of the $[Tp^{Ph2}M(dtc)]$ complexes the cations are radically different with only very weak M-S interactions in the frontier orbitals, HOMO to HOMO-8. However, as expected the LUMO is an antibonding M-S σ^* orbital and similar to the HOMO found in the neutral complexes. The only other significant M-S interaction is the LUMO+1 which is a $*\pi$ orbital containing the dithiocarbamate LUMO (dtc-LUMO Figure 27) and a metal d_{yz} orbital. The lack of M-S interactions in the cations may explain the instability of the $[Tp^{Ph2}M(dtc)]^+$ species as the dithiocarbamate ligand may be insufficiently bound resulting in loss of the ligand. This may also explain why the oxidation of $[Tp^{Ph2}Co(dtc)]$ results in the formation of $[Co(dtc)_3]$ and not the anticipated cation.

The cobalt complexes have an N_3S_2 donor set and thus might be expected to exhibit spin crossover behaviour. Samples of the complexes were sent to Prof. Keith Murray as part of a new collaboration between Walailak University and Monash University in Australia for magnetic susceptibility studies over a large temperature range. The results are shown in Figure 29. The above data reveal that sadly there is no spin crossover for these systems instead the complexes exhibit behaviour typical of high spin d^7 Co^{II} and therefore three unpaired electrons.

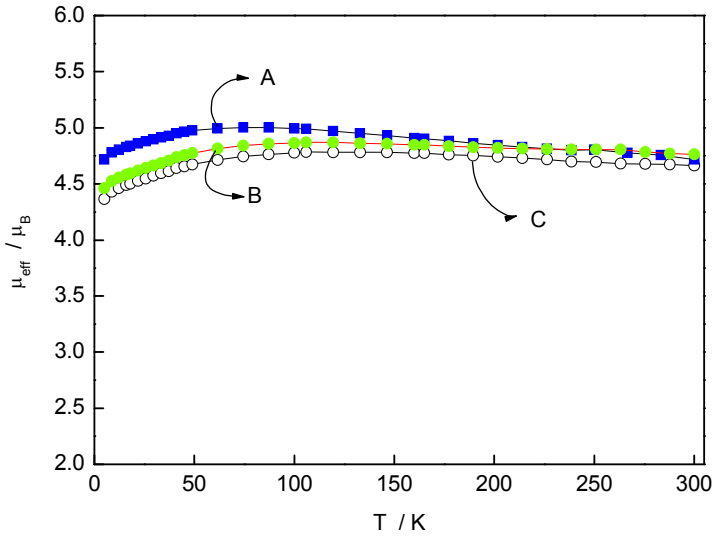

Figure 29 SQUID magnetic susceptibility data for a) [$Tp^{Ph2}Co(S_2CNEt_2)$], b) [$Tp^{Ph2}Co(S_2Cpyr)$] and c) [$Tp^{Ph2}Co(S_2CNBz_2)$].

The reaction of [$Tp^{Ph2}MBr$] with NaS_2CNpy_2 yields brown (Co) or dark green (Ni) solids [$Tp^{Ph2}M(S_2CNpy_2)$] (M = Co **29**, Ni **30**) in good yields. IR spectroscopic studies show BH stretches consistent with κ^3-coordinated Tp^{Ph2} ligands. A further set of bands are found at *ca*. 1475 and 1010 cm^{-1} for the C=Npy_2 and C=S of the dtc ligand. Lastly, a band at *ca*. 1635 cm^{-1} is assigned to C=N band of the pyridyl rings.

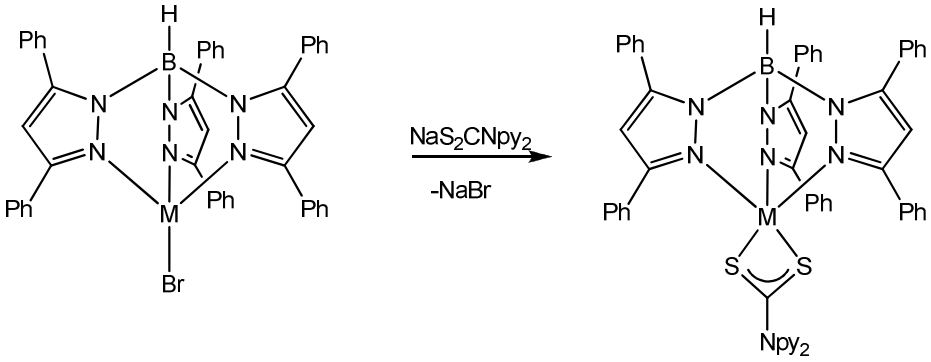

UV-Vis spectroscopy shows that the spectra are significantly different from those of the dtc complexes suggesting that the ligand may be *N*,*N*-bound rather than *S*,*S*-bound. This is particularly true in the case of the nickel complex **30** (see Figure 30).

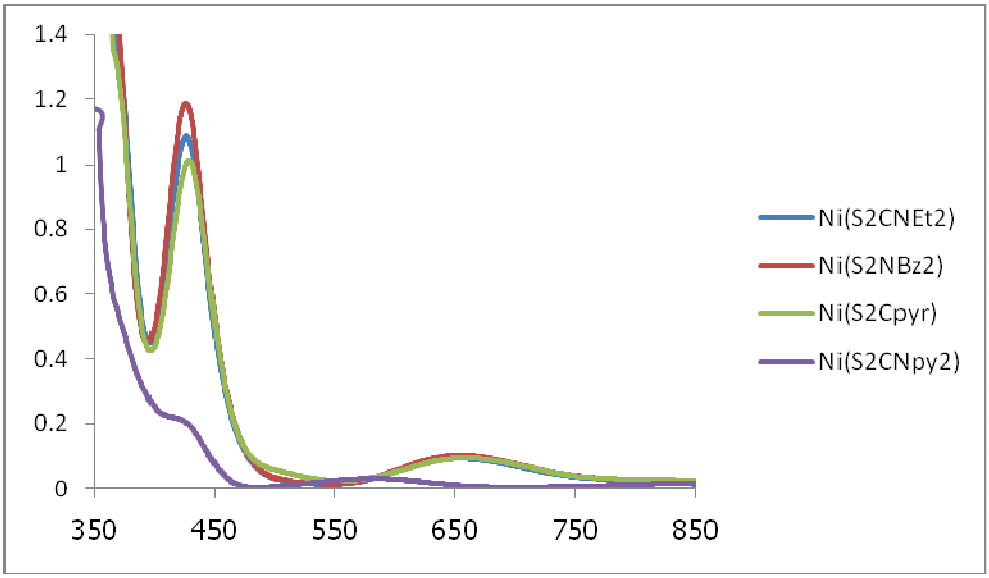

Figure 30 UV-Vis spectra of Tp^{Ph2}Ni(dtc) **26**-**28** and **30** complexes in CH_2Cl_2.

Attempts were made to grow crystals of **29** and **30** and in the case of **30** were successful. The crystals however proved to be [Tp^{Ph2}Ni(dpa)]Br and not [Tp^{Ph2}Ni(S_2CNpy_2)] suggesting that the product has undergone decomposition. Crystallographic data are shown in Table 12 with the molecular structure shown in Figure 31. The nickel centre is five coordinate with a κ^3 coordinated Tp^{Ph2} ligand with a coordination geometry best described as square pyramidal. The Ni-N bond lengths are typical of high spin five coordinate Ni^{II}.

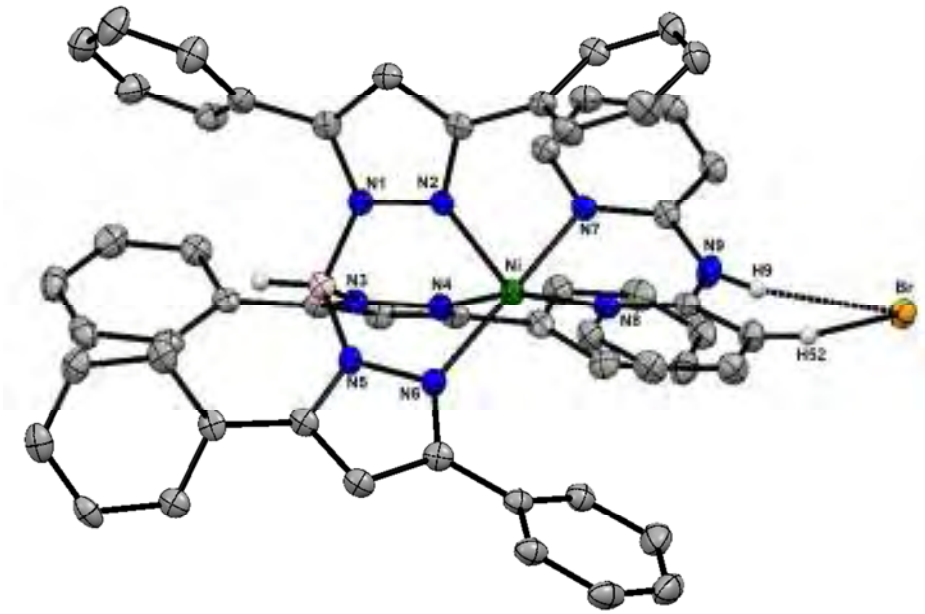

Figure 31 ORTEP diagram of [Tp^{Ph2}Ni(dpa)]Br **31** drawn with 50% ellipsoids showing the H-bonding interactions.

Table 12 Selected bond lengths and angles for **31** (Å, °).

Bond lengths (Å)		Bond angles (°)	
Ni-N2	2.006 (2)	N2-Ni-N4	97.52 (9)
Ni-N4	2.072 (2)	N4-Ni-N6	84.44 (9)
Ni-N6	2.078 (2)	N2-Ni-N6	89.55 (8)
Ni-N7	2.032 (2)	N7-Ni-N8	88.45 (9)
Ni-N8	2.024 (2)	τ	0.23
N-H···Br	2.406 (2)	N-H···Br	165.20 (9)
C-H···Br	2.924 (2)	C-H···Br	140.32 (9)

The most significant feature of the structure is a strong H-bond between the amino proton and the bromide anion. A further weaker interaction is also observed between one of the aromatic protons on the pyridyl ring (H52) and the bromide anion. As with many of the structures in this report, the 3-phenyl rings are all rotated to accommodate the dipyridylamine ligand.

Synthesis of [Tp^{Ph2}M(dtc)] Dimers and Trimers

The successful synthesis of the [Tp^{Ph2}M(dtc)] complexes and their interesting electrochemical behaviour led us to attempt the preparation of a number of dimers and trimers. This involved the *in situ* preparation of the dithiocarbamate ligand by reacting piperazine with CS_2. Addition of a suitable base then couples the dithiocarbamate ligand to the [Tp^{Ph2}MBr] unit yielding dimers [Tp^{Ph2}M(μ-$S_2CN(CH_2)_4NCS_2$)MTp^{Ph2}] (M = Co **32**, Ni **33**). At this time the dimers have only been characterized by IR spectroscopy but are consistent with the proposed formulation.

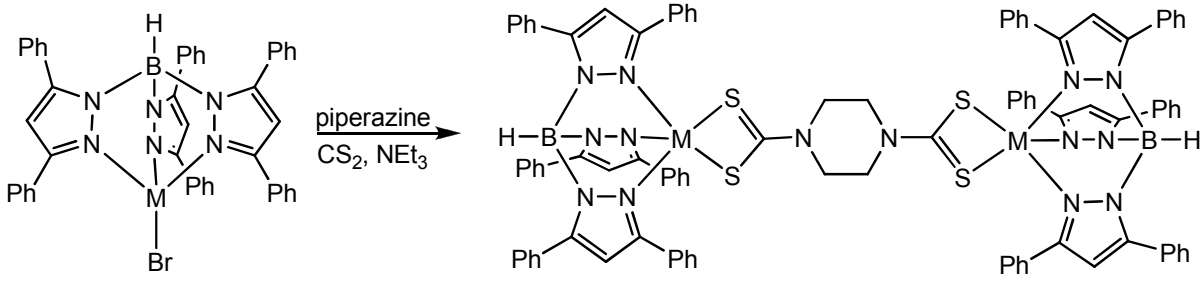

Following the same synthetic procedure we have also been able to trimers using triazacyclononane (tacn). Results are still at a preliminary stage but initial characterization on some of the complexes suggests that the trimers $[Tp^{Ph2}M(\mu_3\text{-}S_2CN(CH_2)_2N(CS_2)\text{-}(CH_2)_2NCS_2)(MTp^{Ph2})_2]$ have been prepared.

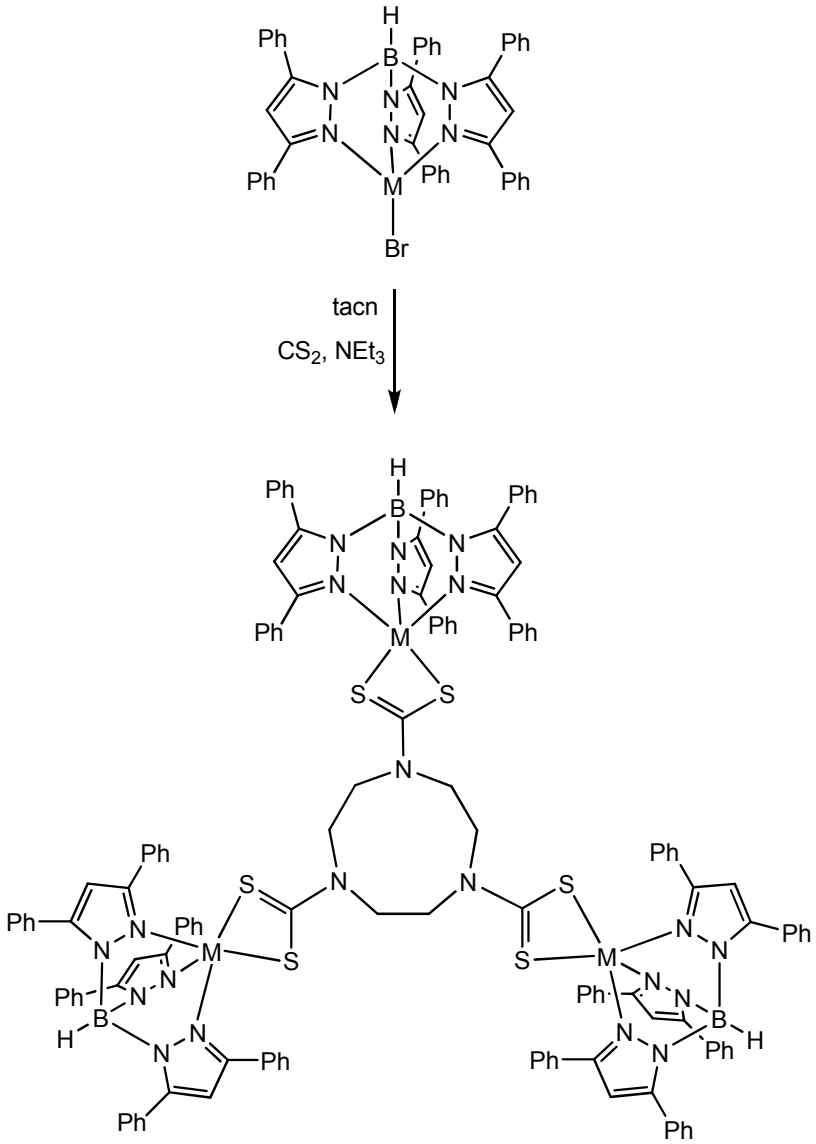

Synthesis of $[Tp^{Ph2}M(\mu\text{-TPA})]_n$

One of the aims of this project is to prepare multinuclear complexes using appropriate linking ligands. Thus, the reaction of two equivalents of $[Tp^{Ph2}M(OAc)]$ (M = Co, Ni) with H_2TPA in the presence of NaOMe gives the complexes $[Tp^{Ph2}M(\mu\text{-TPA})]_n$ (M = Co **32**; Ni **33**) as pastel blue and green solids respectively.

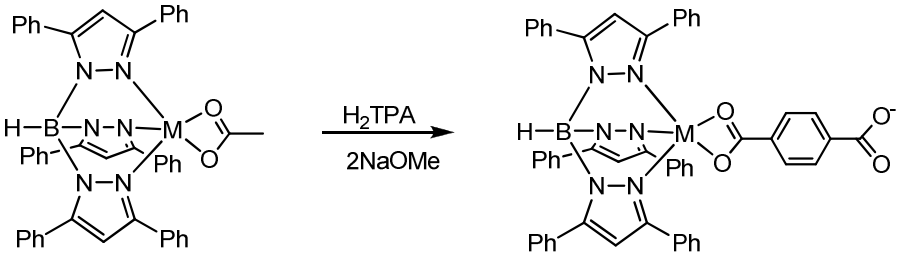

IR spectroscopy of the complexes shows a B-H stretch at 2618 and 2651 cm^{-1} for **32** and **33**, respectively and indicative of κ^3-coordinated Tp^{Ph2} ligands. The complexes are very poorly soluble in most organic solvents suggesting that the compounds are polymers rather than dimers. Further attempts to prepare crystals suitable for X-ray crystallographic studies by the use of H-tubes yielded purple crystals which sadly proved to be $[Tp^{Ph2}Co(OAc)(Hpz^{Ph2})]$.

Synthesis of $[Tp^{R}Co(\mu\text{-}L)CoTp^{R}]$

Dihydroxybenzoquinonate and chloranate have been shown to be useful ligands in the preparation of bridged dimers. The ligands are redox-active and are known to stabilize valence tautomers, in the case of $[TPyACo(\mu\text{-}L)CoTPyA]^{3+}$ {TPyA = tris(pyridylmethyl)amine, L = dihydroxybenzoquinonate (DHBQ) and chloranate (CA)}. We therefore, attempted the synthesis of dimers with tris(pyrazolyl)borate ligands as shown below.

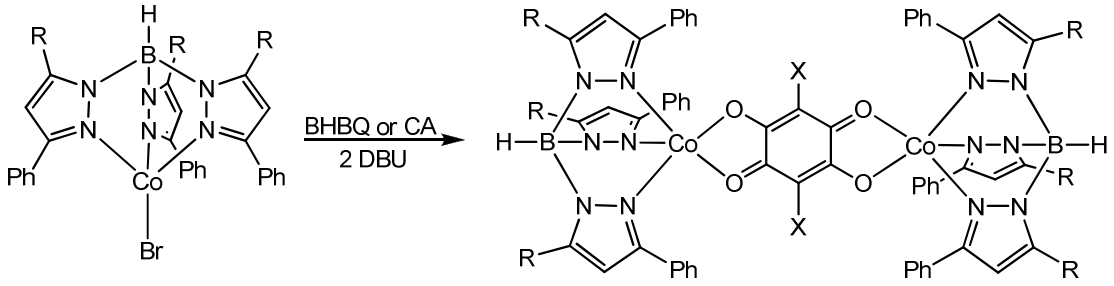

Table 13 Physical and IR spectroscopic data for **34**-**37**.

Complex	Colour	Yield (%)	IR ν_{BH} (cm^{-1})	IR ν_{CO} (cm^{-1})
34	Red-brown	52	2619	1531
35	Brown	47	2619	1518
36	Brown	78	2513	1519
37	Brown	55	2551	1519

The reaction of [$Tp^{R}CoBr$] (R = Ph,Me; Ph_2) with DHBQ or CA in the presence of the weak base DBU yields [$Tp^{R}Co(\mu\text{-}L)CoTp^{R}$] (R = Ph_2; L = $DHBQ^{2-}$ **34**, CA^{2-} **35**; R = Ph,Me; L = $DHBQ^{2-}$ **36**, CA^{2-} **37**) as brown solids. The solids are very poorly soluble in most organic solvents showing very slight solubility only in DMF. IR spectroscopy reveals B-H stretches between 2619 and 2513 cm^{-1} indicative of κ^3 coordinated Tp^{R} ligands (Table 13). The B-H stretches for **36** and **37** are *ca*. 100 cm^{-1} lower than that of **34** and **35** consistent with the more electron rich $Tp^{Ph,Me}$ ligand. The complexes also show a strong CO stretch consistent with bridging dianionic BHBQ or CA ligands.

X-ray crystallographic studies of [$Tp^{Ph,Me}Co(\mu\text{-}CA)CoTp^{Ph,Me}$] have been undertaken and reveal two independent molecules in the same crystal lattice. Interestingly, the two molecules have different coordination environments with five and six coordinate cobalt centres, the latter having an additional water molecule bound to the cobalt centre (see Figures 24 and 25).

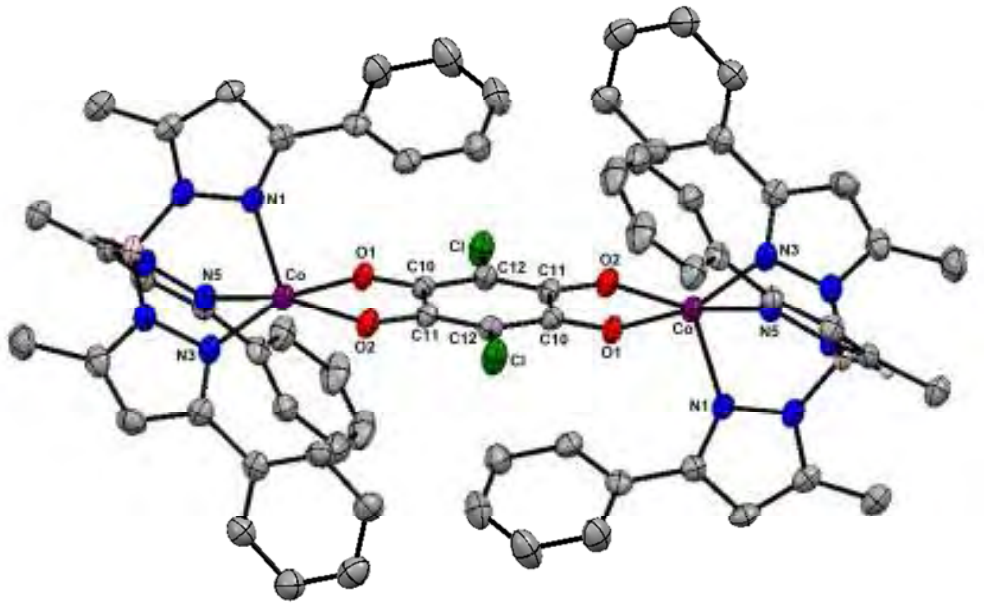

Figure 24 The molecular structure of [$Tp^{Ph,Me}Co(\mu\text{-}CA)CoTp^{Ph,Me}$] **37**, molecule 1. Hydrogen atoms are omitted for clarity.

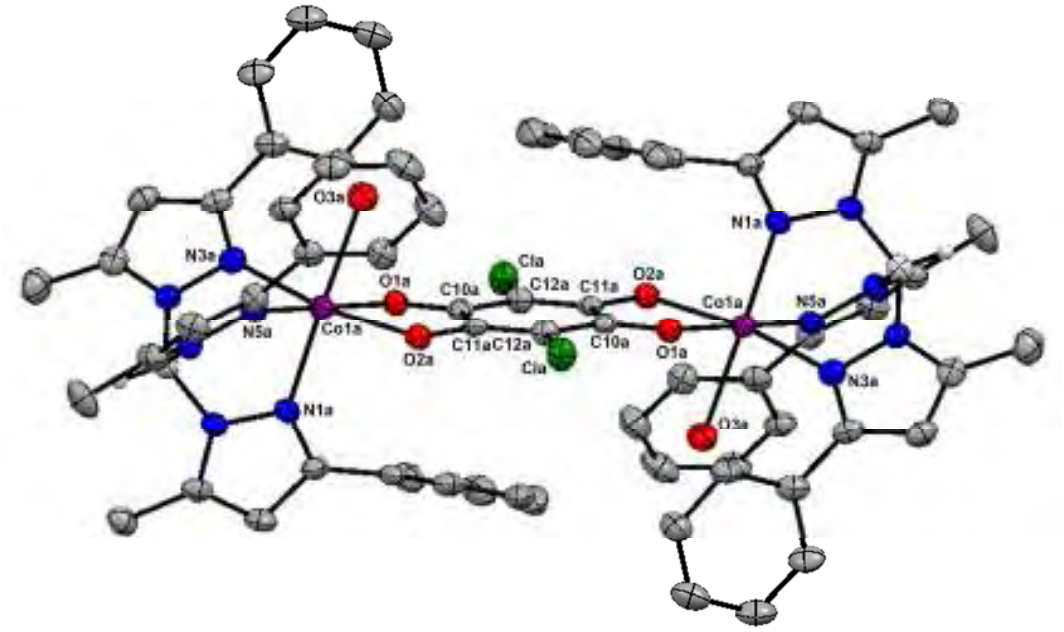

Figure 25 The molecular structure of [$Tp^{Ph,Me}Co(H_2O)(\mu\text{-}CA)(H_2O)CoTp^{Ph,Me}$] **37**, molecule 2. Hydrogen atoms are omitted for clarity.

The geometry for the five coordinate cobalt centre is perfectly square pyramidal (τ = 0) while that of the second cobalt is *pseudo*-octahedral. This is unexpected as large Tp^R ligands are rarely associated with six coordinate metal centres.

Table 14 Selected bond lengths and angles for **37**.

Bond lengths (Å)		**Bond angles (°)**	
Molecule 1			
Co-N1	2.078 (4)	N1-Co-N3	93.9 (1)
Co-N3	2.117 (3)	N1-Co-N5	90.5 (1)
Co-N5	2.061 (3)	N3-Co-N5	83.8 (1)
Co-O1	2.074 (2)	O1-Co-O2	78.7 (1)
Co-O2	2.033 (3)	τ	0.00
Molecule 2			
Co-N1	2.118 (3)	N1-Co-N3	89.4 (1)
Co-N3	2.116 (3)	N1-Co-N5	92.6 (1)
Co-N5	2.164 (4)	N3-Co-N5	86.9 (1)

Co-O1	2.106 (3)	O1-Co-O2	76.9 (1)
Co-O2	2.072 (2)	O1-Co-O3	83.6 (1)
Co-O3	2.225 (3)	N3-Co-O3	88.6 (1)

The Co-N bond lengths are typical of tris(pyrazolyl)borate ligands bound to Co^{II} with the bonds slightly longer in the case of molecule 2 due to the more crowded metal centre (Table 14). The Co-O bond lengths are consistent with the ligand acting as a dianionic semiquinone indicating that no oxidation or reduction of the ligand has occurred, in agreement with the above IR spectroscopic data. The bridging chloranate dianion is planar in both dimers suggesting delocalization of the charge over the ligand framework. It is also noteworthy that in molecule 2 the ligand binds in a slightly angular fashion once again due to steric interactions.

The corresponding nickel complexes have also been prepared by the reaction of $[Tp^{Ph2}NiBr]$ with DHBQ or CA in the presence of the weak base DBU to give $[Tp^{Ph2}Ni(\mu\text{-}L)NiTp^{Ph2}]$ (R = Ph_2; L = $DHBQ^{2-}$ **38**, CA^{2-} **39**) as green-brown solids. As with the cobalt analogues they are extremely insoluble in common organic solvents but IR spectroscopy is consistent with κ^3 coordinated Tp^{Ph2} ligands. Solid state UV-visible spectra of all the complexes are shown in Figure 26.

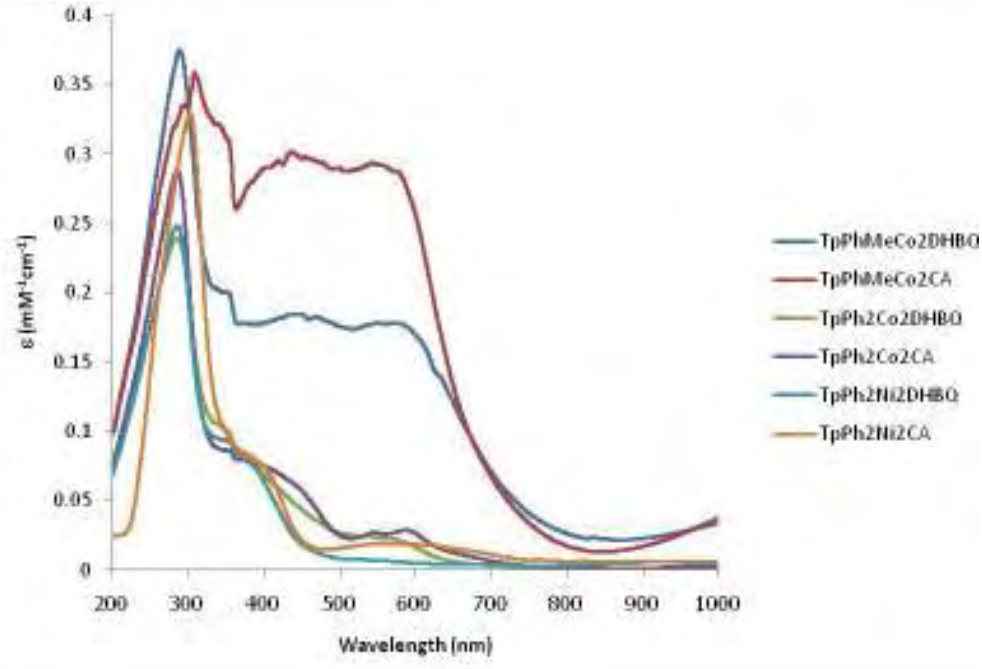

Figure 26 UV-Vis spectra of $[Tp^{R}M(\mu\text{-}L)MTp^{R}]$ **34**-**39** in CH_2Cl_2.

The spectra show strong absorption in the visible and UV region particularly in the case of the $Tp^{Ph,Me}$ complexes. Assignments for the bands are difficult to make but based on the other complexes prepared in the report it would seem likely that many of the stronger are due to the DHBQ and CA ligands.

The insolubility of **34**-**39** led us attempt the synthesis of related compounds with a smaller more soluble Tp ligand namely, Tp*. Thus, the reaction of [Tp*MBr] (M = Co, Ni) with DHBQ followed by addition of NEt_3 appears to give [Tp*M(μ-DHBQ)MTp*] (M = Co **40**, Ni **41**) based on preliminary IR spectroscopic results. Sadly, the compounds are still poorly soluble in organic solvents. It therefore appears as though combinations of Tp^R and anilate ligands always yield insoluble products.

4. Project Outcomes

4.1. Publications

Three international papers have been published in *Acta Crystallographica Section E* and *Transition Metal Chemistry* concerning the X-ray crystal structures of $[Co(phen)_3][BF_4]_2$.MeCN and $[Tp^{Ph2}NiBr]$ and the chemistry of $[Tp^RNi(bpym)]^+$.

1. D. J. Harding, P. Harding and H. Adams, Tris(phenanthroline-κ^2*N,N*′)cobalt(II) tetrafluoridoborate acetonitrile solvate, *Acta Cryst. Section E*, 2008, **E64**, m1538.
2. D. J. Harding, P. Harding and H. Adams, [Tris(3,5-diphenylpyrazolyl)hydroborato]-nickel(II) bromide *Acta Cryst. Section E*, 2009, **E65**, m773.
3. D. J. Harding, P. Harding, J. Kivnang and H. Adams, Cationic Tris(pyrazolyl)borate Bipyrimidine Complexes, *Trans. Metal Chem*., 2010, doi:10.1007/s11243-010-9358-x.
4. D. J. Harding, P. Harding, S. Dokmaisrijan and H. Adams Redox-Active Nickel and Cobalt Tris(pyrazolyl)borate Dithiocarbamate Complexes: Air-Stable Co(II) Dithiocarbamates, in preparation.

A further publication on the nickel complexes $[Tp^{Ph2}Ni(\beta\text{-dkt})]$ will be prepared shortly. Further development of the chemistry of $[Tp^RM(\mu\text{-L})MTp^R]$ should also provide another publication.

4.2. Presentations

Three oral and two poster presentations have been made upon this work.

1. D. J. Harding, Cobalt and nickel tris(pyrazolyl)borate complexes: a lesson in research.
2. D. J. Harding, Redox-active cobalt tris(pyrazolyl)borate and β-diketonate complexes.
3. D. J. Harding, Cationic Tris(pyrazolyl)borate Bipyrimidine Complexes: Potential Molecular Building Blocks.
4. D. J. Harding and P. Harding, Synthesis and Electrochemical Studies of Cobalt and Nickel Cyanometallates.
5. D. J. Harding and P. Harding, Cobalt and Nickel Tris(pyrazolyl)borate Dithiocarbamates: Stabilization of M^{III}.

4.3. Collaborations with International Institutes and Awards

As a result of this project we have developed two new collaborations:

1. Professor Mike Shaw at Southern Illinois University Edwardsville, USA is working with us on developing spectroelectrochemistry here in Thailand.
2. Professor Keith Murray at Monash University, Australia has collaborated with us providing valuable access to a SQUID magnetometer for more in depth magnetic studies.

A further success to come from this research has been the '*Best Research Scholar Award*' awarded by Walailak University to Associate Professor Dr David J. Harding.

Appendix One

International Publication

Acta Crystallographica Section E
Structure Reports Online
ISSN 1600-5368
Editors: **W. T. A. Harrison, J. Simpson and M. Weil**

Tris(phenanthroline-κ^2N,N')cobalt(II) tetrafluoridoborate acetonitrile solvate

David J. Harding, Phimphaka Harding and Harry Adams

Acta Cryst. (2008). E**64**, m1538

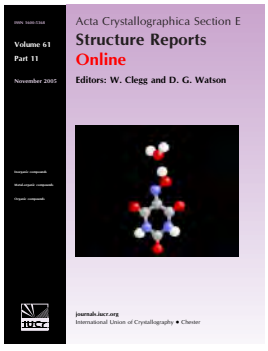

Acta Crystallographica Section E
Structure Reports Online
ISSN 1600-5368

Tris(phenanthroline-κ^2N,N')cobalt(II) tetrafluoridoborate acetonitrile solvate

David J. Harding,[a]* Phimphaka Harding[a] and Harry Adams[b]

[a]Molecular Technology Unit Cell, Department of Chemistry, Walailak University, Thasala, Nakorn Si Thammarat 80161, Thailand, and [b]Department of Chemistry, Faculty of Science, University of Sheffield, Brook Hill, Sheffield S3 7HF, England
Correspondence e-mail: hdavid@wu.ac.th

Received 29 October 2008; accepted 7 November 2008

Key indicators: single-crystal X-ray study; T = 150 K; mean σ(C–C) = 0.007 Å; R factor = 0.072; wR factor = 0.213; data-to-parameter ratio = 12.5.

In the crystal structure of the title compound, $[Co(C_{12}H_8N_2)_3](BF_4)_2{\cdot}CH_3CN$, the molecular packing involves dimers of distorted octahedrally coordinated cations which are held together by one π–π [centroid–centroid = 3.542 (4) Å] and two C—H$\cdots\pi$ interactions [2.573 (4) Å] resulting in a P4AE (Parallel Fourfold Aryl Embrace) motif. The anions are found in aryl boxes formed from the phenanthroline ligands.

Related literature

For other $[Co(phen)_3]^{2+}$ complexes, see: Boys *et al.* (1984); Geraghty *et al.* (1999); Russell *et al.* (2001); Tershansy *et al.* (2005).

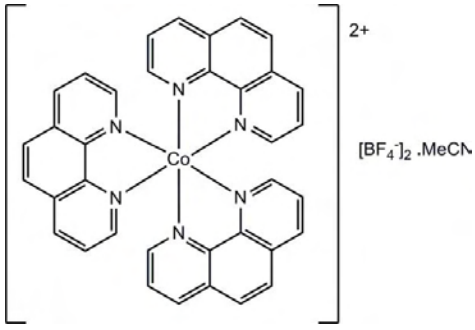

Experimental

Crystal data

$[Co(C_{12}H_8N_2)_3](BF_4)_2{\cdot}C_2H_3N$
M_r = 814.22
Monoclinic, $P2_1/n$
a = 18.0443 (2) Å
b = 9.36230 (10) Å
c = 22.0702 (2) Å
β = 107.3610 (10)°
V = 3558.60 (6) Å^3
Z = 4
Mo $K\alpha$ radiation
μ = 0.56 mm^{-1}
T = 150 (2) K
0.32 × 0.28 × 0.12 mm

Data collection

Bruker SMART CCD area-detector diffractometer
Absorption correction: multi-scan (*SADABS*; Bruker, 1997)
T_{min} = 0.840, T_{max} = 0.935
56541 measured reflections
6276 independent reflections
5268 reflections with $I > 2\sigma(I)$
R_{int} = 0.046

Refinement

$R[F^2 > 2\sigma(F^2)]$ = 0.072
$wR(F^2)$ = 0.213
S = 1.03
6276 reflections
501 parameters
H-atom parameters constrained
$\Delta\rho_{max}$ = 2.96 e Å^{-3}
$\Delta\rho_{min}$ = −0.94 e Å^{-3}

Table 1
Selected geometric parameters (Å, °).

Co1—N4	2.123 (4)	Co1—N1	2.131 (3)
Co1—N2	2.129 (4)	Co1—N5	2.133 (4)
Co1—N6	2.129 (4)	Co1—N3	2.142 (4)

Data collection: *SMART* (Bruker, 1997); cell refinement: *SAINT* (Bruker, 1997); data reduction: *SAINT*; program(s) used to solve structure: *SHELXS97* (Sheldrick, 2008); program(s) used to refine structure: *SHELXL97* (Sheldrick, 2008); molecular graphics: *SHELXTL* (Sheldrick, 2008); software used to prepare material for publication: *SHELXTL*.

The authors gratefully acknowledge the Thailand Research fund for supporting this work (grant No. RMU5080029).

Supplementary data and figures for this paper are available from the IUCr electronic archives (Reference: AT2665).

References

Boys, D., Escobar, C. & Wittke, O. (1984). *Acta Cryst.* C**40**, 1359–1362.
Bruker (1997). *SMART*, *SAINT* and *SADABS*. Bruker AXS Inc., Madison, Wisconsin, USA.
Geraghty, M., McCann, M., Devereux, M. & McKee, V. (1999). *Inorg. Chim. Acta*, **293**, 160–166.
Russell, V., Scudder, M. & Dance, I. (2001). *J. Chem. Soc. Dalton Trans.* pp. 789–799.
Sheldrick, G. M. (2008). *Acta Cryst.* A**64**, 112–122.
Tershansy, M. A., Goforth, A. M., Smith, M. D., Peterson, L. R. Jr & zur Loye, H.-C. (2005). *Acta Cryst.* E**61**, m1680–m1681.

supplementary materials

Acta Cryst. (2008). E**64**, m1538 [**doi:10.1107/S1600536808036611**]

Tris(phenanthroline-κ^2N,N')cobalt(II) tetrafluoridoborate acetonitrile solvate

D. J. Harding, P. Harding and H. Adams

Comment

The reaction of anhydrous cobalt(II) chloride with $AgBF_4$ in the presence of phenanthroline yields the coordination compound tris(phenanthroline)cobalt(II) tetrafluoroborate (**1**), $[Co(phen)_3][BF_4]_2.MeCN$. Crystals were grown by allowing ether to diffuse into a concentrated solution of the complex in MeCN. The title complex crystallizes in the space group $P2_1/n$ in contrast to the related compound $[Co(phen)_3][BF_4]_2.H_2O.EtOH$ which crystallizes in $P\bar{1}$ (Russell *et al.*, 2001). The structure of (**1**) is shown in Fig. 1 while important bond lengths and angles are given in Table 1. The cobalt centre is octahedrally coordinated with Co—N bond lengths and N—Co—N angles for the chelating phenanthroline ligands essentially identical to those reported for other $[Co(phen)_3]^{2+}$ complexes (Boys *et al.*, 1984; Geraghty *et al.*, 1999; Russell *et al.*, 2001; Tershansy *et al.*, 2005).

The crystal lattice of (**1**) contains dimers of $[Co(phen)_3]^{2+}$ cations in which there is a P4AE (Parallel Fourfold Aryl Embrace) motif involving one π–π [centroid···centroid 3.542 (4) Å] and two C—H···π interactions between the phenanthroline ligands as shown in Fig. 2 (Cg1 is the centroid of the ring C31–C35; Russell *et al.*, 2001). The offset between the central aryl ring of the two phenanthroline ligands is 6.443 (3) Å and indicative of overlap of a single aryl ring (Russell *et al.*, 2001). The dimers found in (**1**) are isolated from each other unlike in the structure of $[Co(phen)_3][BF_4]_2.H_2O.EtOH$ where a further P4AE interaction results in formation of a zig-zag chain. A further difference is that the anions are not found in hydrophilic channels between chains of the cations but rather in aryl boxes formed from six phenanthroline ligands. This difference is presumeably the result of a lack of suitable hydrogen bonding solvent in the current structure.

Experimental

Cobalt(II) chloride (130 mg, 1 mmol) was suspended in MeCN (20 ml). $AgBF_4$ (389 mg, 2 mmol) was then added resulting in precipitation of a white solid. The solution was filtered through celite to remove AgCl and phenanthroline (541 mg, 3 mmol) was added giving an orange solution. The volume of the solution was reduced in vacuo to *ca.* 10 ml and then layered with Et_2O (60 ml). After two days yellow crystals formed (602 mg, 74%) Analysis calculated for $C_{38}H_{27}N_7B_2F_8Co$: C 56.06, H 3.34, N 12.04%; found: C 56.27, H 3.40, N 12.41%. ESI^+ MS: (*m/z*) Anal. Calc. 814.22; found: $[M]^+$ 814.19.

Refinement

Hydrogen atoms were placed geometrically and refined with a riding model and with U_{iso} constrained to be 1.2 (aromatic CH) or 1.5 (Me) times U_{eq} of the carrier atom.

Figures

Fig. 1. The molecular structure of (**1**) showing the atom-labelling scheme. Displacement ellipsoids are drawn at the 50% probability level.

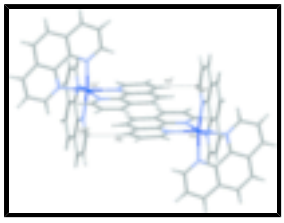

Fig. 2. The molecular packing in (**1**) showing the C—H···π and π–π interactions which make up the P4AE structural motif. Only selected H atoms are labelled for clarity. [Symmetry codes:(i) -*x*, -*y*, 1 - *z*].

Tris(phenanthroline-κ^{2}N,N')cobalt(II) tetrafluoridoborate acetonitrile solvate

Crystal data

$[Co(C_{12}H_8N_2)_3](BF_4)_2·C_2H_3N$	F_{000} = 1652
M_r = 814.22	D_x = 1.520 Mg m^{-3}
Monoclinic, $P2_1/n$	Mo $K\alpha$ radiation λ = 0.71073 Å
Hall symbol: -P 2yn	Cell parameters from 9965 reflections
a = 18.0443 (2) Å	θ = 2.4–24.8º
b = 9.36230 (10) Å	μ = 0.57 mm^{-1}
c = 22.0702 (2) Å	T = 150 (2) K
β = 107.3610 (10)º	Plate, yellow
V = 3558.60 (6) Å^3	0.32 × 0.28 × 0.12 mm
Z = 4	

Data collection

Bruker SMART CCD area-detector diffractometer	6276 independent reflections
Radiation source: fine-focus sealed tube	5268 reflections with $I > 2\sigma(I)$
Monochromator: graphite	R_{int} = 0.046
Detector resolution: 100 pixels mm^{-1}	θ_{max} = 25.0º
T = 150(2) K	θ_{min} = 1.3º
φ and ω scans	h = −21→21
Absorption correction: multi-scan (SADABS; Bruker, 1997)	k = −11→11
T_{min} = 0.840, T_{max} = 0.935	l = −26→26
56541 measured reflections	

Refinement

Refinement on F^2	Secondary atom site location: difference Fourier map
Least-squares matrix: full	Hydrogen site location: inferred from neighbouring sites
$R[F^2 > 2\sigma(F^2)] = 0.072$	H-atom parameters constrained
$wR(F^2) = 0.213$	$w = 1/[\sigma^2(F_o^2) + (0.1194P)^2 + 14.1582P]$ where $P = (F_o^2 + 2F_c^2)/3$
$S = 1.03$	$(\Delta/\sigma)_{max} < 0.001$
6276 reflections	$\Delta\rho_{max} = 2.96$ e Å^{-3}
501 parameters	$\Delta\rho_{min} = -0.94$ e Å^{-3}
Primary atom site location: structure-invariant direct methods	Extinction correction: none

Special details

Geometry. All e.s.d.'s (except the e.s.d. in the dihedral angle between two l.s. planes) are estimated using the full covariance matrix. The cell e.s.d.'s are taken into account individually in the estimation of e.s.d.'s in distances, angles and torsion angles; correlations between e.s.d.'s in cell parameters are only used when they are defined by crystal symmetry. An approximate (isotropic) treatment of cell e.s.d.'s is used for estimating e.s.d.'s involving l.s. planes.

Refinement. Refinement of F^2 against ALL reflections. The weighted *R*-factor *wR* and goodness of fit *S* are based on F^2, conventional *R*-factors *R* are based on *F*, with *F* set to zero for negative F^2. The threshold expression of $F^2 > \sigma(F^2)$ is used only for calculating *R*-factors(gt) *etc*. and is not relevant to the choice of reflections for refinement. *R*-factors based on F^2 are statistically about twice as large as those based on *F*, and *R*-factors based on ALL data will be even larger.

Fractional atomic coordinates and isotropic or equivalent isotropic displacement parameters (Å^2)

	x	*y*	*z*	U_{iso}*/U_{eq}
Co1	0.22845 (3)	0.04969 (6)	0.47231 (3)	0.0198 (2)
N1	0.1221 (2)	−0.0494 (4)	0.47236 (17)	0.0223 (8)
N2	0.1549 (2)	0.1052 (4)	0.38050 (17)	0.0233 (8)
N3	0.2689 (2)	−0.1362 (4)	0.43523 (17)	0.0235 (8)
N4	0.3331 (2)	0.1259 (4)	0.45860 (17)	0.0232 (8)

N5	0.2832 (2)	0.0047 (4)	0.57022 (17)	0.0235 (8)
N6	0.20568 (19)	0.2398 (4)	0.51664 (17)	0.0216 (8)
C1	0.1066 (3)	−0.1261 (5)	0.5179 (2)	0.0252 (9)
H1	0.1448	−0.1343	0.5568	0.030*
C2	0.0356 (3)	−0.1949 (5)	0.5099 (2)	0.0289 (10)
H2	0.0267	−0.2474	0.5428	0.035*
C3	−0.0204 (3)	−0.1836 (5)	0.4530 (2)	0.0313 (11)
H3	−0.0675	−0.2307	0.4465	0.038*
C4	−0.0075 (2)	−0.1013 (5)	0.4041 (2)	0.0278 (10)
C5	−0.0641 (3)	−0.0811 (6)	0.3436 (2)	0.0339 (11)
H5	−0.1121	−0.1258	0.3351	0.041*
C6	−0.0489 (3)	0.0016 (6)	0.2988 (2)	0.0365 (12)
H6	−0.0872	0.0154	0.2604	0.044*
C7	0.0253 (3)	0.0685 (5)	0.3093 (2)	0.0289 (10)
C8	0.0446 (3)	0.1556 (6)	0.2640 (2)	0.0348 (11)
H8	0.0081	0.1739	0.2250	0.042*
C9	0.1171 (3)	0.2124 (6)	0.2777 (2)	0.0349 (11)
H9	0.1303	0.2701	0.2482	0.042*
C10	0.1712 (3)	0.1839 (5)	0.3359 (2)	0.0290 (10)
H10	0.2210	0.2213	0.3440	0.035*
C11	0.0829 (2)	0.0478 (5)	0.3671 (2)	0.0237 (9)
C12	0.0656 (2)	−0.0368 (5)	0.4164 (2)	0.0234 (9)
C13	0.2350 (3)	−0.2627 (5)	0.4210 (2)	0.0312 (10)
H13	0.1877	−0.2785	0.4288	0.037*
C14	0.2679 (3)	−0.3736 (5)	0.3948 (2)	0.0379 (12)
H14	0.2419	−0.4600	0.3843	0.046*
C15	0.3377 (3)	−0.3543 (6)	0.3847 (2)	0.0375 (12)
H15	0.3605	−0.4282	0.3685	0.045*
C16	0.3749 (3)	−0.2222 (5)	0.3990 (2)	0.0319 (11)
C17	0.4484 (3)	−0.1899 (7)	0.3889 (2)	0.0408 (13)
H17	0.4745	−0.2613	0.3742	0.049*
C18	0.4802 (3)	−0.0585 (7)	0.4003 (3)	0.0430 (14)
H18	0.5273	−0.0409	0.3927	0.052*
C19	0.4429 (3)	0.0541 (6)	0.4237 (2)	0.0331 (11)
C20	0.4724 (3)	0.1939 (6)	0.4353 (2)	0.0393 (12)
H20	0.5186	0.2180	0.4274	0.047*
C21	0.4328 (3)	0.2934 (6)	0.4580 (2)	0.0374 (12)
H21	0.4521	0.3859	0.4659	0.045*
C22	0.3631 (3)	0.2568 (5)	0.4695 (2)	0.0288 (10)
H22	0.3368	0.3261	0.4852	0.035*
C23	0.3720 (2)	0.0255 (5)	0.4363 (2)	0.0242 (9)
C24	0.3377 (2)	−0.1148 (5)	0.42359 (19)	0.0238 (9)
C25	0.3210 (3)	−0.1131 (5)	0.5963 (2)	0.0315 (10)
H25	0.3253	−0.1884	0.5701	0.038*
C26	0.3545 (3)	−0.1271 (7)	0.6623 (3)	0.0437 (14)
H26	0.3812	−0.2099	0.6792	0.052*
C27	0.3477 (3)	−0.0184 (7)	0.7013 (3)	0.0437 (14)
H27	0.3696	−0.0269	0.7450	0.052*
C28	0.3075 (3)	0.1062 (6)	0.6756 (2)	0.0333 (11)

C29	0.2966 (3)	0.2253 (6)	0.7135 (2)	0.0405 (13)
H29	0.3175	0.2215	0.7574	0.049*
C30	0.2569 (3)	0.3414 (6)	0.6863 (2)	0.0383 (12)
H30	0.2506	0.4167	0.7118	0.046*
C31	0.2242 (3)	0.3520 (5)	0.6191 (2)	0.0301 (10)
C32	0.1828 (3)	0.4708 (5)	0.5884 (3)	0.0370 (12)
H32	0.1749	0.5486	0.6120	0.044*
C33	0.1537 (3)	0.4724 (5)	0.5234 (3)	0.0369 (12)
H33	0.1258	0.5507	0.5025	0.044*
C34	0.1667 (3)	0.3550 (5)	0.4893 (2)	0.0271 (10)
H34	0.1471	0.3572	0.4452	0.033*
C35	0.2344 (2)	0.2377 (5)	0.5808 (2)	0.0235 (9)
C36	0.2759 (2)	0.1130 (5)	0.6095 (2)	0.0244 (9)
B1	0.5917 (3)	0.4996 (7)	0.3923 (3)	0.0366 (13)
B2	0.4925 (4)	1.0025 (7)	0.1490 (4)	0.0475 (17)
F1	0.5174 (3)	0.4621 (5)	0.3646 (2)	0.0922 (17)
F2	0.6209 (3)	0.4429 (4)	0.45093 (17)	0.0689 (12)
F3	0.60229 (15)	0.6448 (3)	0.39024 (15)	0.0399 (7)
F4	0.6351 (3)	0.4370 (5)	0.3547 (2)	0.0865 (15)
F5	0.4886 (3)	0.9846 (5)	0.2141 (2)	0.0738 (12)
F6	0.5557 (2)	1.0845 (4)	0.15558 (16)	0.0625 (11)
F7	0.4259 (2)	1.0742 (5)	0.1195 (2)	0.0742 (13)
F8	0.4948 (3)	0.8703 (4)	0.1273 (2)	0.0852 (14)
C1S	0.9015 (5)	0.2643 (9)	0.7541 (3)	0.079 (2)
H1S1	0.8986	0.3610	0.7677	0.118*
H1S2	0.9017	0.2640	0.7106	0.118*
H1S3	0.9482	0.2205	0.7802	0.118*
C2S	0.8353 (5)	0.1856 (8)	0.7595 (4)	0.072 (2)
N1S	0.7831 (5)	0.1217 (10)	0.7631 (4)	0.098 (2)*

Atomic displacement parameters (Å^2)

	U^{11}	U^{22}	U^{33}	U^{12}	U^{13}	U^{23}
Co1	0.0168 (3)	0.0217 (3)	0.0215 (3)	−0.0008 (2)	0.0067 (2)	−0.0004 (2)
N1	0.0199 (17)	0.0226 (18)	0.0255 (19)	−0.0003 (14)	0.0086 (15)	−0.0029 (14)
N2	0.0244 (18)	0.0242 (18)	0.0228 (19)	−0.0015 (15)	0.0094 (15)	−0.0027 (15)
N3	0.0224 (18)	0.0256 (19)	0.0237 (19)	0.0007 (15)	0.0086 (15)	−0.0003 (15)
N4	0.0196 (17)	0.028 (2)	0.0206 (18)	−0.0017 (15)	0.0048 (14)	0.0022 (15)
N5	0.0180 (17)	0.0275 (19)	0.0243 (19)	0.0005 (15)	0.0055 (14)	0.0053 (15)
N6	0.0198 (17)	0.0225 (18)	0.0239 (19)	−0.0019 (14)	0.0085 (14)	−0.0003 (14)
C1	0.024 (2)	0.025 (2)	0.029 (2)	0.0014 (18)	0.0118 (18)	0.0010 (18)
C2	0.030 (2)	0.027 (2)	0.037 (3)	−0.0012 (19)	0.020 (2)	−0.0002 (19)
C3	0.023 (2)	0.026 (2)	0.049 (3)	−0.0038 (18)	0.016 (2)	−0.005 (2)
C4	0.019 (2)	0.029 (2)	0.038 (3)	0.0007 (18)	0.0127 (19)	−0.008 (2)
C5	0.019 (2)	0.040 (3)	0.039 (3)	−0.001 (2)	0.003 (2)	−0.008 (2)
C6	0.025 (2)	0.041 (3)	0.036 (3)	0.001 (2)	−0.003 (2)	−0.007 (2)
C7	0.027 (2)	0.031 (2)	0.027 (2)	0.0050 (19)	0.0053 (19)	−0.0032 (19)
C8	0.037 (3)	0.040 (3)	0.023 (2)	0.005 (2)	0.003 (2)	−0.002 (2)

C9	0.042 (3)	0.039 (3)	0.024 (2)	−0.001 (2)	0.012 (2)	0.002 (2)
C10	0.031 (2)	0.031 (2)	0.026 (2)	−0.003 (2)	0.0093 (19)	−0.0006 (19)
C11	0.021 (2)	0.024 (2)	0.025 (2)	0.0012 (17)	0.0064 (18)	−0.0034 (17)
C12	0.020 (2)	0.024 (2)	0.027 (2)	0.0009 (17)	0.0081 (18)	−0.0053 (17)
C13	0.035 (3)	0.027 (2)	0.034 (3)	−0.001 (2)	0.013 (2)	−0.0016 (19)
C14	0.052 (3)	0.025 (2)	0.034 (3)	0.002 (2)	0.009 (2)	−0.004 (2)
C15	0.046 (3)	0.037 (3)	0.032 (3)	0.015 (2)	0.016 (2)	−0.002 (2)
C16	0.033 (2)	0.041 (3)	0.021 (2)	0.012 (2)	0.0076 (19)	0.001 (2)
C17	0.030 (3)	0.066 (4)	0.030 (3)	0.012 (3)	0.014 (2)	−0.006 (2)
C18	0.027 (2)	0.073 (4)	0.035 (3)	0.003 (3)	0.019 (2)	−0.004 (3)
C19	0.022 (2)	0.056 (3)	0.022 (2)	−0.002 (2)	0.0085 (19)	0.005 (2)
C20	0.024 (2)	0.062 (3)	0.033 (3)	−0.015 (2)	0.011 (2)	0.004 (2)
C21	0.033 (3)	0.042 (3)	0.034 (3)	−0.016 (2)	0.006 (2)	0.002 (2)
C22	0.028 (2)	0.031 (2)	0.025 (2)	−0.0075 (19)	0.0041 (18)	0.0014 (19)
C23	0.020 (2)	0.035 (2)	0.016 (2)	0.0003 (18)	0.0035 (16)	0.0008 (17)
C24	0.024 (2)	0.032 (2)	0.015 (2)	0.0033 (18)	0.0057 (16)	0.0008 (17)
C25	0.023 (2)	0.036 (3)	0.036 (3)	0.004 (2)	0.010 (2)	0.008 (2)
C26	0.031 (3)	0.056 (3)	0.043 (3)	0.009 (2)	0.007 (2)	0.023 (3)
C27	0.030 (3)	0.068 (4)	0.030 (3)	0.002 (3)	0.004 (2)	0.016 (3)
C28	0.024 (2)	0.052 (3)	0.022 (2)	−0.008 (2)	0.0049 (19)	0.006 (2)
C29	0.040 (3)	0.064 (4)	0.018 (2)	−0.014 (3)	0.009 (2)	−0.007 (2)
C30	0.040 (3)	0.045 (3)	0.034 (3)	−0.011 (2)	0.017 (2)	−0.014 (2)
C31	0.029 (2)	0.034 (3)	0.032 (3)	−0.010 (2)	0.015 (2)	−0.011 (2)
C32	0.042 (3)	0.026 (2)	0.051 (3)	−0.005 (2)	0.026 (3)	−0.012 (2)
C33	0.045 (3)	0.027 (3)	0.045 (3)	0.004 (2)	0.023 (2)	0.001 (2)
C34	0.027 (2)	0.027 (2)	0.030 (2)	0.0017 (18)	0.0120 (19)	0.0040 (18)
C35	0.018 (2)	0.028 (2)	0.026 (2)	−0.0055 (17)	0.0089 (17)	−0.0021 (18)
C36	0.0172 (19)	0.033 (2)	0.023 (2)	−0.0053 (18)	0.0060 (17)	0.0001 (18)
B1	0.035 (3)	0.042 (3)	0.032 (3)	−0.010 (3)	0.008 (2)	0.001 (3)
B2	0.034 (3)	0.035 (3)	0.061 (4)	−0.006 (3)	−0.004 (3)	0.006 (3)
F1	0.066 (3)	0.086 (3)	0.096 (3)	−0.043 (2)	−0.020 (2)	0.043 (3)
F2	0.096 (3)	0.051 (2)	0.040 (2)	0.005 (2)	−0.0088 (19)	0.0005 (16)
F3	0.0271 (14)	0.0351 (16)	0.060 (2)	−0.0011 (12)	0.0168 (13)	0.0045 (14)
F4	0.129 (4)	0.062 (3)	0.089 (3)	−0.011 (3)	0.066 (3)	−0.017 (2)
F5	0.078 (3)	0.089 (3)	0.059 (2)	−0.013 (2)	0.027 (2)	0.001 (2)
F6	0.055 (2)	0.075 (2)	0.043 (2)	−0.0238 (18)	−0.0066 (16)	0.0258 (18)
F7	0.0396 (19)	0.105 (3)	0.069 (3)	0.012 (2)	0.0018 (18)	−0.033 (2)
F8	0.132 (4)	0.048 (2)	0.091 (3)	0.007 (2)	0.057 (3)	−0.008 (2)
C1S	0.116 (7)	0.074 (5)	0.045 (4)	0.001 (5)	0.023 (4)	0.008 (4)
C2S	0.094 (6)	0.059 (4)	0.080 (5)	0.030 (4)	0.051 (5)	0.024 (4)

Geometric parameters (Å, °)

Co1—N4	2.123 (4)	C17—C18	1.349 (8)
Co1—N2	2.129 (4)	C17—H17	0.9300
Co1—N6	2.129 (4)	C18—C19	1.428 (8)
Co1—N1	2.131 (3)	C18—H18	0.9300
Co1—N5	2.133 (4)	C19—C20	1.407 (8)
Co1—N3	2.142 (4)	C19—C23	1.413 (6)

N1—C1	1.331 (6)	C20—C21	1.357 (8)
N1—C12	1.353 (6)	C20—H20	0.9300
N2—C10	1.331 (6)	C21—C22	1.398 (7)
N2—C11	1.355 (6)	C21—H21	0.9300
N3—C13	1.327 (6)	C22—H22	0.9300
N3—C24	1.355 (6)	C23—C24	1.444 (7)
N4—C22	1.332 (6)	C25—C26	1.406 (7)
N4—C23	1.351 (6)	C25—H25	0.9300
N5—C25	1.334 (6)	C26—C27	1.362 (9)
N5—C36	1.366 (6)	C26—H26	0.9300
N6—C34	1.331 (6)	C27—C28	1.401 (8)
N6—C35	1.356 (6)	C27—H27	0.9300
C1—C2	1.398 (6)	C28—C36	1.400 (6)
C1—H1	0.9300	C28—C29	1.441 (8)
C2—C3	1.361 (7)	C29—C30	1.342 (8)
C2—H2	0.9300	C29—H29	0.9300
C3—C4	1.400 (7)	C30—C31	1.428 (7)
C3—H3	0.9300	C30—H30	0.9300
C4—C12	1.401 (6)	C31—C32	1.396 (7)
C4—C5	1.432 (7)	C31—C35	1.409 (6)
C5—C6	1.346 (8)	C32—C33	1.373 (8)
C5—H5	0.9300	C32—H32	0.9300
C6—C7	1.432 (7)	C33—C34	1.392 (7)
C6—H6	0.9300	C33—H33	0.9300
C7—C11	1.399 (6)	C34—H34	0.9300
C7—C8	1.413 (7)	C35—C36	1.429 (6)
C8—C9	1.359 (7)	B1—F1	1.344 (7)
C8—H8	0.9300	B1—F2	1.351 (7)
C9—C10	1.388 (7)	B1—F3	1.376 (7)
C9—H9	0.9300	B1—F4	1.426 (8)
C10—H10	0.9300	B2—F8	1.333 (8)
C11—C12	1.451 (6)	B2—F6	1.346 (7)
C13—C14	1.405 (7)	B2—F7	1.360 (7)
C13—H13	0.9300	B2—F5	1.468 (9)
C14—C15	1.353 (8)	C1S—C2S	1.438 (12)
C14—H14	0.9300	C1S—H1S1	0.9600
C15—C16	1.398 (8)	C1S—H1S2	0.9600
C15—H15	0.9300	C1S—H1S3	0.9600
C16—C24	1.405 (6)	C2S—N1S	1.139 (11)
C16—C17	1.440 (7)		
N4—Co1—N2	96.35 (14)	C24—C16—C17	118.5 (5)
N4—Co1—N6	94.96 (14)	C18—C17—C16	121.5 (5)
N2—Co1—N6	94.71 (14)	C18—C17—H17	119.3
N4—Co1—N1	170.19 (14)	C16—C17—H17	119.3
N2—Co1—N1	78.55 (14)	C17—C18—C19	121.4 (5)
N6—Co1—N1	93.82 (13)	C17—C18—H18	119.3
N4—Co1—N5	92.75 (13)	C19—C18—H18	119.3
N2—Co1—N5	168.89 (14)	C20—C19—C23	117.1 (5)
N6—Co1—N5	78.11 (14)	C20—C19—C18	124.0 (5)

N1—Co1—N5	93.34 (14)	C23—C19—C18	118.9 (5)
N4—Co1—N3	78.43 (14)	C21—C20—C19	119.6 (4)
N2—Co1—N3	91.24 (14)	C21—C20—H20	120.2
N6—Co1—N3	171.57 (13)	C19—C20—H20	120.2
N1—Co1—N3	93.21 (13)	C20—C21—C22	120.0 (5)
N5—Co1—N3	96.84 (14)	C20—C21—H21	120.0
C1—N1—C12	117.8 (4)	C22—C21—H21	120.0
C1—N1—Co1	128.9 (3)	N4—C22—C21	122.1 (5)
C12—N1—Co1	113.2 (3)	N4—C22—H22	118.9
C10—N2—C11	117.9 (4)	C21—C22—H22	118.9
C10—N2—Co1	128.8 (3)	N4—C23—C19	122.6 (4)
C11—N2—Co1	113.3 (3)	N4—C23—C24	117.7 (4)
C13—N3—C24	118.1 (4)	C19—C23—C24	119.7 (4)
C13—N3—Co1	129.0 (3)	N3—C24—C16	122.6 (4)
C24—N3—Co1	112.9 (3)	N3—C24—C23	117.5 (4)
C22—N4—C23	118.6 (4)	C16—C24—C23	119.9 (4)
C22—N4—Co1	127.9 (3)	N5—C25—C26	122.1 (5)
C23—N4—Co1	113.5 (3)	N5—C25—H25	119.0
C25—N5—C36	118.2 (4)	C26—C25—H25	119.0
C25—N5—Co1	128.6 (3)	C27—C26—C25	119.5 (5)
C36—N5—Co1	113.2 (3)	C27—C26—H26	120.2
C34—N6—C35	118.1 (4)	C25—C26—H26	120.2
C34—N6—Co1	128.1 (3)	C26—C27—C28	120.0 (5)
C35—N6—Co1	113.7 (3)	C26—C27—H27	120.0
N1—C1—C2	123.0 (4)	C28—C27—H27	120.0
N1—C1—H1	118.5	C36—C28—C27	117.4 (5)
C2—C1—H1	118.5	C36—C28—C29	119.1 (5)
C3—C2—C1	118.7 (4)	C27—C28—C29	123.6 (5)
C3—C2—H2	120.6	C30—C29—C28	120.9 (5)
C1—C2—H2	120.6	C30—C29—H29	119.5
C2—C3—C4	120.4 (4)	C28—C29—H29	119.5
C2—C3—H3	119.8	C29—C30—C31	121.4 (5)
C4—C3—H3	119.8	C29—C30—H30	119.3
C3—C4—C12	116.9 (4)	C31—C30—H30	119.3
C3—C4—C5	123.7 (4)	C32—C31—C35	117.5 (4)
C12—C4—C5	119.4 (4)	C32—C31—C30	123.6 (5)
C6—C5—C4	121.1 (4)	C35—C31—C30	118.8 (5)
C6—C5—H5	119.5	C33—C32—C31	119.8 (4)
C4—C5—H5	119.5	C33—C32—H32	120.1
C5—C6—C7	121.2 (4)	C31—C32—H32	120.1
C5—C6—H6	119.4	C32—C33—C34	119.0 (5)
C7—C6—H6	119.4	C32—C33—H33	120.5
C11—C7—C8	116.9 (4)	C34—C33—H33	120.5
C11—C7—C6	119.3 (4)	N6—C34—C33	123.1 (4)
C8—C7—C6	123.7 (4)	N6—C34—H34	118.4
C9—C8—C7	119.5 (4)	C33—C34—H34	118.4
C9—C8—H8	120.2	N6—C35—C31	122.5 (4)
C7—C8—H8	120.2	N6—C35—C36	117.5 (4)
C8—C9—C10	119.7 (5)	C31—C35—C36	120.0 (4)

C8—C9—H9	120.1	N5—C36—C28	122.8 (4)
C10—C9—H9	120.1	N5—C36—C35	117.5 (4)
N2—C10—C9	122.7 (4)	C28—C36—C35	119.7 (4)
N2—C10—H10	118.6	F1—B1—F2	112.6 (5)
C9—C10—H10	118.6	F1—B1—F3	111.9 (5)
N2—C11—C7	123.1 (4)	F2—B1—F3	113.7 (5)
N2—C11—C12	117.4 (4)	F1—B1—F4	105.9 (5)
C7—C11—C12	119.5 (4)	F2—B1—F4	105.7 (5)
N1—C12—C4	123.2 (4)	F3—B1—F4	106.3 (4)
N1—C12—C11	117.4 (4)	F8—B2—F6	116.8 (6)
C4—C12—C11	119.4 (4)	F8—B2—F7	113.9 (5)
N3—C13—C14	122.3 (5)	F6—B2—F7	111.6 (5)
N3—C13—H13	118.8	F8—B2—F5	105.2 (5)
C14—C13—H13	118.8	F6—B2—F5	104.2 (5)
C15—C14—C13	119.9 (5)	F7—B2—F5	103.5 (6)
C15—C14—H14	120.1	C2S—C1S—H1S1	109.5
C13—C14—H14	120.1	C2S—C1S—H1S2	109.5
C14—C15—C16	119.3 (5)	H1S1—C1S—H1S2	109.5
C14—C15—H15	120.4	C2S—C1S—H1S3	109.5
C16—C15—H15	120.4	H1S1—C1S—H1S3	109.5
C15—C16—C24	117.8 (4)	H1S2—C1S—H1S3	109.5
C15—C16—C17	123.6 (5)	N1S—C2S—C1S	178.8 (10)

Fig. 1

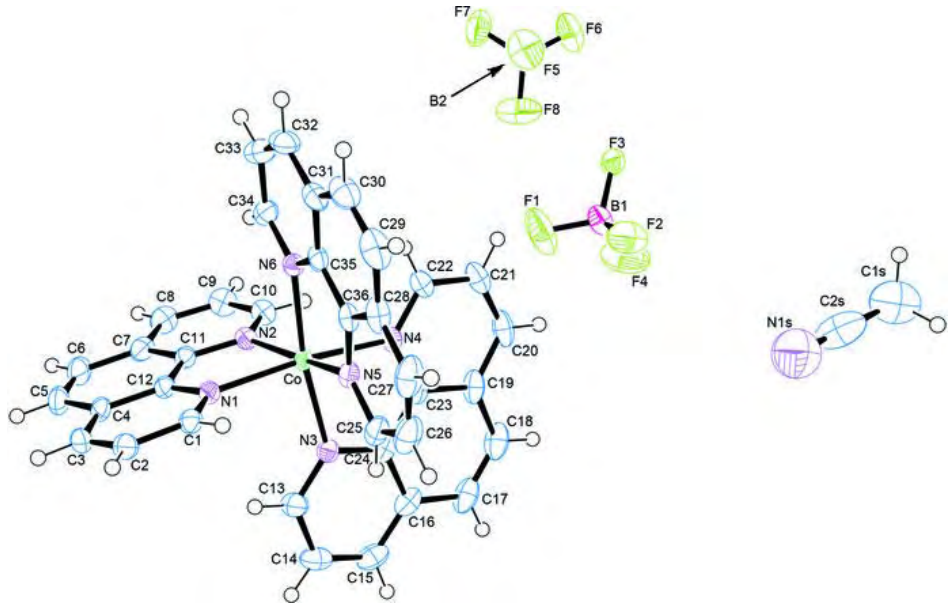

Fig. 2

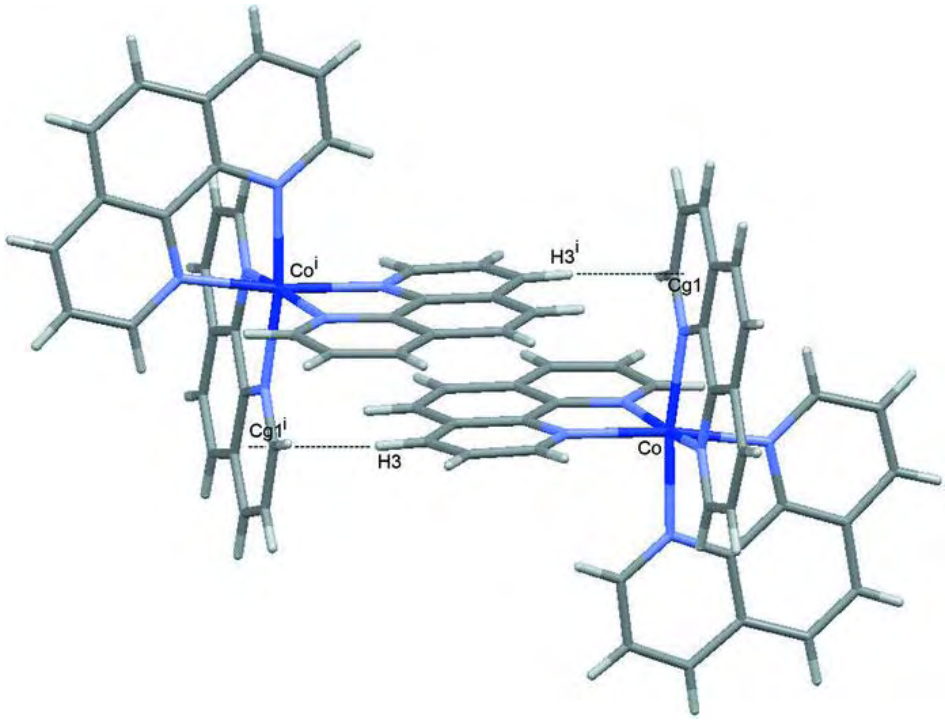

Appendix Two

International Publication

Acta Crystallographica Section E
Structure Reports Online
ISSN 1600-5368

[Tris(3,5-diphenylpyrazolyl)hydroborato]nickel(II) bromide

David J. Harding,[a]* Phimphaka Harding[a] and Harry Adams[b]

[a]Molecular Technology Research Unit, Department of Chemistry, Walailak University, Thasala, Nakhon Si Thammarat 80161, Thailand, and [b]Department of Chemistry, Faculty of Science, University of Sheffield, Brook Hill, Sheffield S3 7HF, England
Correspondence e-mail: hdavid@wu.ac.th

Received 14 May 2009; accepted 6 June 2009

Key indicators: single-crystal X-ray study; T = 150 K; mean σ(C–C) = 0.004 Å; R factor = 0.028; wR factor = 0.063; data-to-parameter ratio = 12.7.

In the title tris(pyrazolyl)borate (Tp^{Ph2}) complex, [$NiBr(C_{45}H_{34}BN_6)$], the Ni, Br and B atoms lie on a crystallographic threefold axis and a distorted NiN_3Br tetrahedral geometry arises for the metal ion. In the crystal, C—H···(C=C) and C—H···π interactions help to establish the polar crystal packing.

Related literature

For other Tp^RNiX (X = Cl, Br) complexes, see: Desrochers *et al.* (2003, 2006); Kunrath *et al.* (2003); Uehara *et al.* (2002); Guo *et al.* (1998); Harding *et al.* (2007). For ionic radius data, see: Shannon (1976).

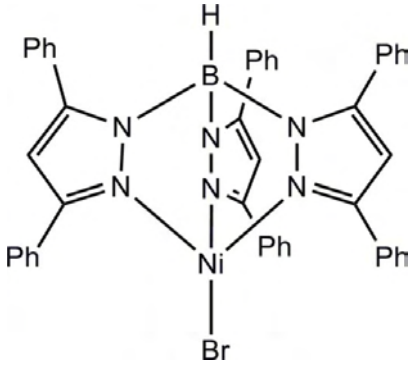

Experimental

Crystal data

[$NiBr(C_{45}H_{34}BN_6)$]
M_r = 808.21
Trigonal, $R\overline{3}$
a = 12.8227 (8) Å
c = 19.327 (3) Å
V = 2752.0 (5) Å^3
Z = 3
Mo $K\alpha$ radiation
μ = 1.66 mm^{-1}
T = 150 K
0.24 × 0.24 × 0.21 mm

Data collection

Bruker SMART CCD diffractometer
Absorption correction: multi-scan (*SADABS*; Bruker, 1997)
T_{min} = 0.691, T_{max} = 0.722
5609 measured reflections
2075 independent reflections
1943 reflections with $I > 2\sigma(I)$
R_{int} = 0.037

Refinement

$R[F^2 > 2\sigma(F^2)]$ = 0.028
$wR(F^2)$ = 0.063
S = 1.06
2075 reflections
163 parameters
1 restraint
H-atom parameters constrained
$\Delta\rho_{max}$ = 0.27 e Å^{-3}
$\Delta\rho_{min}$ = −0.29 e Å^{-3}
Absolute structure: Flack (1983), 670 Friedel pairs
Flack parameter: 0.020 (8)

Table 1
Selected geometric parameters (Å, °).

Ni1—Br1	2.3523 (6)	Ni1—N1	2.041 (2)
N1—Ni1—N1^{i}	93.11 (8)	N1—Ni1—Br1	123.04 (6)

Symmetry code: (i) $-x+y+1, -x+1, z$.

Table 2
Hydrogen-bond geometry (Å, °).

D—H···A	D—H	H···A	D···A	D—H···A
C5—H5···$Cg1^{ii}$	0.95	2.73	3.589 (3)	151

Symmetry code: (ii) $-x+y+\frac{5}{3}, -x+\frac{1}{3}, z-\frac{2}{3}$.

Data collection: *SMART* (Bruker, 1997); cell refinement: *SAINT* (Bruker, 1997); data reduction: *SAINT*; program(s) used to solve structure: *SHELXS97* (Sheldrick, 2008); program(s) used to refine structure: *SHELXL97* (Sheldrick, 2008); molecular graphics: *SHELXTL* (Sheldrick, 2008); software used to prepare material for publication: *SHELXTL*.

The authors gratefully acknowledge the Thailand Research Fund (grant No. RMU5080029) and the National Research Council of Thailand (grant No. WU51106) for support of this work.

Supplementary data and figures for this paper are available from the IUCr electronic archives (Reference: HB2976).

References

Bruker (1997). *SMART*, *SAINT* and *SADABS*. Bruker AXS Inc., Madison, Wisconsin, USA.
Desrochers, P. J., LeLievre, L., Johnson, R. J., Lamb, B. T., Phelps, A. L., Cordes, A. W., Gu, W. & Cramer, S. P. (2003). *Inorg. Chem.* **42**, 7945–7950.
Desrochers, P. J., Telser, J., Zvyagin, S. A., Ozarowski, A., Krzystek, J. & Vicic, D. A. (2006). *Inorg. Chem.* **45**, 8930–8941.
Flack, H. D. (1983). *Acta Cryst.* A**39**, 876–881.
Guo, S., Ding, E., Yin, Y. & Yu, K. (1998). *Polyhedron*, **17**, 3841–3849.
Harding, D. J., Harding, P., Adams, H. & Tuntulani, T. (2007). *Inorg. Chim. Acta*, **360**, 3335–3340.
Kunrath, F. A., de Souza, R. F., Casagrande, O. L. Jr, Brooks, N. R. & Young, V. G. Jr (2003). *Organometallics*, **22**, 4739–4743.
Shannon, R. D. (1976). *Acta Cryst.* A**32**, 751–767.
Sheldrick, G. M. (2008). *Acta Cryst.* A**64**, 112–122.
Uehara, K., Hikichi, S. & Akita, M. (2002). *J. Chem. Soc. Dalton Trans.* pp. 3529–3538.

supplementary materials

Acta Cryst. (2009). E**65**, m773 [**doi:10.1107/S1600536809021606**]

[Tris(3,5-diphenylpyrazolyl)hydroborato]nickel(II) bromide

D. J. Harding, P. Harding and H. Adams

Comment

Tris(pyrazolyl)borates are versatile and popular ligands in coordination chemistry with many complexes now known. Despite the C_3 symmetry present in many tris(pyrazolyl)borate ligands few tetrahedral complexes crystallize in space groups containing a C_3 axis (Desrochers *et al.*, 2003, 2006; Kunrath *et al.*, 2003; Uehara *et al.*, 2002). Rare examples which do contain a C_3 axis include [Tp^{Ph2}NiCl] and [Tp^{Ph2}Ni(OAc)] despite the later being formally five-coordinate (Guo *et al.*, 1998; Harding *et al.*, 2007). In the following paper we report a further example namely, the title compound, [Tp^{Ph2}NiBr], (I).

The reaction of $NiBr_2.2H_2O$ with KTp^{Ph2} readily affords the title complex as a red-purple solid in moderate yield. Crystals were grown by allowing hexanes to diffuse into a concentrated solution of the complex in CH_2Cl_2. The compound crystallizes in the trigonal *R3* space group. The structure is shown in Figure 1 while important bond lengths and angles are given in the supporting tables. The geometry around the nickel centre is best described as distorted tetrahedral {N1—Ni—$N1^{i}$ = 93.11 (8), N1—Ni—Br1 = 123.04 (6)}. The Ni—N bond lengths are very slightly longer by *ca*. 0.01 Å than those found in [Tp^{Ph2}NiCl] (Guo *et al.*, 1998). A similar difference is observed in the structures of [Tp*NiCl] and [Tp*NiBr] (Desrochers *et al.*, 2003, 2006). The Ni—Br distance is 2.3523 (6) Å, *ca* 0.15 Å longer than the corresponding Ni—Cl distance in [Tp^{Ph2}NiCl], and consistent with the difference in the bromine and chlorine covalent radii (0.15 Å; Shannon, 1976). Interestingly, the Ni—Br bond length in (I) is significantly longer than that observed for [Tp*NiBr] (2.291 (2) Å). A similar increase, albeit not so marked, is also found between [Tp^{Ph2}NiCl] and [Tp*NiCl] (ΔNi-Cl = 0.03 Å) suggesting that the larger Tp^{Ph2} ligand may be responsible for the longer nickel-halide bond distances.

The crystal packing in the structure of (I) contains several C—H···π interactions between the phenyl rings of neighbouring Tp^{Ph2} ligands (see Figure 2). The hydrogen atoms H6 and H11 are directed at the π bonds between C1—N1 and C4—C5, respectively {(C1—N1)π···H6 2.657 (3) Å; (C4—C5)π···H11 2.834 (5) Å} while H5 interacts with a phenyl ring (*Cg*1···H5 2.730 (3) Å; *Cg*1 is the centroid of ring C10—C15). Similar interactions occur on all three faces of the Tp^{Ph2} ligand creating a network of triangular columns such that all the [Tp^{Ph2}NiBr] molecules point in the same direction and the phenyl rings adopt a propeller configuration.

Experimental

$NiBr_2.2H_2O$ (34 mg, 0.14 mmol) was dissolved in THF (5 ml) giving a green solution and then stirred for 5 min. KTp^{Ph2} (95 mg, 0.15 mmol) was dissolved in THF (5 ml) giving a pale yellow solution. Addition of the KTp^{Ph2} solution to the Ni solution resulted in a colour change to a red-pink solution. The solution was stirred for 16 hrs. The solution was reduced to dryness, redissolved in fresh THF (2 ml) and filtered through celite. The purple-pink solution was layered with hexanes (10 ml). After two days purple-pink blocks of (I) appeared. These were washed with EtOH (3 *x* 3 ml) and hexanes (2 *x* 5

ml) (59 mg, 54%). ν_{max}(KBr)/cm^{-1} 3059w, 2966w, 2854w (νCH), 2626w (νBH). δ_H (300 MHz; $CDCl_3$; $SiMe_4$), 7.63 (br m, *m*- and *p*-Ph, 18H), 8.53 (br s, *o*-Ph, 6H), 8.86 (br s, *o*-Ph, 6H). UV–Vis λ_{max}(CH_2Cl_2)/nm 318 (ε/dm^{3}mol^{-1}cm^{-1} 3140), 502 (600), 828 (120), 926 (160). m/*z* (ESI) 727 [M—Br$^-$]$^+$. Anal. Calc. for $C_{45}H_{34}N_6BBrNi$ [Tp^{Ph2}NiBr]: C, 66.87; H, 4.24; N 10.40 Found: C, 66.62; H, 4.29; N, 10.17%

Figures

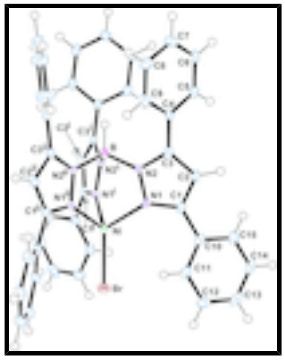

Fig. 1. The molecular structure of (I) with displacement ellipsoids drawn at the 50% probability level. [Symmetry codes:(i) -*x* + *y*+1, -*x* + 1, *z*; (ii) -*y* + 1, *x*-*y*, *z*].

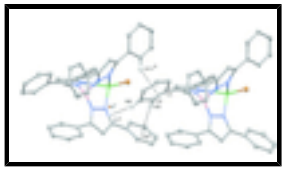

Fig. 2. The molecular packing in (I) showing the three C—H···π interactions. Only selected atoms are labelled or shown for clairty [Symmetry codes:(i) 4/3 - *x* + *y*, 2/3 - *x*, -1/3 + *z*; (ii) 4/3 - *y*, -1/3 + *x*-*y*, -1/3 + *z*].

[Tris(3,5-diphenylpyrazolyl)hydroborato]nickel(II) bromide

Crystal data

[NiBr($C_{45}H_{34}BN_6$)]	Z = 3
M_r = 808.21	F_{000} = 1242
Trigonal, *R*3	D_x = 1.463 Mg m^{-3}
Hall symbol: R 3	Mo *K*α radiation λ = 0.71073 Å
a = 12.8227 (8) Å	Cell parameters from 2851 reflections
b = 12.8227 (8) Å	θ = 2.8–30.6º
c = 19.327 (3) Å	μ = 1.66 mm^{-1}
α = 90º	*T* = 150 K
β = 90º	Block, purple–pink
γ = 120º	0.24 × 0.24 × 0.21 mm
V = 2752.0 (5) Å^3	

Data collection

Bruker SMART CCD diffractometer	2075 independent reflections
Radiation source: fine-focus sealed tube	1943 reflections with $I > 2\sigma(I)$
Monochromator: graphite	R_{int} = 0.037

Detector resolution: 100 pixels mm^{-1}

T = 150 K

φ scans

Absorption correction: multi-scan (SADABS; Bruker, 1997)

T_{min} = 0.691, T_{max} = 0.722

5609 measured reflections

θ_{max} = 27.5º

θ_{min} = 2.1º

h = −16→16

k = −11→16

l = −21→25

Refinement

Refinement on F^2

Least-squares matrix: full

$R[F^2 > 2\sigma(F^2)]$ = 0.028

$wR(F^2)$ = 0.063

S = 1.06

2075 reflections

163 parameters

1 restraint

Primary atom site location: structure-invariant direct methods

Secondary atom site location: difference Fourier map

Hydrogen site location: inferred from neighbouring sites

H-atom parameters constrained

$w = 1/[\sigma^2(F_o^2) + (0.0169P)^2]$ where $P = (F_o^2 + 2F_c^2)/3$

$(\Delta/\sigma)_{max}$ = 0.001

$\Delta\rho_{max}$ = 0.27 e $Å^{-3}$

$\Delta\rho_{min}$ = −0.29 e $Å^{-3}$

Extinction correction: none

Absolute structure: Flack (1983), 670 Friedel pairs

Flack parameter: 0.020 (8)

Special details

Geometry. All e.s.d.'s (except the e.s.d. in the dihedral angle between two l.s. planes) are estimated using the full covariance matrix. The cell e.s.d.'s are taken into account individually in the estimation of e.s.d.'s in distances, angles and torsion angles; correlations between e.s.d.'s in cell parameters are only used when they are defined by crystal symmetry. An approximate (isotropic) treatment of cell e.s.d.'s is used for estimating e.s.d.'s involving l.s. planes.

Refinement. Refinement of F^2 against ALL reflections. The weighted R-factor wR and goodness of fit S are based on F^2, conventional R-factors R are based on F, with F set to zero for negative F^2. The threshold expression of $F^2 > \sigma(F^2)$ is used only for calculating R-factors(gt) *etc*. and is not relevant to the choice of reflections for refinement. R-factors based on F^2 are statistically about twice as large as those based on F, and R- factors based on ALL data will be even larger.

Fractional atomic coordinates and isotropic or equivalent isotropic displacement parameters ($Å^2$)

	x	y	z	U_{iso}*/U_{eq}
Br1	0.6667	0.3333	0.732391 (16)	0.02249 (14)
Ni1	0.6667	0.3333	0.61068 (2)	0.01335 (14)
N1	0.75319 (18)	0.26622 (19)	0.55312 (10)	0.0127 (4)
N2	0.75175 (19)	0.29001 (19)	0.48407 (10)	0.0128 (4)
B1	0.6667	0.3333	0.4567 (3)	0.0139 (10)
H1B	0.6667	0.3333	0.3983	0.017*
C1	0.8082 (2)	0.2003 (2)	0.55910 (12)	0.0146 (5)
C2	0.8419 (3)	0.1815 (3)	0.49355 (13)	0.0166 (6)
H2	0.8812	0.1373	0.4829	0.020*

C3	0.8064 (2)	0.2405 (2)	0.44716 (12)	0.0136 (5)
C4	0.8224 (3)	0.2532 (3)	0.37198 (14)	0.0135 (5)
C5	0.7922 (2)	0.1509 (2)	0.33065 (13)	0.0173 (6)
H5	0.7601	0.0738	0.3515	0.021*
C6	0.8094 (3)	0.1632 (3)	0.25990 (16)	0.0182 (7)
H6	0.7890	0.0942	0.2325	0.022*
C7	0.8557 (2)	0.2743 (3)	0.22844 (13)	0.0201 (6)
H7	0.8668	0.2814	0.1797	0.024*
C8	0.8860 (3)	0.3759 (3)	0.26839 (13)	0.0215 (6)
H8	0.9179	0.4525	0.2469	0.026*
C9	0.8698 (3)	0.3652 (3)	0.33951 (14)	0.0190 (6)
H9	0.8913	0.4350	0.3665	0.023*
C10	0.8239 (2)	0.1510 (3)	0.62468 (13)	0.0163 (6)
C11	0.8460 (2)	0.2131 (3)	0.68680 (14)	0.0185 (6)
H11	0.8564	0.2919	0.6872	0.022*
C12	0.8530 (3)	0.1605 (3)	0.74866 (17)	0.0230 (7)
H12	0.8650	0.2023	0.7912	0.028*
C13	0.8422 (3)	0.0472 (3)	0.74807 (16)	0.0269 (7)
H13	0.8468	0.0113	0.7901	0.032*
C14	0.8246 (3)	−0.0137 (3)	0.68574 (15)	0.0234 (7)
H14	0.8191	−0.0904	0.6849	0.028*
C15	0.8150 (3)	0.0381 (3)	0.62476 (16)	0.0209 (6)
H15	0.8022	−0.0041	0.5824	0.025*

Atomic displacement parameters (Å^2)

	U^{11}	U^{22}	U^{33}	U^{12}	U^{13}	U^{23}
Br1	0.02665 (19)	0.02665 (19)	0.0142 (2)	0.01332 (9)	0.000	0.000
Ni1	0.0140 (2)	0.0140 (2)	0.0120 (3)	0.00702 (10)	0.000	0.000
N1	0.0107 (10)	0.0149 (11)	0.0121 (9)	0.0061 (9)	−0.0007 (8)	0.0007 (8)
N2	0.0137 (11)	0.0146 (11)	0.0096 (8)	0.0068 (9)	0.0007 (8)	0.0006 (8)
B1	0.0112 (15)	0.0112 (15)	0.019 (2)	0.0056 (8)	0.000	0.000
C1	0.0121 (13)	0.0105 (13)	0.0199 (12)	0.0047 (11)	−0.0016 (10)	0.0005 (10)
C2	0.0186 (14)	0.0165 (15)	0.0191 (16)	0.0122 (13)	−0.0028 (13)	0.0009 (12)
C3	0.0097 (13)	0.0094 (12)	0.0189 (12)	0.0026 (11)	−0.0001 (9)	0.0010 (9)
C4	0.0106 (13)	0.0148 (14)	0.0169 (12)	0.0077 (11)	0.0010 (10)	−0.0012 (11)
C5	0.0171 (15)	0.0124 (14)	0.0221 (13)	0.0071 (12)	0.0005 (11)	0.0031 (11)
C6	0.0191 (16)	0.0155 (15)	0.0234 (16)	0.0113 (13)	−0.0015 (13)	−0.0039 (13)
C7	0.0180 (15)	0.0237 (15)	0.0153 (12)	0.0080 (13)	0.0044 (11)	0.0003 (11)
C8	0.0210 (15)	0.0179 (15)	0.0210 (12)	0.0062 (12)	0.0060 (11)	0.0053 (11)
C9	0.0199 (16)	0.0172 (15)	0.0193 (13)	0.0087 (13)	0.0016 (11)	−0.0029 (11)
C10	0.0089 (13)	0.0166 (14)	0.0215 (13)	0.0049 (11)	0.0001 (10)	0.0043 (11)
C11	0.0136 (14)	0.0155 (14)	0.0233 (13)	0.0050 (12)	−0.0050 (11)	0.0012 (11)
C12	0.0204 (17)	0.0291 (19)	0.0180 (15)	0.0112 (15)	−0.0034 (13)	0.0002 (14)
C13	0.0206 (16)	0.0304 (17)	0.0268 (14)	0.0105 (14)	−0.0022 (13)	0.0126 (13)
C14	0.0206 (16)	0.0195 (16)	0.0333 (16)	0.0124 (13)	−0.0008 (12)	0.0075 (13)
C15	0.0185 (15)	0.0194 (16)	0.0257 (14)	0.0101 (14)	−0.0019 (12)	−0.0011 (12)

Geometric parameters (Å, °)

Ni1—Br1	2.3523 (6)	C5—H5	0.9500
Ni1—N1	2.041 (2)	C6—C7	1.380 (4)
Ni1—N1^{i}	2.041 (2)	C6—H6	0.9500
Ni1—N1^{ii}	2.041 (2)	C7—C8	1.392 (4)
N1—C1	1.350 (3)	C7—H7	0.9500
N1—N2	1.371 (3)	C8—C9	1.387 (4)
N2—C3	1.360 (3)	C8—H8	0.9500
N2—B1	1.544 (3)	C9—H9	0.9500
B1—N2^{i}	1.544 (3)	C10—C11	1.389 (4)
B1—N2^{ii}	1.544 (3)	C10—C15	1.394 (4)
B1—H1B	1.1278	C11—C12	1.397 (4)
C1—C2	1.398 (4)	C11—H11	0.9500
C1—C10	1.475 (3)	C12—C13	1.390 (5)
C2—C3	1.388 (3)	C12—H12	0.9500
C2—H2	0.9500	C13—C14	1.391 (5)
C3—C4	1.465 (4)	C13—H13	0.9500
C4—C9	1.397 (4)	C14—C15	1.388 (4)
C4—C5	1.415 (4)	C14—H14	0.9500
C5—C6	1.381 (4)	C15—H15	0.9500
N1—Ni1—N1^{i}	93.11 (8)	C4—C5—H5	120.0
N1—Ni1—N1^{ii}	93.11 (8)	C7—C6—C5	121.0 (3)
N1^{i}—Ni1—N1^{ii}	93.11 (8)	C7—C6—H6	119.5
N1—Ni1—Br1	123.04 (6)	C5—C6—H6	119.5
N1^{i}—Ni1—Br1	123.04 (6)	C6—C7—C8	119.7 (2)
N1^{ii}—Ni1—Br1	123.04 (6)	C6—C7—H7	120.1
C1—N1—N2	106.99 (19)	C8—C7—H7	120.1
C1—N1—Ni1	141.45 (17)	C9—C8—C7	119.9 (3)
N2—N1—Ni1	111.47 (15)	C9—C8—H8	120.0
C3—N2—N1	109.82 (19)	C7—C8—H8	120.0
C3—N2—B1	127.6 (2)	C8—C9—C4	120.9 (3)
N1—N2—B1	120.3 (2)	C8—C9—H9	119.5
N2—B1—N2^{i}	108.89 (19)	C4—C9—H9	119.5
N2—B1—N2^{ii}	108.89 (19)	C11—C10—C15	118.8 (3)
N2^{i}—B1—N2^{ii}	108.89 (19)	C11—C10—C1	121.9 (3)
N2—B1—H1B	110.0	C15—C10—C1	119.2 (2)
N2^{i}—B1—H1B	110.0	C10—C11—C12	120.4 (3)
N2^{ii}—B1—H1B	110.0	C10—C11—H11	119.8
N1—C1—C2	109.5 (2)	C12—C11—H11	119.8
N1—C1—C10	124.6 (2)	C13—C12—C11	120.1 (3)
C2—C1—C10	125.8 (2)	C13—C12—H12	120.0
C3—C2—C1	106.1 (2)	C11—C12—H12	120.0
C3—C2—H2	127.0	C14—C13—C12	119.8 (3)
C1—C2—H2	127.0	C14—C13—H13	120.1

N2—C3—C2	107.6 (2)	C12—C13—H13	120.1
N2—C3—C4	122.9 (2)	C15—C14—C13	119.7 (3)
C2—C3—C4	129.5 (2)	C15—C14—H14	120.2
C9—C4—C5	118.4 (2)	C13—C14—H14	120.2
C9—C4—C3	121.7 (3)	C14—C15—C10	121.1 (3)
C5—C4—C3	119.9 (2)	C14—C15—H15	119.4
C6—C5—C4	119.9 (3)	C10—C15—H15	119.4
C6—C5—H5	120.0		

Symmetry codes: (i) −*x*+*y*+1, −*x*+1, *z*; (ii) −*y*+1, *x*−*y*, *z*.

Hydrogen-bond geometry (Å, °)

D—H···*A*	*D*—H	H···*A*	*D*···*A*	*D*—H···*A*
C5—H5···Cg1^{iii}	0.95	2.73	3.589 (3)	151

Symmetry codes: (iii) −*x*+*y*+5/3, −*x*+1/3, *z*−2/3.

Fig. 1

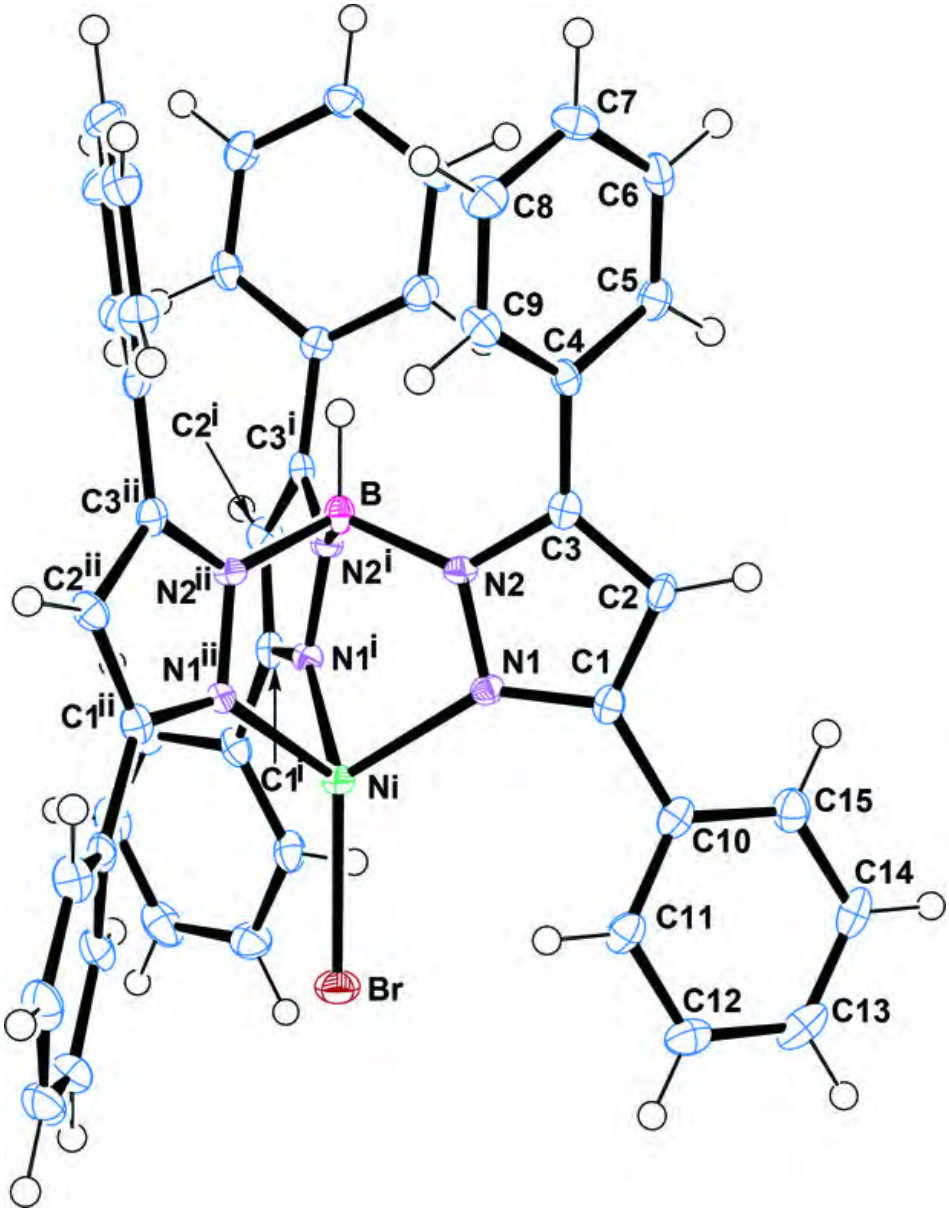
C7
C8
C6
C5
C9
C4
C2i
C3i
B
C3ii
C3
C2ii
N2ii
N2i
N2
C2
N1ii
N1i
N1
C1
C1ii
C1i
Ni
C15
C10
C14
C11
Br
C12
C13

Fig. 2

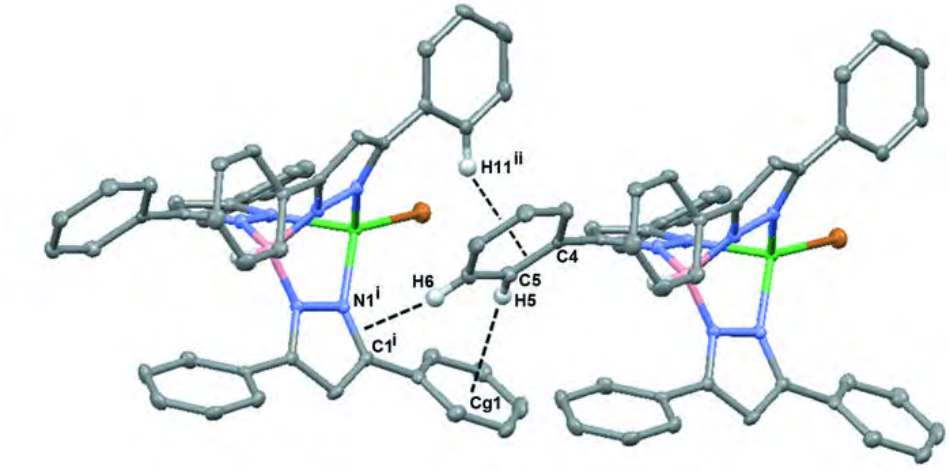

Appendix Three

International Publication

Transition Met Chem
DOI 10.1007/s11243-010-9358-x

Cationic tris(pyrazolyl)borate bipyrimidine complexes

David J. Harding · Phimphaka Harding · Jutaporn Kivnang · Harry Adams

Received: 16 March 2010 / Accepted: 6 April 2010

Abstract The cationic complexes, $[Tp^{R}Ni(bpym)]^{+}$ {Tp^{R} = tris(3,5-diphenylpyrazolyl)borate, R = Ph_2 **1**; tris(3-phenyl-5-methylpyrazolyl)borate, R = Ph,Me **2**} were synthesized by reacting $[Tp^{R}NiBr]$ (R = Ph_2; Ph,Me) with bipyrimidine followed by subsequent addition of KPF_6 in CH_2Cl_2. The green solids have been characterized by IR, UV–Vis and ^1H NMR spectroscopy. Crystallographic studies of $[Tp^{Ph,Me}Ni(bpym)]PF_6$ reveal a five-coordinate square pyramidal nickel centre with a κ^3-coordinated $Tp^{Ph,Me}$ ligand and a chelating bipyrimidine ligand. Cyclic voltammetric studies show *irreversible* reduction with the degree of reversibility dependent on the type of Tp^{R} ligand.

Introduction

2,2′-Bipyrimidine (bpym) is a useful ligand in coordination chemistry able to act as a chelating bidentate [1–3] or bridging bis-bidentate ligand [4–14]. Dimers containing the M(μ-bpym)M unit are particularly common with examples including $[(H_2O)_4M(\mu\text{-bpym})M(H_2O)_4][SO_4]_2$ [4–8] and $[(hfac)_2M(\mu\text{-bpym})M(hfac)_2]$ (M = Mn, Fe, Co, Ni, Cu) [11, 12]. More recently, hetereodinuclear systems have also been prepared [13]. Such complexes are of interest as the bpym ligand facilitates weak magnetic exchange between the metals which although antiferromagnetic in most cases can be ferromagnetic. In addition to dimers, coordination polymers and multidimensional networks incorporating bipyrimidine are also well known [14]. Despite this wealth of chemistry, control over the size and shape of these networks is often extremely difficult to achieve, and the nature of the products thus formed is largely serendipitous. The use of facially capping ligands, such as tris(pyrazolyl)borate Tp^{R} (R = alkyl or aryl groups), [15] to block one face of the metal has proven to be effective in reducing the dimensionality of transition metal clusters and thus we have embarked on the synthesis of precursors in which both bpym and tris(pyrazolyl)borate are present. In this work, we describe the synthesis and characterization of the first mononuclear tris(pyrazolyl)borate and bipyrimidine complexes that may function as potential molecular building blocks.

Experimental

General considerations

All manipulations were performed in air with HPLC grade solvents. Potassium tris(3,5-diphenylpyrazolyl)borate (KTp^{Ph2}) and tris(3-phenyl-5-methylpyrazolyl)borate ($KTp^{Ph,Me}$) were prepared by literature procedures [16, 17]. $[Tp^{Ph2}NiBr]$ [18] and $[Tp^{Ph,Me}NiBr]$ [19] were prepared as previously reported. All other chemicals were purchased from Aldrich Chemical Company and used as received.

Electronic supplementary material The online version of this article (doi:10.1007/s11243-010-9358-x) contains supplementary material, which is available to authorized users.

D. J. Harding (✉) · P. Harding
Molecular Technology Research Unit, Department of Chemistry, Walailak University, Thasala, Nakhon Si Thammarat 80161, Thailand
e-mail: hdavid@wu.ac.th

J. Kivnang
Inorganic Materials Research Unit, Department of Chemistry, Taksin University, Songkhla 90000, Thailand

H. Adams
Department of Chemistry, University of Sheffield, Brook Hill, Sheffield S3 7HF, UK

Published online: 22 April 2010

Infrared spectra (as KBr discs) were recorded on a Perkin-Elmer Spectrum One infrared spectrophotometer in the range 400–4,000 cm^{-1}. Electronic spectra were recorded in CH_2Cl_2 at room temperature on a Shimadzu UV–Visible spectrophotometer. ^1H NMR spectra were recorded on a Bruker 300 MHz FT-NMR spectrometer at 25 °C in $CDCl_3$ with $SiMe_4$ added as an internal standard. Magnetic susceptabilities of **1** and **2** were determined using the Evan's method with appropriate diamagnetic corrections applied. [20]. Elemental analyses were carried out on a Eurovector EA3000 analyser. ESI–MS were carried out on a Bruker Daltonics 7.0T Apex 4 FTICR Mass Spectrometer. Electrochemical studies were carried out using a palmsensPC Vs 2.11 potentiosat in conjunction with a three-electrode cell. The auxiliary electrode was a platinum rod and the working electrode was a platinum disc (2.0 mm diameter). The reference electrode was a Ag–AgCl electrode (2 M LiCl). Solutions, in CH_2Cl_2 dried over CaH_2, were 5×10^{-4} mol dm^{-3} in the test compound and 0.1 mol dm^{-3} in $[NBu^n_4][PF_6]$ as the supporting electrolyte. Under these conditions, $E^{o\prime}$ for the one-electron oxidation of $[Fe(\eta\text{-}C_5H_5)_2]$ added to the test solutions as an internal calibrant is 0.52 V.

Preparation of $[Tp^{Ph2}Ni(bpym)]PF_6$ **1**

$[Tp^{Ph2}NiBr]$ (242 mg, 0.3 mmol) was dissolved in CH_2Cl_2 (10 ml) giving a purple-pink solution. Bpym (48 mg, 0.3 mmol) was added resulting in a change to emerald green. The solution was stirred for 30 min. KPF_6 (57 mg, 0.31 mmol) was then added and the solution stirred for 2 h resulting in an emerald green solution. The solution was filtered through Celite and reduced to dryness *in vacuo*. The solid was redissolved in CH_2Cl_2 (4 ml) and layered with hexane (15 ml). After 2 days, dark green crystals formed which were washed with Et_2O (2 × 5 ml) and air dried (278 mg, 90%). ν_{max}(KBr)/cm^{-1} 3,060 (ν_{CH}), 2,640 (ν_{BH}), 1,578 (ν_{CN}), 845, 558 (ν_{PF}). ^1H NMR (300 MHz; $CDCl_3$) δ/ppm −10.82 (vbr s, *BH*, 1 H), 5.92 (s, *Ph*, 6H), 7.58 (s, *Ph*, 6H), 7.66 (s, *Ph*, 4H), 8.45 (s, *Ph*, 6H), 8.76 (s, *Ph*, 4H), 10.35 (vbr s, *Ph*, 4H), 14.59 (s, bpym-*CH*, 2H), 35.50 (s, bpym-*CH*, 2H), 71.14 (br s, pz-*CH*, 3H). UV–Vis $\lambda_{max}(CH_2Cl_2)$/nm 340sh (ε/dm^3 mol^{-1} cm^{-1} 2,200), 593 (51), 810 (34). *m/z* (ESI) 885 $[M\text{-}PF_6^-]^+$, 727 $[M\text{-}PF_6^-\text{-}bpym]^+$. Magnetic moment ($\mu_{eff}/\mu_B$, 297 K): 3.57. $C_{53}H_{40}N_{10}BPF_6Ni$: requires C, 61.72, H 3.91, N 13.58; found: C, 61.74, H 4.19, N 13.85%.

Preparation of $[Tp^{Ph,Me}Ni(bpym)]PF_6$ **2**

To a stirred pink suspension of $[Tp^{Ph,Me}NiBr]$ (62 mg, 0.1 mmol) in CH_2Cl_2 (10 ml) was added bpym (16 mg, 0.1 mmol) to give a green solution. The solution was stirred at room temperature for 1 h. KPF_6 (18 mg, 0.1 mmol) was added and the solution stirred for 2 h. The solution was filtered through Celite, and hexane (15 ml) was layered on top. After two days, dark green crystals appeared which were washed with Et_2O and air dried (63 mg, 75%). ν_{max}(KBr)/cm^{-1} 3058, 2963, 2927 (ν_{CH}), 2547 (ν_{BH}), 1578 (ν_{CN}), 847, 558 (ν_{PF}). ^1H NMR (300 MHz; $CDCl_3$) δ/ppm −9.77 (vbr s, *BH*, 1 H), 3.83 (s, *CH_3*, 9H), 5.89 (s, *Ph*, 7H), 8.62 (s, *Ph*, 4H), 9.80 (vbr s, *Ph*, 4H), 14.35 (s, bpym-*CH*, 2H), 34.96 (s, bpym-*CH*, 2H), 70.83 (br s, pz-*CH*, 3H). UV–Vis $\lambda_{max}(CH_2Cl_2)$/nm 408sh (ε/dm^3 mol^{-1} cm^{-1} 354), 598 (102), 812 (89). *m/z* (ESI) 699 $[M\text{-}PF_6^-]^+$, 541 $[M\text{-}PF_6^-\text{-bpym}]^+$. Magnetic moment ($\mu_{eff}/\mu_B$, 297 K): 3.35. $C_{38}H_{34}N_{10}BPF_6Ni{\cdot}0.5CH_2Cl_2$: requires C, 52.09, H 3.97, N 15.78; found: C, 52.02, H 3.98, N 15.93%.

X-ray crystallography

X-ray quality crystals of **2** were grown by allowing hexane to diffuse into a concentrated solution of the complex in CH_2Cl_2. Crystals were mounted on a glass fibre using perfluoropolyether oil and cooled rapidly to 150(2) K in a stream of cold nitrogen. All diffraction data were collected on a Bruker Smart CCD area detector with graphite monochromated Mo Kα(λ = 0.71073 Å). After data collection, an empirical absorption correction (SADABS) was applied [21], and the structure was then solved by direct methods and refined on all F^2 data using the SHELX suite of programs [22]. The non-hydrogen atoms were refined with anisotropic thermal parameters; hydrogen atoms were included in calculated positions and refined with isotropic thermal parameters which were *ca*. 1.2× (aromatic CH) or 1.5× (Me), the equivalent isotropic thermal parameters of their parent carbon atoms.

Results and discussion

Preparation of $[Tp^RNi(bpym)]PF_6$

The reaction of $[Tp^RNiBr]$ (R = Ph_2; Ph,Me) [18, 19] with bipyrimidine in CH_2Cl_2 followed by the addition of KPF_6 gives the cationic complexes $[Tp^RNi(bpym)]PF_6$ (R = Ph_2 **1**; Ph,Me **2**) as dark green solids in good yields (Scheme 1). Although Akita et al. [19] have reported the preparation of a range of cationic complexes $[Tp^{Ph,Me}ML]^+$ (M = Co, Ni; L = chelating ligand), our synthesis differs from theirs in that we use KPF_6 with CH_2Cl_2 as a solvent rather than AgOTf and MeCN. This proved to be crucial in the synthesis of **1** as $[Tp^{Ph2}NiBr]$ has very low solubility in MeCN and provides a new synthetic strategy for the synthesis of

Scheme 1 Preparation of $[Tp^{Ph2}Ni(bpym)]^+$ **1** and $[Tp^{Ph,Me}Ni(bpym)]^+$ **2**

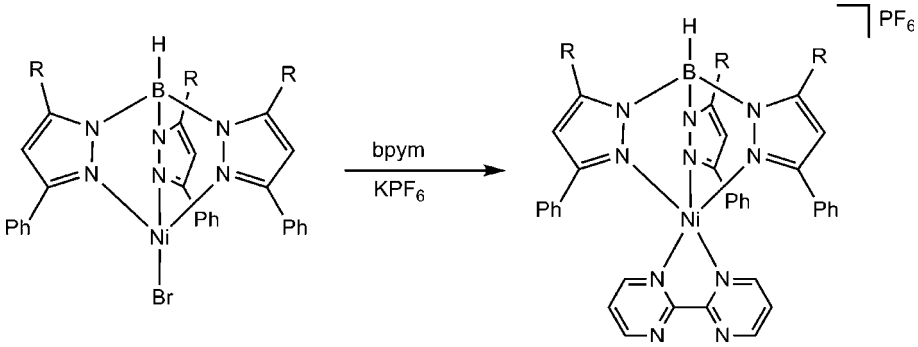

cationic tris(pyrazolyl)borate complexes that eliminates the need for troublesome and expensive silver salts.

Spectroscopic characterization of $[Tp^RNi(bpym)]PF_6$

IR spectroscopic studies of **1** and **2** show B–H stretches at 2,634 and 2,545 cm^{-1}, respectively, indicative of κ^3-coordinated Tp^R ligands [23]. In addition, there is strong band at *ca.* 1,580 cm^{-1} assigned to a C=N stretch of the bipyrimidine ligand [24]. The coordination mode of the bipyrimidine ligand cannot unfortunately be determined by IR spectroscopy as the band at *ca.* 1,565 cm^{-1} typically used for this purpose is masked by bands due to the Tp^R ligands [4–8]. Further bands are also observed at 845, 558 and 847, 558 cm^{-1} for **1** and **2**, respectively, consistent with the presence of PF_6^- counter anions.

The UV–Vis spectra of **1** and **2** reveal two bands at 810, 593 ($\varepsilon = 34$, 51 $dm^3\ mol^{-1}\ cm^{-1}$) and 812, 598 nm ($\varepsilon = 89$, 102 $dm^3\ mol^{-1}\ cm^{-1}$), respectively, consistent with d–d transitions and similar to those reported for other five-coordinate nickel Tp^R complexes [17–19, 25]. A further more intense band ($\varepsilon = 2{,}200$ and 354 $dm^3\ mol^{-1}\ cm^{-1}$ for **1** and **2**, respectively) at lower wavelengths is also observed for both complexes and is tentatively assigned to an MLCT band.

The ^1H NMR spectra of both complexes reveal appropriately shifted resonances due to the paramagnetic nickel centre with the borohydride resonances found at −10.82 and −9.77 ppm for **1** and **2**, respectively [25–27]. The presence of a single pyrazolyl hydrogen peak at 71.14 and 70.83 ppm for **1** and **2**, respectively, and a single methyl resonance for **2** indicate fast rotation of the Tp^R ligand. Such fluxional behaviour and relatively sharp NMR are frequently observed in four- and five-coordinate first row transition tris(pyrazolyl)borate metal compounds such as $[Tp^RNi(OAc)]$ (R = Me_3; Me_2; Me_2,Br) [25], $[Tp^{Ph,Me}Ni(SR)]$ (R = aryl) [26] and $[Tp^{Ph,Me}Ni(S_2CNR_2)]$ (R = Et, Ph) [27]. Interestingly, we were unable to locate two of the protons on the bipyrimidine ligand which are presumably lost due to their close proximity to the paramagnetic nickel centre. Magnetic susceptabilities of 3.57 and 3.35 μ_B were observed for **1** and **2**, respectively, and are consistent with two unpaired electrons for both complexes and further support fluxionality in these systems, as complexes with the square-based pyramidal geometry observed in the crystal structure (vide infra) would be expected to be diamagnetic.

X-ray crystal structure of $[Tp^{Ph,Me}Ni(bpym)]PF_6$ **2**

Crystals of **2** were grown by diffusion of hexanes into a concentrated solution of the complex in CH_2Cl_2. The compound crystallizes in the triclinic $P\bar{1}$ space group with two independent molecules in the lattice and a molecule of CH_2Cl_2. The molecular structure of one of the independent molecules is shown in Fig. 1. The two independent molecules show five-coordinate nickel metal centres with a κ^3-coordinated $Tp^{Ph,Me}$ ligand, consistent with the above IR data. The coordination geometry is best described as square pyramidal with trigonality indices of 0.12 and 0.07

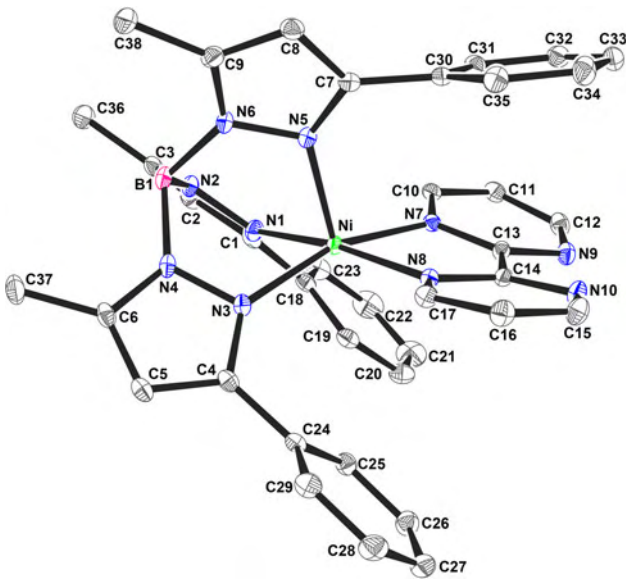

Fig. 1 Molecular structure of $[Tp^{Ph,Me}Ni(bpym)]^+$ **2** (molecule 1) drawn at 30% probability level. The PF_6^- counter anion, CH_2Cl_2 molecule and hydrogen atoms have been omitted for clarity

Table 1 Selected bond lengths and angles for **2**

Bond lengths (Å)		Bond angles (°)	
Molecule 1			
Ni–N1	2.051 (3)	N1–Ni–N3	85.42 (9)
Ni–N3	2.048 (2)	N1–Ni–N5	94.09 (9)
Ni–N5	2.018 (2)	N3–Ni–N5	92.11 (9)
Ni–N7	2.070 (2)	N7–Ni–N8	78.34 (8)
Ni–N8	2.066 (2)	τ	0.12
Molecule 2			
Ni–N1a	1.987 (2)	N1a–Ni–N3a	91.01 (8)
Ni–N3a	2.038 (2)	N1a–Ni–N5a	93.92 (8)
Ni–N5a	2.068 (3)	N3a–Ni–N5a	86.46 (8)
Ni–N7a	2.063 (2)	N7a–Ni–N8a	78.10 (8)
Ni–N8a	2.074 (3)	τ	0.07

for the two independent molecules and is similar to that reported for the related bipyridine complex [$Tp^{Ph,Me}$Ni(-bipy)]OTf ($\tau = 0.06$) [28]. As expected, the bipyrimidine ligand adopts a bidentate-chelating coordination mode but is significantly twisted about the C13–C14 bond and thus contains non-coplanar pyrimidine rings. This is particularly evident in the case of molecule 1 where the torsion angle is

Table 2 Crystallographic data for [$Tp^{Ph,Me}$Ni(bpym)]PF_6·0.5CH_2Cl_2 **2**

Complex	**2**
Chemical formula	$C_{38.5}H_{35}BClF_6N_{10}NiP$
M_r	887.71
Crystal system	Triclinic
Space group	$P\bar{1}$
a/Å	12.6110 (3)
b/Å	16.0919 (3)
c/Å	21.5709 (5)
α/°	80.4620 (10)
β/°	73.4060 (10)
γ/°	70.0030 (10)
Volume/Å^3	3930.99 (15)
Z	4
D_c/g cm^{-3}	1.500
μ(Mo-Kα)/mm^{-1}	0.675
T/K	150 (2)
Reflections collected	76248
Independent reflections (R_{int})	18026 (0.0478)
R_1, wR_2 [$I > 2\sigma(I)$][a]	0.0455, 0.1217
R_1, wR_2 (all data)	0.0638, 0.1110

[a] $R_1 = \Sigma||F_o| - |F_c||/\Sigma|F_o|$, $wR_2[\Sigma w(F_o^2 - F_c^2)^2/\Sigma w(F_o^2)^2]^{1/2}$

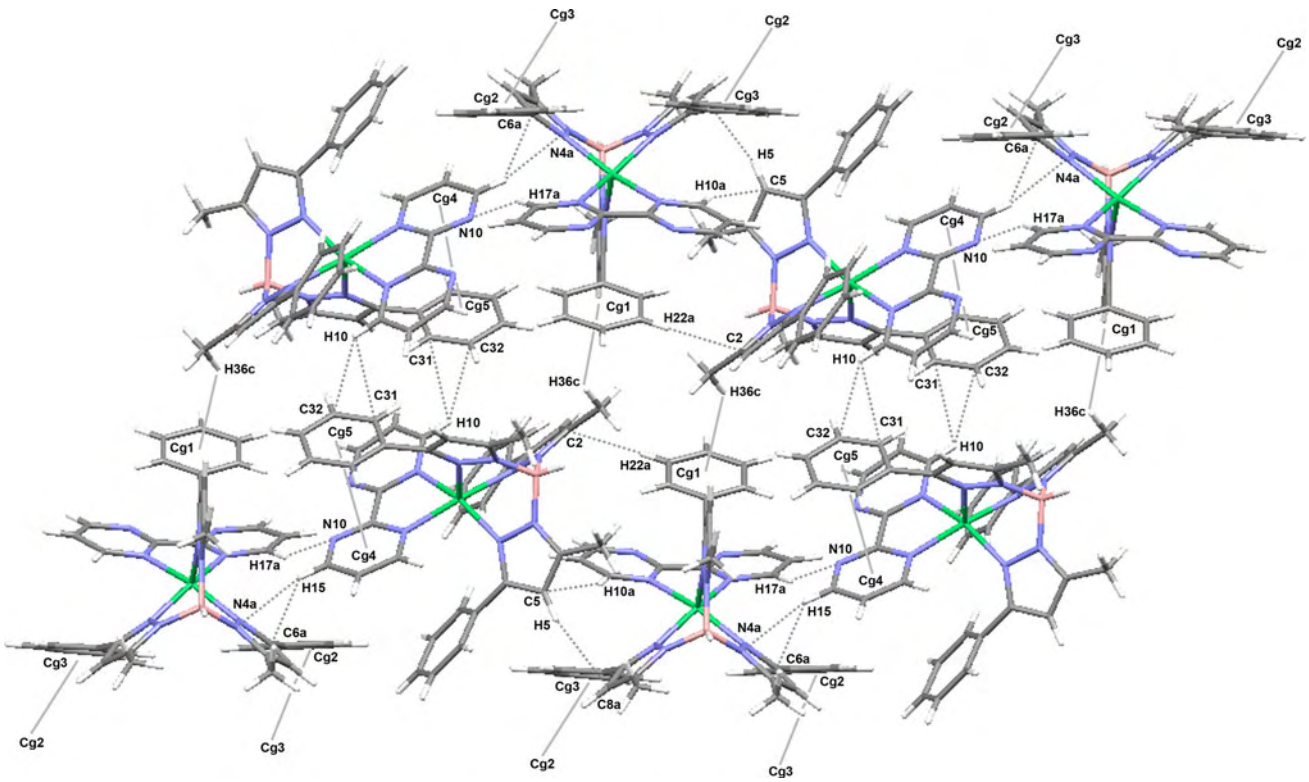

Fig. 2 Mercury plot of [$Tp^{Ph,Me}$Ni(bpym)]$^+$ **2** showing the intramolecular and intermolecular interactions between the molecules. The PF_6^- counter anions and CH_2Cl_2 molecules have been omitted for clarity

8.14° (N7–C13–C14–N8) compared with 2.68° (N7a–C13a–C14a–N8a) for molecule 2. The Ni–N bond lengths for the tris(pyrazolyl)borate ligand are in accord with those reported for other nickel $Tp^{Ph,Me}$ complexes and reveal symmetrical coordination of the $Tp^{Ph,Me}$ ligand [18]. The Ni–N bond lengths for the bipyrimidine ligand are similar to those found in $[(H_2O)_4Ni(\mu\text{-bpym})Ni(H_2O)_4]^{4+}$ despite the difference in coordination number (2.092 and 2.097 Å) [4]. The chelate angle for the bipyrimidine ligand is typical for coordinated diimine ligands [4–10] (Tables 1, 2).

The structure contains extensive intermolecular interactions (Fig. 2). There are three CH···π interactions between the two independent molecules involving the hydrogen atom of one of the Tp phenyl rings and one of the pyrimidine rings of the bpym ligand and the pyrazole rings of the neighbouring $Tp^{Ph,Me}$ ligand (C5···H10a = 2.879(3) Å, C2···H22a = 2.790(4) Å). The final interaction is between the pyrazole hydrogen atom and an adjacent pyrazole ring (C8a···H5 = 2.790(3) Å). Each set of independent molecules is then linked to neighbouring sets by a hydrogen bonding interaction (H17a···N10 = 2.737(3) Å) and a further CH···π interaction (H15···N4a–C6aπ = 2.608(3) Å) forming a linear chain. This chain is then connected to another chain through two CH···π interactions; one between one of the hydrogen atoms on the bpym ligand and a neighbouring Tp phenyl ring and the other between a methyl hydrogen and the centroid of another Tp phenyl ring (H10···C31–C32π = 2.775(3) Å, H36c···Cg1 = 2.834(2) Å where Cg1 is the centroid of the ring described by C18a–C23a). Further, π···π interactions connect these two chains to further sets of chains completing the structure (Cg2···Cg3 = 4.388(2) Å, Cg2 and Cg3 are the centroids of the rings described by C24a–C29a and C30a–C35a, respectively). Finally, an intramolecular interaction between the phenyl ring of the $Tp^{Ph,Me}$ ligand that lies directly above the bipyrimidine ligand is oriented to provide preferential overlap with one of the aromatic rings suggesting π···π interactions (Cg4···Cg5 = 3.687(2) Å where Cg4 and Cg5 are the centroids of the rings described by N8–C14–N10–C15–C17 and C30–C35, respectively).

Cyclic voltammetry

Cyclic voltammetric studies of the two compounds reveal irreversible reduction at −1.26 V and −1.36 V for **1** and **2**, respectively. Interestingly, the degree of reversibility is dependent on the type of Tp^R ligand used with the Tp^{Ph2} ligand showing the most reversibility (Fig. 3). This seems to suggest that the larger Tp^{Ph2} ligand is better able to stabilize the product formed upon reduction. Cyclic voltammograms at lower scan rates reveal that the couple becomes increasingly irreversible, indicating that in both cases, the reduction is chemically irreversible. The lack of sufficient related nickel Tp^R complexes makes comparisons difficult, but similar observations have been made for the bipyrimidine complex [(bpym)Ni(Mes)Br] which reduces irreversibly at −1.49 V [3].

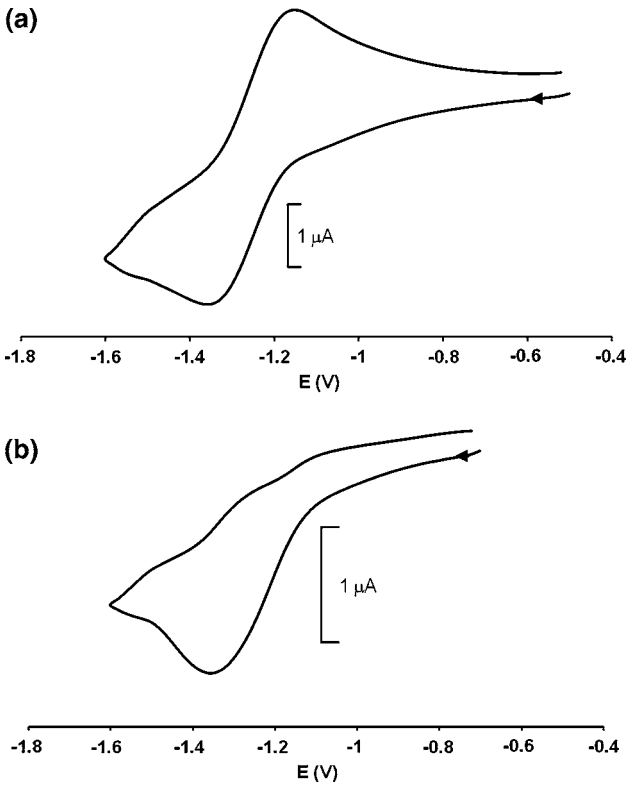

Fig. 3 Cyclic voltammograms of (**a**) $[Tp^{Ph2}Ni(bpym)]^+$ **1** and (**b**) $[Tp^{Ph,Me}Ni(bpym)]^+$ **2** in $CH_2Cl_2/[NBu^n_4][PF_6]$ solution at 298 K with potentials versus $FeCp_2^{0/+}$

Conclusions

In conclusion, we have successfully synthesized two novel cationic tris(pyrazolyl)borate nickel complexes with a potentially bridging bipyrimidine ligand. X-ray crystallographic studies reveal that the tris(pyrazolyl)borate is κ^3 coordinated while the bipyrimidine ligand exhibits a chelating coordination mode. Electrochemical studies show irreversible reduction with the degree of reversibility dependent on the type of tris(pyrazolyl)borate ligand.

Supplementary material

CCDC 770357 contains the supplementary crystallographic data for this paper. These data can be obtained free of charge from the Cambridge Crystallographic Data Centre via www.ccdc.cam.ac.uk/data_request/cif.

Acknowledgments We gratefully acknowledge the Thailand Research Fund (Grant No. RMU5080029) and the National Research Office of Thailand for funding this research (Grant no. WU51106). The School of Chemistry, University of Bristol is thanked for elemental analysis and MS services.

References

1. Castro I, Sletten J, Glaerum LK, Cano J, Lloret F, Faus J, Julve M (1995) J Chem Soc Dalton Trans 3207
2. Castro I, Sletten J, Glaerum LK, Lloret F, Faus J, Julve M (1994) J Chem. Soc Dalton Trans 2777
3. Klein A, Kaiser A, Sarkar B, Wanner M, Fiedler J (2007) Eur J Inorg Chem 965
4. De Munno G, Julve M, Lloret F, Derory A (1993) J Chem Soc Dalton Trans 1179
5. Munno G, Julve M, Lloret F, Cano J, Caneschi A (1995) Inorg Chem 34:2048
6. Munno G, Julve M, Lloret F, Faus J, Caneschi, A (1994) J Chem Soc Dalton Trans 1175
7. Munno G, Ruiz R, Lloret F, Faus J, Sessoli R, Julve M (1995) Inorg Chem 34:408
8. Hong DM, Chu YY, Wei HH (1996) Polyhedron 15:447
9. Real A, Zarembowitch J, Kahn O, Solans X (1987) Inorg Chem 26:2939
10. Andrés E, Munno G, Julve M, Real JA, Lloret F (1993) J Chem Soc Dalton Trans 2169
11. Brewer G, Sinn E (1985) Inorg Chem 24:4580
12. Barquín M, González Garmendia MJ, Bellido V (1999) Transition Met Chem 24:584
13. Barquín M, González Garmendia MJ, Bellido V (1999) Transition Met Chem 24:546
14. Martín S, Gotzone Barandika M, Cortés R, Ruiz de Larramendi JI, Karmele Urtiaga M, Lezama L, Isabel Arriortua M, Rojo T (2001) Eur J Inorg Chem 2107
15. Trofimenko S (1999) Scorpionates: The Coordination Chemistry of Polypyrazolyl-borate Ligands. Imperial College Press, London
16. Kitajima N, Fujisawa K, Fujimoto C, Moro-oka Y, Hashimoto S, Kitagawa T, Toriumi K, Tatsumi K, Nakamura A (1992) J Am Chem Soc 114:1277
17. Desrochers PJ, Cutts RW, Rice PK, Golden ML, Graham JB, Barclay TM, Cordes AW (1999) Inorg Chem 38:5690
18. Uehara K, Hikichi S, Akita M (2002) J Chem Soc Dalton Trans 3529
19. Harding DJ, Harding P, Adams H, Tuntulani T (2007) Inorg Chim Acta 360:3335
20. Bain GA, Berry JF (2008) J Chem Ed 85:532
21. Bruker (2005) SMART, XSCANS, SHEXTL and SADABS. Bruker AXS Inc., Madison
22. Sheldrick GM (1997) SHELX-97 and SHELXS-97. University of Göttingen, Germany
23. Akita M, Ohta K, Takahashi Y, Hikichi S, Moro-oka Y (1997) Organometallics 16:4121
24. Nakamoto K (ed) (2009) In: Infrared and Raman spectra of inorganic and coordination compounds: part B, 6th edn. New Jersey, Wiley, pp 257–285
25. Hikichi S, Sasakura Y, Yoshizawa M, Ohzu Y, Moro-oka Y, Akita M (2002) Bull Chem Soc Jpn 75:1255
26. Matsunaga Y, Fujisawa K, Ibi N, Miyashita Y, Okamoto K (2005) Inorg Chem 44:325
27. Ma H, Chattopadhyay S, Petersen JL, Jensen MP (2008) Inorg Chem 47:7966
28. Addison AW, Rao TN, Reedijk J, Van Rijn J, Verschoor GC (1984) J Chem Soc Dalton Trans 1349

Appendix Four

Manuscript

Redox-Active Nickel and Cobalt Tris(pyrazolyl)borate Dithiocarbamate Complexes: Air-Stable Co(II) Dithiocarbamates

David J. Harding,*[a] Phimphaka Harding,[a] Supaporn Dokmaisrijan,[a] and Harry Adams[b]

Received (in XXX, XXX) Xth XXXXXXXXX 200X, Accepted Xth XXXXXXXXX 200X
First published on the web Xth XXXXXXXXX 200X
DOI: 10.1039/b000000x

A series of new cobalt(II) and nickel(II) tris(3,5-diphenylpyrazolyl)borate (Tp^{Ph2}) dithiocarbamate complexes [Tp^{Ph2}M(dtc)] (M = Co, dtc = S_2CNEt_2 **1**, S_2CNBz_2 **2** and $S_2CN(CH_2)_4$ **3**; M = Ni, dtc = S_2CNEt_2 **4**, S_2CNBz_2 **5** and $S_2CN(CH_2)_4$ **6**) have been prepared by the reaction of [Tp^{Ph2}MBr] with Nadtc in CH_2Cl_2. IR spectroscopy indicates that the Tp^{Ph2} ligand is κ^3 coordinated while the dithiocarbamate ligand is κ^2 coordinated. ^{1}H NMR and UV-Vis spectroscopy are consistent with high spin, five-coordinate metal centres. X-ray crystallographic studies of **1**, **3** and **6** confirm the κ^3 coordination of the Tp^{Ph2} ligand and reveal an intermediate five-coordinate geometry with an asymmetrically coordinated dithiocarbamate ligand. Electrochemical studies of **1**-**6** reveal a metal centred *quasi-reversible* one-electron oxidation to M(III). Attempted oxidation of [Tp^{Ph2}Co(dtc)] with [$FeCpCp^{COMe}$]BF_4 yields [Co(dtc)$_3$], Hpz^{Ph2} and a further product which may be [$Tp^{Ph2}CoBp^{Ph2}$]BF_4. DFT calculations indicate that the low redox potentials in these complexes result from a strongly antibonding M-S σ* HOMO.

Introduction

Tris(pyrazolyl)borates, Tp^R (R denotes substituents on the pyrazole rings) are one of the most widely used facially capping ligands in coordination chemistry.[1,2] Their popularity arises from their ease of synthesis and the readiness with which their steric and electronic properties may be varied by altering the substituents on the pyrazole rings.[1] While Tp and Tp^{Me2} are widely used in the preparation of half-sandwich complexes of second and third row transition metals with first row transition metals chemically inert sandwich compounds, [Tp_2M] form.[1] However, by employing sterically hindered scorpionates such as $Tp^{t\text{-}Bu}$, Tp^{Ph} and $Tp^{i\text{-}Pr}$ half-sandwich complexes [Tp^RMX] (X = halide or pseudohalide) can be prepared.[3-6] Thus, [Tp^RCoL] (L = anionic ligand) complexes have been prepared as spectroscopic probes for the zinc analogues [Tp^RZn(L)] and structural and functional models for the native zinc enzymes.[7-10] Cobalt and nickel thiolate complexes, [Tp^RM(SR′)] have also been prepared to provide insight into how the subtle differences between cobalt, nickel and copper affect the reactivity of the copper models for blue copper proteins.[11-13] Furthermore, Akita and co-workers have synthesized numerous organometallic species [Tp^RMR] (M = Co, Ni; R = allyl, alkyl, aryl or alkynyl) to provide insight into catalytic transformations or for use as polymerization catalysts.[14-17] Finally, [$Tp^{Ph,Me}$M($Hpz^{Ph,Me}$)L] (M = Co, Ni; L = 2,6-di-*tert*-butyl-4-carboxyphenoxide) have been synthesized in an attempt to prepare molecular magnets.[18]

Despite the wealth of research into coablt and nickel tris(pyrazolyl)borate complexes the redox chemistry of these systems remains extremely poorly developed. Theopold has shown that the reduction of [$Tp^{t\text{-}Bu,Me}$CoI] with magnesium gives [$Tp^{t\text{-}Bu,Me}Co(N_2)$] which then undergoes a wide range of reactions to form [$Tp^{t\text{-}Bu,Me}$Co(L)] (L = CO, alkene) or [$Tp^{t\text{-}Bu,Me}$CoX] (X = Cl, OH, H).[19-21] The oxidation of [{Tp^RM}$_2$(μ-OH)$_2$] (R = Me_2, Me_3, *i*-Pr_2) has also been explored by Akita *et al*.[22] More recently, work in our group has extended the number of such redox-active complexes to include a series of cobalt complexes, [Tp^{Ph2}Co(β-dkt)] (β-dkt = β-diketonate) which undergo irreversible oxidation.[23] Lastly, a new series of nickel dithiocarbamate complexes, [Tp^RNi(dtc)] (R = Me_2; Ph,Me; dtc = dithiocarbamate) have been prepared by Jensen *et al* with quasi-reversible oxidation being observed in all cases.[24-25] As part of our continuing interest in redox-active tris(pyrazolyl)borate complexes supported by the poorly represented Tp^{Ph2} ligand we have undertaken a study of cobalt and nickel dithiocarbamate Tp^{Ph2} complexes and their redox chemistry. Our findings are reported in the following paper.

Results and discussion

Synthesis and characterisation

The reaction of [Tp^{Ph2}MBr] (M = Co or Ni) with NaS_2CNR_2 (R = Et, Bz) or $NaS_2CN(CH_2)_4$ in CH_2Cl_2 gave the expected dithiocarbamate complexes [Tp^{Ph2}M(S_2CNR_2)] (M = Co, R = Et **1**, Bz **2**; M = Ni, R = Et **4**, Bz **5**) and [Tp^{Ph2}M(S_2Cpyr)] (M = Co **3**, Ni **6**) in good or excellent yields as purple-brown (M = Co) or green (M = Ni) solids (Scheme 1).

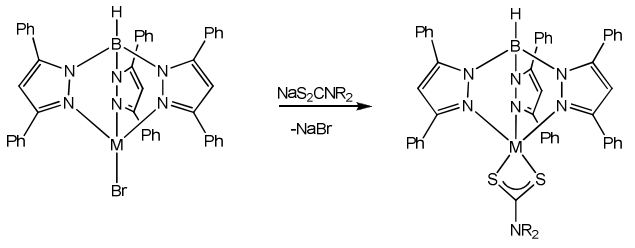

Scheme 1 Synthesis of [Tp^{Ph2}M(dtc)] **1**, **2**, **4**, **5**.

Table 1 Physical, spectroscopic and electrochemical data for [Tp^{Ph2}M(dtc)] **1-6**

Complex	Colour	Yield (%)	IR/cm^{-1} [a]			$E^{o'}/V$ [b]	λ_{max}/nm ($\varepsilon/M^{-1}cm^{-1}$)
			ν_{BH}	ν_{CN}	ν_{CS}		
1	Purple-brown	63	2623	1478	1010	0.49	408 (859), 536 (63)
2	Purple-brown	69	2613	1475	1009	0.56	404 (974), 535 (72)
3	Purple	64	2626	1479	1011	0.54	402 (1,071), 505 (73)
4	Dark green	85	2624	1478	1011	0.57	372sh (1,460), 426 (1,190), 654 (95)
5	Dark green	84	2610	1471	1011	0.64	365sh (1,860), 426 (1,187), 655 (103)
6	Green	77	2626	1479	1011	0.62	372sh, (1,360), 429 (1,011), 658 (95)

[a] As KBr discs [b] At 100 mVs^{-1} versus Ag/AgCl

The compounds are soluble in polar organic solvents such as CH_2Cl_2 and acetone. Succesful synthesis of the cobalt complexes requires longer reaction times than the corresponding nickel complexes, typically 5-6 hours compared with 2 hours, as [Tp^{Ph2}CoBr] is only sparingly soluble in CH_2Cl_2 while [Tp^{Ph2}NiBr] dissolves readily. The synthesis of the air-stable cobalt(II) dithiocarbamate complexes, **1-3**, is particularly notable as cobalt(II) dithiocarbamate complexes are comparitively rare and usually highly susceptible to oxidation.[26] Moreover, while **1-3** are readily synthesized attempts to prepare the $Tp^{Ph,Me}$ analogues under the same conditions led to a complex mixture of products including the cobalt(III) tris(dithiocarbamate) complexes, [$Co(dtc)_3$], suggesting that the electron poor Tp^{Ph2} ligand is vital to the successful synthesis of stable Co(II) dithiocarbamate compounds.

IR spectroscopy reveals B-H stretches between 2610 and 2626 cm^{-1} indicative of κ^3 coordinated Tp^{Ph2} ligands (Table 1). There are also very strong C-N streches between 1479 and 1471 cm^{-1} confirming the presence of a dithiocarbamate ligand in the metal coordination sphere.[27] The corresponding C-S streches are weak bands observed between 1011 and 1009 cm^{-1}. Similar stretches are observed in the closely related [Tp*Ni(dtc)] complexes.[24]

Solution spectra of **1-6** were recorded in CH_2Cl_2 and are shown in Figure 1. In the case of the cobalt complexes there are two main features in the spectra one at *ca*. 400 nm and another between 505 and 535 nm. The former of these bands has a large molar extinction coefficient and by comparison with the analogous complex [$Tp^{Ph,Me}$Co(thiomaltolate)] which has a similar band at 391 nm is assigned as a sulfur-to-Co(II) LMCT band.[8] The other band is assigned to a d-d transition as the related five-coordinate complex [$Tp^{i\text{-}Pr2}$Co(SMeIm)] (SMeIm = 2-mercapto-1-methylimidazolate) has a band at 563 nm.[13] The analogous nickel complexes, **4-6** have two features a shoulder at *ca*. 370 nm and further band between 426 and 429 nm indicative of sulfur-to-Ni(II) LMCT bands. For comparison, the recently reported [$Tp^{Ph,Me}$Ni(dtc)] (dtc = S_2CNEt_2, S_2CNPh_2) complexes also exhibit bands at 420 and 428 nm, respectively and in the case of [$Tp^{Ph,Me}$Ni(S_2CNEt_2)] a shoulder at 380 nm.[25] The CT bands at *ca*. 370 nm are thought to correspond to the S-Ni σ bond while the lower energy bands are caused by the S-metal π bond in accordance with the assignments made by Fujisawa *et al* in the cobalt and nickel complexes [$Tp^{i\text{-}Pr2}$M(SMeIm)].[13]

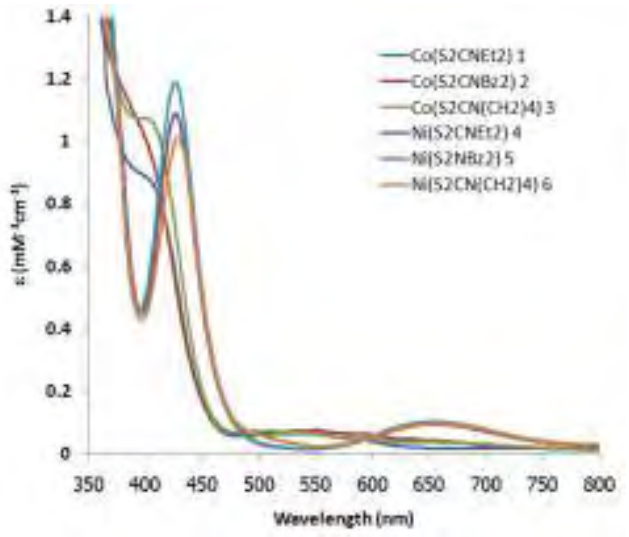

Figure 1 UV-Vis spectra of [Tp^{Ph2}M(dtc)].

Interestingly, while the cobalt complexes reveal a weak blue shift in going from **1** to **3** an opposite trend is observed for **4-6** where the band is red-shifted with decreasing *S*,*S*′-chelate donor strength. Furthermore, the sulfur-to-metal(II) CT bands of the cobalt series are found on average 22 nm lower than their nickel counterparts. A comparable albeit larger shift is observed in [Tp*M(CysEt)] (M = Co, Ni, CysEt = *l*-cysteine ethyl ester) where the difference is 48 nm.[28,29] In addition to the above charge transfer bands there is also a d-d transition between 654 and 658 nm. Once again similar bands are observed in previously reported [Tp^{R}Ni(dtc)] complexs.[24-25] Overall, the spectra are consistent with five-coordinate, high spin M(II) complexes.

^{1}H NMR spectroscopic studies

^{1}H NMR spectra of **1-6** were recorded in $CDCl_3$ and have been assigned by comparison with the previously reported [$Tp^{Ph,Me}$Ni(dtc)] (dtc = S_2CNEt_2, S_2CNPh_2) complexes and in the case of **1-3** with [$Tp^{Ph,Me}$Co(O-S)] (O-S = thiomaltolate, 1,2-hydroxypyridinethionate, 3,4-hydroxypyridinethionate),[8] [Tp^{Ph}Co(lactate)][29] and [Bp^{Ph2}Co{HB(3,5-pz^{Ph2})(pz^{Me2})$_2$}].[30] The ^{1}H NMR spectra reveal paramagnetically shifted resonances (Table 2) with the cobalt compounds exhibiting particularly large shifts over a range of 200 ppm (Figure 2). The borohydride resonances are very broad and for **1-3** and **4-6** are found between 116 and 119 ppm and *ca*. -11 ppm,

Table 2 ^{1}H NMR spectroscopic data for [Tp^{Ph2}M(dtc)] **1-6**.[a]

Complex	Tp^{Ph2} ligand								Dithiocarbamate ligand	
	5Ph (*o*)	5Ph (*m*)	5Ph (*p*)	3Ph (*o*)	3Ph (*m*)	3Ph (*p*)	4H	BH	N-CH_2	R
1	36.7	22.4	18.2	-73.5	3.7	3.8	49.0	119.1	101.6	32.4 (Me)
2	35.9	22.0	17.8	-71.2	3.2	3.9	49.8	115.6	93.3	36.9 (*o*-Ph), 15.2 (*m*-Ph), 13.8 (*p*-Ph)
3	36.6	22.3	18.1	-73.6	2.9	3.7	49.1	118.6	102.4	28.2 (CH_2)
4	7.7	7.0	7.4	4.8	6.9	7.2	59.3	-11.1	39.0	1.1 (Me)
5	7.8	7.1	7.4	4.7	6.7	7.1	61.0	-11.3	30.7	8.4 (*o*-Ph), 7.6 (*m*-Ph), 8.0 (*p*-Ph)
6	7.8	7.1	7.4	4.8	6.9	7.3	59.9	-10.9	38.8	4.9 (CH_2)

[a] In $CDCl_3$.

respectively. In both sets of complexes there is a single peak for the pyrazolyl protons indicative of fast rotation of the Tp^{Ph2} ligand. Such fluxional behaviour is well documented in first row transition metal Tp^R complexes. For **1-3** the hydrogen atoms of the 3-phenyl ring are observed between -74 and -71 ppm, 2.9 and 3.7 ppm and 3.7 and 3.9 ppm for the *ortho*, *meta* and *para* protons respectively. In contrast, the 5-phenyl ring protons are strongly deshielded and found between 17.8 and 36.7 ppm.

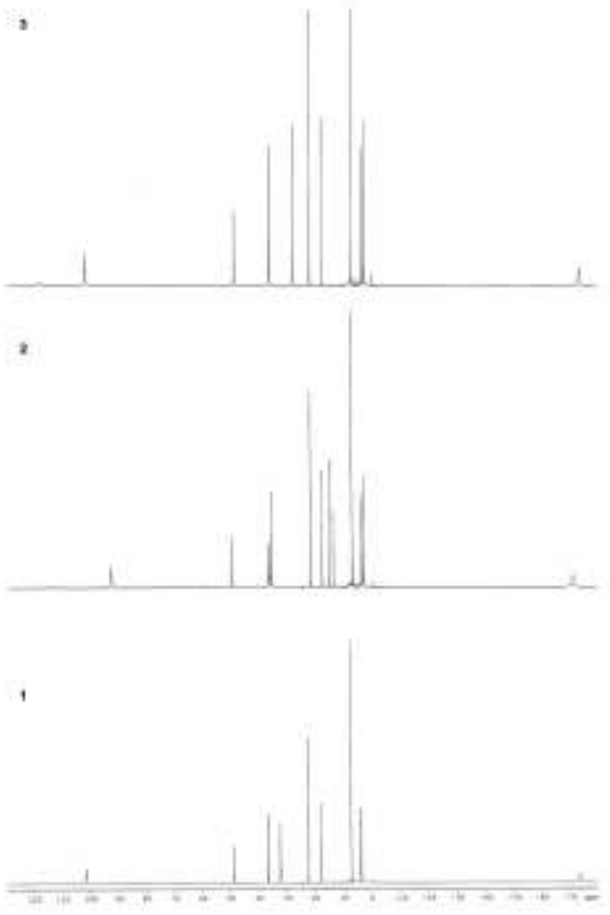

Figure 2 ^{1}H NMR spectra of [Tp^{Ph2}Co(dtc)] **1-3**.

The nickel complexes exhibit similar resonances between 4.7 and 7.3 ppm and 7.1 and 7.8 ppm for the 3-phenyl and 5-phenyl protons respectively. As with **1-3** the *ortho*-hydrogens of the 3-phenyl substituents are broad and shifted upfield of the other aomatic protons for the Tp^{Ph2} ligand. The dithiocarbamate ligand has sharp resonances for the N-CH_2R protons between 102 and 93 ppm and 39 and 31 ppm for **1-3** and **4-6** respectively. Interestingly, in the case of the benzyl dithiocarbamate ligand the resonance is always *ca*. 9 ppm upfield of the other dithiocarbamates. The other protons for the dithiocarabamte ligands are readily identified and assigned based on their position and integration intensity, although the CH_2 protons for the pyrrolidene ring in **6** are found to overlap with *ortho* protons of the Tp^{Ph2} ligand.

X-ray crystallographic studies

The molecular structures of [Tp^{Ph2}Co(S_2CNEt_2)] **1**, [Tp^{Ph2}Co($S_2CN(CH_2)_4$)] **3** and [Tp^{Ph2}Ni($S_2CN(CH_2)_4$)] **6** have been determined by X-ray crystallography. Crystallographic data are presented in Tables 3 and 4 while the structures are shown in Figures 3 and 4 for **1** and **6**, respectively. In the case of **3** and **6** two of the carbons in the pyrrolidene ring of the dithiocarbamate ligand are crystallographically disorded over two positions. All complexes show five-coordinate metal centres with κ^3 coordinated Tp^{Ph2} ligands and a geometry intermediate between square pyramidal and trigonal bipyramidal being slightly closer to the former. In contrast, the related [Tp^{Ph,Me}Ni(dtc)] (dtc = S_2CNEt_2, S_2CNPh_2) complexes are four-coordinate and square planar in the solid state, although a five-coordinate geometry exists in solution.[25] However, [Tp*Ni(S_2CNEt_2)][24] and the xanthate complex [Tp^{Ph,Me}Ni(S_2COEt)][25] are five-coordinate. In this instance it would appear that the more electron poor Tp^{Ph2} ligand leads to coordination of the apical nitrogen in both the solid state and in solution while the more electron rich Tp^{Ph,Me} ligand is able to stabilize a four- rather than five-coordinate species.

Table 3 Bond Lengths and angles for complexes **1**, **3** and **6**

	1	**3**	**6**	**Tp*Ni(S_2CNEt_2)**[a]
Bond Lengths/Å				
M-N1	2.164(2)	2.0876(17)	2.049(2)	2.063(2)
M-N3	2.080(2)	2.1674(17)	2.085(2)	2.065(2)
M-N5	2.106(2)	2.0709(17)	2.051(2)	2.027(2)
M-S1	2.4267(8)	2.3676(10)	2.3510(9)	2.3747(8)
M-S2	2.3891(8)	2.4461(10)	2.4357(10)	2.4099(7)

C46-S1	1.716(3)	1.726(2)	1.696(3)	1.710(3)
C46-S2	1.735(3)	1.716(2)	1.715(3)	1.707(3)
C46-N7	1.335(3)	1.318(3)	1.322(4)	1.329(4)
Bond Angles/^{o}				
N1-M-N3	87.83(8)	81.47(6)	84.23(10)	88.39(8)
N1-M-N5	81.16(8)	95.75(7)	95.31(9)	93.47(9)
N3-M-N5	94.39(8)	87.56(7)	89.64(9)	88.68(8)
N3-M-S2	121.32(6)	171.78(4)	173.04(7)	171.95(6)
N5-M-S2	144.24(6)	100.51(5)	97.12(7)	98.19(6)
N1-M-S2	100.36(6)	99.13(5)	96.71(7)	95.33(6)
N3-M-S1	103.01(6)	99.57(5)	101.29(7)	99.59(6)
N5-M-S1	97.25(6)	119.97(5)	115.12(7)	112.05(7)
N1-M-S1	169.15(6)	144.27(5)	148.92(7)	153.27(7)
S1-M-S2	74.61(3)	75.11(2)	74.38(3)	73.99(3)
N7-C46-S1	122.0(2)	121.07(16)	121.7(3)	122.7(2)
N7-C46-S2	122.4(2)	121.90(16)	122.2(3)	122.4(2)
S1-C46-S2	115.54(15)	117.02(12)	116.11(19)	114.8(1)
τ^{b}	0.42	0.46	0.40	0.31

[a] Data from reference 24. [b] Reference 31

The importance of steric effects is highlighted by [Tp*Ni(S_2CNEt_2)] which although more electron rich than both Tp^{Ph2} and $Tp^{Ph,Me}$ still results in a five-coordinate complex presumably due to the smaller steric bulk of Tp*. It is clear that a subtle combination of both steric and electronic effects influences the prefered coordinating mode of the Tp^{R} ligands in such dithiocarbamate complexes.

The Ni-N_{pz} and Ni-S bond lengths in **6** are very similar to those found in [Tp*Ni(S_2CNEt_2)] and [Tp^{PhMe}Ni(S_2COEt)] where the bond lengths are Ni-N_{pz} 2.042-2.078(2) Å; Ni-S1 2.399(1), Ni-S2 2.379(1) Å and Ni-N_{pz} 2.027-2.065(2) Å and Ni-S1 2.4099(7), Ni-S2 2.3747(8) Å, respectively and consistent with a paramagnetic Ni(II) centre.

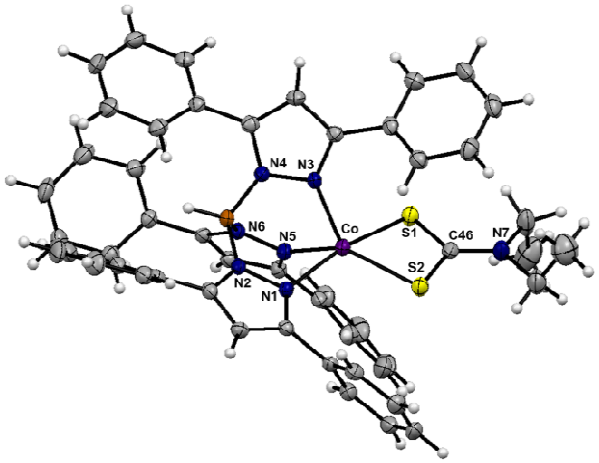

Figure 3 ORTEP diagram of [Tp^{Ph2}Co(S_2CNEt_2)] **1**, drawn with 50% ellipsoids.

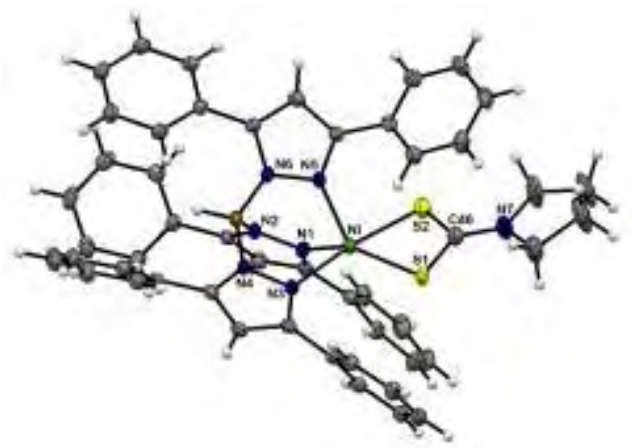

Figure 4 ORTEP diagram of [Tp^{Ph2}Ni($S_2CN(CH_2)_4$)] **6**, drawn with 50% ellipsoids.

On average the cobalt-nitrogen bond lengths are *ca*. 0.05 Å longer than in **6** and consistent with the different ionic radii of Co(II) and Ni(II).[32] A further difference between the cobalt and nickel complexes is that while the Tp^{Ph2} ligand is symmetrically coordinated in **6** one of the pyrazole arms of the Tp^{Ph2} ligand is elongated by between *ca*. 0.06-0.08 Å in **1** and **3** (see Table 3). Such asymmetric binding of the Tp^{Ph2} ligand has previously been observed in the structure of [Tp^{Ph2}Co(OAc)(Hpz^{Ph2})].[33] Furthermore, in all the complexes asymmetric binding of the dithiocarbamate is observed although the degree of asymmetry is dependent on the particular dithiocarbamate present. Thus ΔM-S = 0.038(1) Å for **1** and 0.079(1) and 0.085(1) Å for **3** and **6** respectively. Interestingly, for [Tp*Ni(S_2CNEt_2)] ΔM-S = 0.035(1) Å suggesting that the constrained pyrrolidene dithiocarbamate ligand may cause asymmetric binding in Tp^{R} dithiocarbamate complexes. The dithiocarbamate ligands display small bite angles between 74.4 and 75.1^{o} and similar with those reported for [Tp*Ni(S_2CNEt_2)] (73.99(3)^{o}) and [$Tp^{Ph,Me}$Ni(S_2COEt)] (74.75(2)^{o}).[24,25] The carbon-nitrogen and carbon-sulfur bond lengths are typical for bound dithiocarbamate ligands with values intermediate between those expected for carbon-element single and double bonds.

Electrochemistry

Electrochemical studies reveal that both the Co and Ni complexes undergo *quasi-reversible* oxidation to Co(III) and Ni(III) respectively. The Co series are shown in Figure 5 as representative examples. The quasi-reversibilty of the redox couples of **4**-**6** matches those of the previously reported [Tp^{R}Ni(dtc)] (R = Ph,Me; Me_2) compounds.[24,25] It is noteworthy that the reduction of [Co(dtc)$_3$] to [Co(dtc)$_3$]$^{-}$ is also quasi-reversible.[34] The cobalt complexes are *ca*. 80 mV more easily oxidized than the corresponding nickel compounds reflecting the greater stability of the Co(III) oxidation state (see Table 2). Surprisingly, the [Tp^{Ph2}Co(dtc)] complexes are more easily oxidized than the [Tp^{Ph2}Co(β-diketonate)] complexes by on average 750 mV.[23] This is extraordinary given that the only difference is the exchange of a β-diketonate ligand for a dithiocarbamate ligand. [Tp^{Ph2}Ni(S_2CNEt_2)] is found to be 130 mV more difficult to

Table 4 Crystallographic data and structure refinement for complexes **1**, **3** and **6**.

	1	**2**	**6**
Formula	$C_{50}H_{44}BCoN_7S_2$	$C_{50}H_{42}BCoN_7S_2$	$C_{50}H_{42}BNiN_7S_2$
Molecular weight / gmol^{-1}	876.78	874.77	874.55
Crystal system	Monoclinic	Monoclinic	Monoclinic
Space group	$P2_1/c$	$P2_1/c$	$P2_1/c$
a / Å	14.076(2)	13.960(5)	14.026(3)
b / Å	25.405(4)	25.122(10)	25.042(5)
c / Å	12.5980(19)	12.649(5)	12.672(2)
α / °	90	90	90
β / °	103.749(9)	102.047(5)	102.630(3)
γ / °	90	90	90
T / K	150(2)	150(2)	150(2)
Cell volume / Å^3	4376.1(11)	4339(3)	4343.2(14)
Z	4	4	4
Absorption coefficient / mm^{-1}	0.532	0.536	0.587
Reflections collected	95001	38601	38822
Independent reflections, R_{int}	10063, 0.0990	8443, 0.0441	8434, 0.0594
Max. and min. transmission	0.9438 and 0.8234	0.8643 and 0.8060	0.8528 and 0.7905
Restraints/parameters	0/552	39/569	33 / 569
Final R indices [I>2σ(I)]:R_1, wR_2	0.0525, 0.1012	0.0364, 0.0888	0.0483, 0.1135

oxidize [Tp^{Ph,Me}Ni(S_2CNEt$_2$)] indicating that substituents on the Tp^R ligand are able to influence the redox potential more than the dithiocarbamate ligands.[25] It may also explain the difficulty encountered in successfully synthesizing the [Tp^{Ph,Me}Co(dtc)] complexes noted earlier as these would be expected to more easily oxidized than their Tp^{Ph2} counterparts.

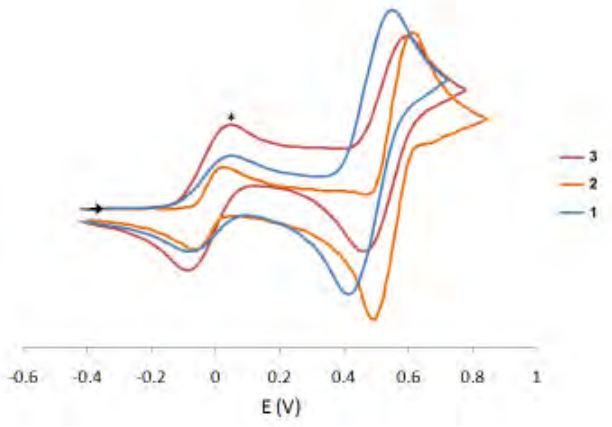

Figure 5 Cyclic voltammograms of [Tp^{Ph2}Co(dtc)] **1-3**, in CH_2Cl_2 at 100mVs^{-1} (*[FeCp*$_2$]).

The complexes are oxidized in the order Et < pyr < Bz over a range of 70 mV suggesting that the substituent groups are also able to influence the oxidation potential and reflect the relative donor strength of the different dithiocarbamate ligands. The difference between the pyrrolidene and ethyl substituted dithiocarbamates is particularly interesting given that the ligands are so similar. This suggests that ring strain in the dithiocarbamate ligand may favour the dithiocarbamate resonance form over the thioureide form thereby reducing electron density at the metal (Figure 6).

Figure 6 Dithiocarbamate and thioureide resonance forms.

A decrease in the reduction potential of [Fe(S_2C$_4$H$_4$)$_3$] has also been ascribed to a decrease in the thioureide resonance form.[35]

Attempted oxidation of [Tp^{Ph2}Co(dtc)]

The oxidation potentials of **1**-**3** suggested that oxidation could be achieved using mild oxidizing agents. We therefore attempted the oxidation of [Tp^{Ph2}Co(dtc)] with acetyl ferrocenium, [FeCpCp^{COMe}]BF$_4$. The reaction proved to be not as simple as expected and after crystallization three products were evident. The first of these were colourless needles which proved to be Hpz^{Ph2} on the basis of IR and ^{1}H NMR spectroscopy. The other products were green and pink crystals. In the case of **2** we were able to structurally characterize one of these products. The crystals proved to be [Co(S_2CNBz$_2$)$_3$] with two molecules in the asymmetric unit (Figure 7). The structure has previously been reported and the bond lengths and angles found in our structure are essentially identical. The presence of free pyrazole in the reaction mixture suggests that the final product may be [Tp^{Ph2}CoBp^{Ph2}]BF$_4$. A five-coordinate mixed pyrazole Tp^R and Bp^{Ph2} cobalt complex, [HB(pz^{Me2})$_2$(pz^{Ph2})CoBp^{Ph2}] has previously been prepared by Wołoweic *et al* lending support to this hypothesis.[30]

Table5 Computed and X-ray crystallographically determined bond lengths for [Tp^{Ph2}M(dtc)] **1**, **3** and **6**.

	1	**1**[a]	**3**	**3**[a]	**6**	**6**[a]
Bond Lengths/Å						
M-N1	2.164	2.171	2.0876	2.109	2.049	2.051
M-N3	2.080	2.077	2.1674	2.170	2.085	2.115
M-N5	2.106	2.110	2.0709	2.075	2.051	2.048
M-S1	2.4267	2.542	2.3676	2.462	2.3510	2.450
M-S2	2.3891	2.457	2.4461	2.548	2.4357	2.536
C46-S1	1.716	1.764	1.726	1.790	1.696	1.788
C46-S2	1.735	1.792	1.716	1.760	1.715	1.756
C46-N7	1.335	1.353	1.318	1.344	1.322	1.346

[a] Computed value.

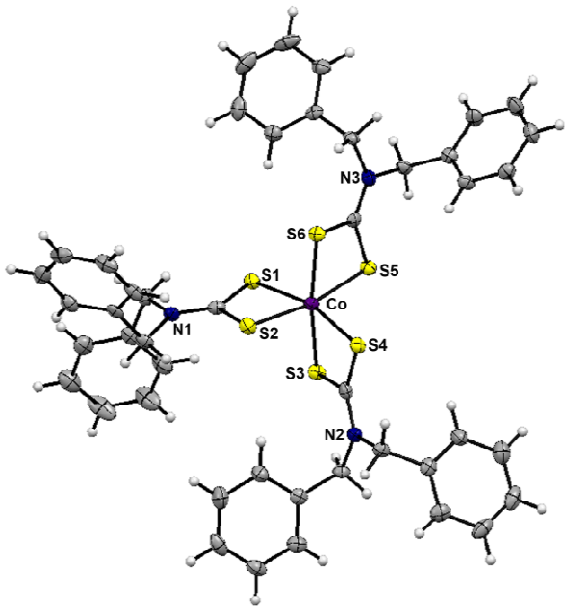

Figure 7 ORTEP diagram of $[Co(S_2CNBz_2)_3]$ drawn with 50% ellipsoids.

The results from the attempt to oxidize **1-3** suggest that initially the oxidation to $[Tp^{Ph2}Co(dtc)]^+$ is successful but that the five-coordinate species is unstable and this intermediate then decomposes to give the more stable tris(dithiocarbamate) Co(III) complexes. Interestingly, $[Co(dtc)_3]^+$ is known to be short lived and prone to reduction to a dimeric Co(III) cation, $[Co_2(dtc)_5]^+$, which in MeCN decomposes further to give $[Co(dtc)_3]$.[36] The free $[Tp^{Ph2}Co]^{2+}$ fragment then presumably attacks a bound Tp^{Ph2} ligand releasing Bp^{Ph2} and Hpz^{Ph2} resulting in the formation of $[Tp^{Ph2}CoBp^{Ph2}]BF_4$. The formation of $[Tp^{Ph2}CoBp^{Ph2}]BF_4$ rather than $[\{Tp^{Ph2}\}_2Co]BF_4$ may be due to the large steric bulk of the Tp^{Ph2} ligand which prevents formation of the sandwich compound.

DFT studies of [Tp^{Ph2}M(dtc)] complexes

In an attempt to better understand the remarkably low oxidation potential of the [Tp^{Ph2}M(dtc)] complexes and the instability of the $[Tp^{Ph2}M(dtc)]^+$ cations we have undertaken DFT calculations of the redox pairs $[Tp^{Ph2}M(dtc)]^{0/+}$. All calculations were performed using the Gaussian 03 software package with the B3LYP functional.[37]

The M-N and M-S bond lengths and the metal bond angles are close to those found in the structurally characterized compounds indicating that the models are accurate representations of [Tp^{Ph2}M(dtc)] (Table 5). Spin unrestricted calculations on the compounds reveal that the both the Co and Ni dithiocarbamate complexes are high spin being more stable than the corresponding low spin state by between 43.7-43.5 and 87.8-78.1 $kJmol^{-1}$ for the Co and Ni series, respectively. In the case of the $[Tp^{Ph2}M(dtc)]^+$ cations a singlet state is found for Ni indicating that it is low spin while for Co surprisingly a triplet state is found although it must be stated that B3LYP often overestimates the energy of different spin states.[38]

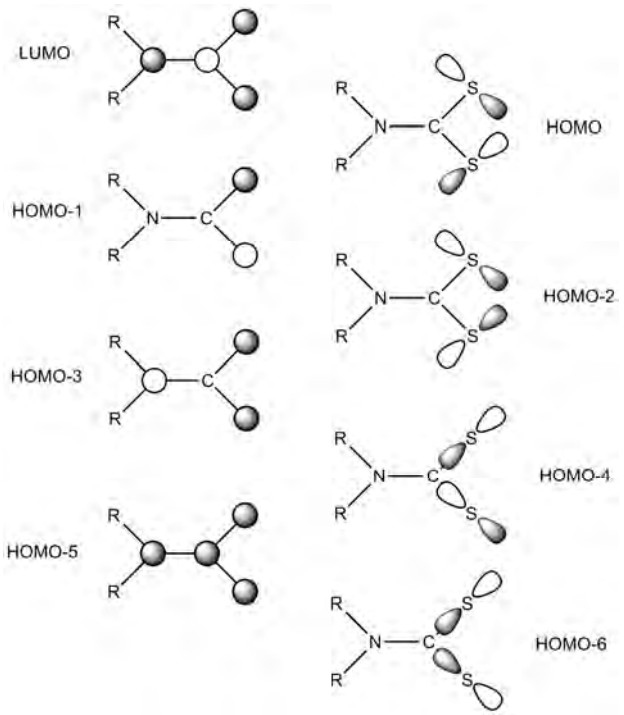

Figure 8 Simplified dithiocarbamate molecular orbitals.

The eight principal orbitals that dithiocarbamate ligands possess in C_{2v} symmetry and which may be used in metal-ligand bonding have previously been described by Bitterwolf and are shown in Figure 8.[39] Metal-dithiocarbamte bonding is thus described by a combination of these orbitals with suitable metal orbitals. In the present compounds the molecular orbitals concerning M-S interactions are shown in Figure 9 for **1** as a representative example.

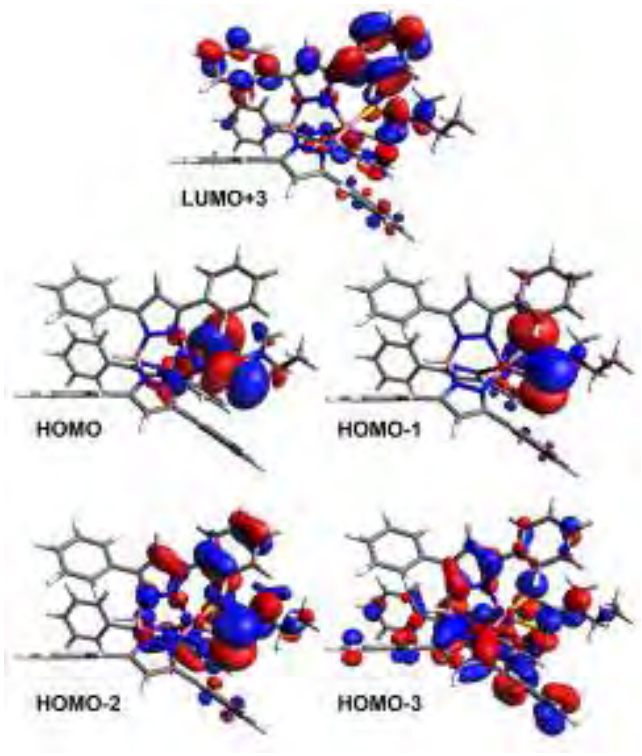

Figure 9 Selected molecular orbitals of $[Tp^{Ph2}Co(S_2CNEt_2)]$ **1** showing the M-S interactions

The HOMO of all the complexes is found to be a strong M-S σ* interaction involving a metal d_{x2-y2} and an asymmetric combination of the sulfur p_x and p_y orbitals (dtc HOMO in Figure 8). The strong antibonding character of the orbital results in the HOMO being destablised and therefore at high energy making oxidation comparitively easy. As expected, the benzyl substituted dithiocarbamate complexes **2** and **5** are found to be stabilised relative to the ethyl and pyrrolidene substituted dithiocarbamate compounds consistent with the higher redox potential observed in the electrochemical studies. Interestingly, no significant difference in the energy of the HOMO is observed between the ethyl and pyrrolidene substituted dithiocarbamate compounds despite there being a 50 mV difference in redox potential. The orbital immediately below the HOMO is composed of an asymmetric combination of the sulfur p_z orbitals (dtc HOMO-1) and a metal d_{xz} orbital resulting in a M-S π* interaction. The HOMO-2 also contains a M-S π* antibonding interaction constructed from a symmetric combination of the sulfur p_z orbitals (dtc HOMO-3) and a metal d_{yz} orbital. A weaker but almost indentical M-S π* antibonding interaction, differing only in the inclusion of a strong M-Tp interaction, is found in the HOMO-3 orbital. The antibonding nature of all of the above interactions is consistent with the findings of Bitterwolf for $[M(dtc)_2]$ (M = Ni, Cu, Zn) where the first three M-S ineractions were all antibonding although the highest of these is empty in the case of the 16-electron Ni complex.[39] In addition, the metal d_{z2} orbital is found in the HOMO-4 orbital and as with $[Ni(dtc)_2]$ is non-bonding with respect to the dithiocarbamate ligand. The dithiocarbamate LUMO is located in the LUMO+3 orbital and is essentially a ligand π* orbital with no significant electron density on the metal. Once again a similar interaction is also observed in $[Ni(dtc)_2]$. These combined M-S interactions complete the picture of M-S bonding in the $[Tp^{Ph2}M(dtc)]$ complexes.

In contrast to the M-S dominated HOMOs of the $[Tp^{Ph2}M(dtc)]$ complexes the cations are radically different with only very weak M-S interactions in the frontier orbitals, HOMO to HOMO-8. However, as expected the LUMO is an antibonding M-S σ* orbital and similar to the HOMO found in the neutral complexes. The only other significant M-S interaction is the LUMO+1 which is a *π orbital containing the dithiocarbamate LUMO (dtc-LUMO Figure 8) and a metal d_{yz} orbital. The lack of M-S interactions in the cations may explain the instability of the $[Tp^{Ph2}M(dtc)]^+$ species as the dithiocarbamate ligand may be insufficiently bound resulting in loss of the ligand. This may also explain why the oxidation of $[Tp^{Ph2}Co(dtc)]$ results in the formation of $[Co(dtc)_3]$ and not the anticipated cation.

Conclusions

In conclusion, a series of novel Co and Ni tris(pyrazolyl)borate complexes have been prepared including rare examples of *air stable* Co(II) dithiocarbamates, $[Tp^{Ph2}Co(dtc)]$. IR, UV-Vis and ^1H NMR spectroscopy are consistent with five-coordinate high spin Co(II) and Ni(II) and reveal rapid rotation of the Tp^{Ph2} ligand in solution. Structural studies confirm that the complexes adopt an intermediate coordination geometry between square pyramidal and trigonal bipyramidal and contrast with the related $[Tp^{Ph,Me}Ni(dtc)]$ complexes which are diamagnetic and square planar. The difference in coordination is due to a change in coordination mode of the Tp^R ligand from κ^3 to κ^2. Electrochemical studies indicate *quasi-reversible* oxidation to Co(III) and Ni(III) with the redox potential tunable over 80 mV by varying the substituents on the dithiocarbamate ligand. Oxidation of $[Tp^{Ph2}Co(dtc)]$ with $[FeCpCp^{COMe}]BF_4$ yields $[Co(dtc)_3]$, Hpz^{Ph2} and possibly $[Tp^{Ph2}CoBp^{Ph2}]BF_4$. DFT calculations indicate that the frontier orbitals of $[Tp^{Ph2}M(dtc)]$ are dominated by the presence of M-S σ* and π* interactions. In contrast, the cations $[Tp^{Ph2}M(dtc)]^+$ possess almost no M-S interactions perhaps explaining the instability of these complexes.

Experimental

General remarks

All manipulations were performed in air with HPLC grade solvents. Tris(3,5-diphenylpyrazolyl)borate (KTp^{Ph2}) was prepared by a literature procedure.[40] $[Tp^{Ph2}MBr]$ were prepared as previously reported. All other chemicals were

purchased from Fluka or Aldrich Chemical Company and used as received.

Infrared spectra (as KBr discs) were recorded on a Perkin-Elmer Spectrum One infrared spectrophotometer in the range 400-4000 cm^{-1}. Electronic spectra were recorded in CH_2Cl_2 at room temperature on a Shimadzu UV-1700 UV-Visible spectrophotometer. ^1H NMR spectra were recorded on a Bruker 300 MHz FT-NMR spectrometer at 25 ^oC in $CDCl_3$ with $SiMe_4$ added as an internal standard. Elemental analysis were carried out on a Eurovector EA3000 analyser. ESI-MS were carried out on a Bruker Daltonics 7.0T Apex 4 FTICR Mass Spectrometer. Electrochemical studies were carried out using a palmsensPC Vs 2.11 potentiosat in conjunction with a three electrode cell. The auxiliary electrode was a platinum rod and the working electrode was a platinum disc (2.0 mm diameter). The reference electrode was a Ag-AgCl electrode. Solutions, in CH_2Cl_2 dried over CaH_2, were 5 x 10^{-4} $mol.dm^{-3}$ in the test compound and 0.1 $mol.dm^{-3}$ in $[NBu^n_4][PF_6]$ as the supporting electrolyte. Under these conditions, $E^{o\prime}$ for the one-electron oxidation of $[Fe(\eta\text{-}C_5H_5)_2]$ added to the test solutions as an internal calibrant is 0.52 V.

Synthesis of complexes

Synthesis of $[Tp^{Ph2}Co(S_2CNEt_2)]$ 1

$[Tp^{Ph2}CoBr]$ (81 mg, 0.1 mmol) was suspended in CH_2Cl_2 (10 ml) giving a turquoise suspension. NaS_2CNEt_2 (24 mg, 0.1 mmol) was added resulting in a change to brown. The solution was stirred for 5 hrs and reduced to dryness *in vacuo*. The solid was redissolved in CH_2Cl_2 (2 ml) and layered with hexanes (15 ml). After 2 days purple-brown crystals formed which were washed with Et_2O (2 x 5 ml) and air dried (56 mg, 63%). ν_{max}(KBr)/cm^{-1} 3055, 2973, 2931 (ν_{CH}), 2623 (ν_{BH}), 1478 ($\nu_{C=N}$), 1010 (ν_{CS}). ^1H NMR ($CDCl_3$, 295 K; δ; ppm) 119.1 (1H, BH), 101.6 (4H, N-CH_2), 49.0 (3H, 4-pz), 36.7 (6H, 5-*o*-Ph), 32.4 (6H, Me), 22.4 (6H, 5-*m*-Ph), 18.2 (3H, 5-*p*-Ph), 3.8 (3H, 3-*p*-Ph), 3.7 (6H, 3-*m*-Ph), -73.5 (6H, 3-*o*-Ph). UV-Vis $\lambda_{max}(CH_2Cl_2)$/nm (ε, $dm^3mol^{-1}cm^{-1}$) 408 (859), 536 (63). *m*/*z* (ESI) 728 $[M\text{-}S_2CNEt_2^-]^+$. *Anal*. Calc. for $C_{50}H_{44}N_7BS_2Co$: C 68.49, H 5.06, N 11.18; Found: C 68.35, H 5.02, N 11.13.

Complexes **2**-**6** were synthesized in a similar manner to **1** using appropriate cobalt or nickel starting materials and recrystallized from the solvents indicated.

Synthesis of $[Tp^{Ph2}Co(S_2CNBz_2)]$ 2

Purple-brown crystals (crystallised from CH_2Cl_2-hexane). 69% yield. ν_{max}(KBr)/cm^{-1} 3056, 3027, 2937 (ν_{CH}), 2613 (ν_{BH}), 1475 ($\nu_{C=N}$), 1009 (ν_{CS}). ^1H NMR ($CDCl_3$, 295 K; δ; ppm) 115.6 (1H, BH), 93.3 (4H, N-CH_2), 49.8 (3H, 4-pz), 36.9 (4H, dtc-*o*-Ph), 35.9 (6H, 5-*o*-Ph), 22.0 (6H, 5-*m*-Ph), 17.8 (3H, 5-*p*-Ph), 15.2 (4H, dtc-*m*-Ph), 13.8 (2H, dtc-*p*-Ph), 3.9 (3H, 3-*p*-Ph), 3.2 (6H, 3-*m*-Ph), -71.2 (6H, 3-*o*-Ph). UV-Vis $\lambda_{max}(CH_2Cl_2)$/nm (ε, $dm^3mol^{-1}cm^{-1}$) 404 (974), 535 (72). *m*/*z* (ESI) 728 $[M\text{-}S_2CNBz_2^-]^+$. *Anal*. Calc. for $C_{60}H_{48}N_7BS_2Co$: C 72.00, H 4.83, N 9.80; Found: C 71.67, H 4.84, N 9.79.

Synthesis of $[Tp^{Ph2}Co(S_2CN(CH_2)_4)]$ 3

Purple crystals (crystallised from CH_2Cl_2-hexane). 64% yield. ν_{max}(KBr)/cm^{-1} 3058, 2970 (ν_{CH}), 2626 (ν_{BH}), 1479 ($\nu_{C=N}$), 1011 (ν_{CS}). ^1H NMR ($CDCl_3$, 295 K; δ; ppm) 118.6 (1H, BH), 102.4 (4H, N-CH_2), 49.1 (3H, 4-pz), 36.6 (6H, 5-*o*-Ph), 28.2 (4H, CH_2), 22.3 (6H, 5-*m*-Ph), 18.1 (3H, 5-*p*-Ph), 3.7 (3H, 3-*p*-Ph), 2.9 (6H, 3-*m*-Ph), -73.6 (6H, 3-*o*-Ph). UV-Vis $\lambda_{max}(CH_2Cl_2)$/nm (ε, $dm^3mol^{-1}cm^{-1}$) 402 (1,071), 505 (73). *m*/*z* (ESI) 728 $[M\text{-}S_2CN(CH_2)_4^-]^+$. *Anal*. Calc. for $C_{50}H_{42}N_7BS_2Co$: C 68.65, H 4.84, N 11.21; Found: C 68.84, H 5.01, N 11.19.

Synthesis of $[Tp^{Ph2}Ni(S_2CNEt_2)]$ 4

Green crystals (crystallised from CH_2Cl_2-hexane). 85% yield. ν_{max}(KBr)/cm^{-1} 3054, 2972, 2930 (ν_{CH}), 2624 (ν_{BH}), 1478 ($\nu_{C=N}$), 1011 (ν_{CS}). ^1H NMR ($CDCl_3$, 295 K; δ; ppm) 59.3 (3H, 4-pz), 39.0 (4H, N-CH_2), 7.7 (6H, 5-*o*-Ph), 7.4 (3H, 5-*p*-Ph), 7.2 (3H, 3-*p*-Ph), 7.0 (6H, 5-*m*-Ph), 6.9 (6H, 3-*m*-Ph), 4.8 (6H, 3-*o*-Ph), 1.1 (6H, Me), -11.1 (1H, BH). UV-Vis $\lambda_{max}(CH_2Cl_2)$/nm (ε, $dm^3mol^{-1}cm^{-1}$) 372sh (1,460), 426 (1,190), 654 (95). *m*/*z* (ESI) 727 $[M\text{-}S_2CNEt_2^-]^+$. *Anal*. Calc. for $C_{50}H_{44}N_7BS_2Ni$: C 68.51, H 5.06, N 11.19; Found: C 68.33, H 4.94, N 11.14.

Synthesis of $[Tp^{Ph2}Ni(S_2CNBz_2)]$ 5

Green crystals (crystallised from CH_2Cl_2-hexane). 84% yield. ν_{max}(KBr)/cm^{-1} 3059, 3025, 2910 (ν_{CH}), 2610 (ν_{BH}), 1471 ($\nu_{C=N}$), 1011 (ν_{CS}). ^1H NMR ($CDCl_3$, 295 K; δ; ppm) 61.0 (3H, 4-pz), 30.7 (4H, N-CH_2), 8.4 (4H, dtc-*o*-Ph), 8.0 (2H, dtc-*p*-Ph), 7.8 (6H, 5-*o*-Ph), 7.6 (4H, dtc-*m*-Ph), 7.4 (3H, 5-*p*-Ph), 7.1 (9H, 3-*p*-Ph and 5-*m*-Ph), 6.7 (6H, 3-*m*-Ph), 4.7 (6H, 3-*o*-Ph), -11.3 (1H, BH). UV-Vis $\lambda_{max}(CH_2Cl_2)$/nm (ε, $dm^3mol^{-1}cm^{-1}$) 365sh (1,860), 426 (1,187), 655 (103). *m*/*z* (ESI) 727 $[M\text{-}S_2CNBz_2^-]^+$. *Anal*. Calc. for $C_{60}H_{48}N_7BS_2Ni$: C 72.01, H 4.83, N 9.80; Found: C 71.88, H 4.79, N 9.72.

Synthesis of $[Tp^{Ph2}Ni(S_2CN(CH_2)_4)]$ 6

Green crystals (crystallised from CH_2Cl_2-hexane). 77% yield. ν_{max}(KBr)/cm^{-1} 3058, 2969, 2869 (ν_{CH}), 2626 (ν_{BH}), 1479 ($\nu_{C=N}$), 1011 (ν_{CS}). ^1H NMR ($CDCl_3$, 295 K; δ; ppm) 59.9 (3H, 4-pz), 38.8 (4H, N-CH_2), 7.8 (6H, 5-*o*-Ph), 7.4 (3H, 5-*p*-Ph), 7.3 (3H, 3-*p*-Ph), 7.1 (6H, 5-*m*-Ph), 6.9 (6H, 3-*m*-Ph), 4.9 (4H, CH_2), 4.8 (6H, 3-*o*-Ph), -10.9 (1H, BH). UV-Vis $\lambda_{max}(CH_2Cl_2)$/nm (ε, $dm^3mol^{-1}cm^{-1}$) 372sh, (1,360), 429 (1,011), 658 (95). *m*/*z* (ESI) 727 $[M\text{-}S_2CN(CH_2)_4^-]^+$. *Anal*. Calc. for $C_{50}H_{42}N_7BS_2Ni$: C 68.67, H 4.84, N 11.21; Found: C 68.74, H 4.77, N 11.43.

X-ray crystallography

Crystal data and data processing parameters for the structures of **1**, **3** and **6** are given in Tables 2 and 3. X-ray quality crystals of **1**, **3** and **6** were grown by allowing hexane to diffuse into a concentrated solution of the complex in CH_2Cl_2. Crystals were mounted on a glass fibre using perfluoropolyether oil and cooled rapidly to 150 K in a stream of cold nitrogen. All diffraction data were collected on a Bruker Smart CCD area detector with graphite monochromated Mo Kα(λ = 0.71073 Å). After data collection, in each case an empirical absorption correction (SADABS) was applied,[41] and the structures were then solved

by direct methods and refined on all F^2 data using the SHELX suite of programs.[42] In all cases non-hydrogen atoms were refined with anisotropic thermal parameters; hydrogen atoms were included in calculated positions and refined with isotropic thermal parameters which were *ca*. 1.2 × (aromatic CH) or 1.5 × (Me) the equivalent isotropic thermal parameters of their parent carbon atoms.

Acknowledgements

We gratefully acknowledge the Thailand Resaerch Fund (Grant No. RMU5080029) and the National Research Office of Thailand for funding this research (Grant No. WU51106). The School of Chemistry, University of Bristol is thanked for elemental analysis and MS services.

Notes and references

[a] *Molecular Technology Research Unit, School of Science, Walailak University, Thasala, Nakhon Si Thammarat, 80161, Thailand. Fax: +66-75-672004; Tel: +66-75-672094; E-mail: hdavid@wu.ac.th*
[b] *Department of Chemistry, University of Sheffield, Brook Hill, Sheffield S3 7HF, England*

† Electronic Supplementary Information (ESI) available: [details of any supplementary information available should be included here]. See DOI: 10.1039/b000000x/

1 S. Trofimenko, *Scorpionates: The Coordination Chemistry of Polypyrazolylborate Ligands*, Imperial College Press: London, 1999.
2 S. Trofimenko, *Chem. Rev*., 1993, **93**, 943.
3 J. C. Calabrese, S. Trofimenko and J. S. Thompson, *J. Chem. Soc., Chem. Commun*., 1986, 1122.
4 S. Trofimenko, J.C. Calabrese, P.J. Domaille and J.S. Thompson, *Inorg. Chem.*, 1987, **26**, 1507.
5 S. Trofimenko, J. C. Calabrese, and J. S. Thompson, *Inorg. Chem.*, 1989, **28**, 1091.
6 S. Trofimenko, J.C. Calabrese, J.K. Kochi, S. Wolowiec, F.B. Hulsbergen and J. Reedijk, *Inorg. Chem*., 1992, **31**, 3943.
7 A. Kremer-Aach, W. Kläui, R. Bell, A. Strerath, H. Wunderlich and D. Mootz, *Inorg. Chem*., 1997, **36**, 1552.
8 F. E. Jacobsen, R. M. Breece, W. K. Myers, D. L. Tierney and S. M. Cohen, *Inorg. Chem*., 2006, **45**, 7306.
9 R. Han, A. Looney, K. McNeill, G. Parkin, A. L. Rheingold and B. S. Haggerty, *J. Inorg. Biochem*., 1993, **49**, 105.
10 C. Bergquist, T. Fillebeen, M. M. Morlok and G. Parkin, *J. Am. Chem. Soc.*, 2003, **125**, 6189.
11 Y. Matsunaga, K. Fujisawa, N. Ibi, Y. Miyashita and K. Okamoto, *Inorg. Chem*., 2005, **44**, 325.
12 S. I. Gorelsky, L. Basumallick, J. Vura-Weis, R. Sarangi, K. O. Hodgson, B. Hedman, K. Fujisawa and E. I. Solomon, *Inorg. Chem*., 2005, **44**, 4947.
13 K. Fujisawa, T. Kakizaki, Y. Miyashita and K. Okamoto, *Inorg. Chim. Acta*, 2008, **361**, 1134.
14 N. Shirasawa, T. T. Nguyet, S. Hikichi, Y. Moro-oka and M. Akita, *Organometallics*, 2001, **20**, 3582.
15 N. Shirasawa, M. Akita, S. Hikichi and Y. Moro-oka, *J. Chem. Soc., Chem. Commun*. 1999, 417.
16 S. Yoshimitsu, S. Hikichi, M. Akita, *Organometallics*, 2002, **21**, 3672.
17 M. Akita, *J. Organomet. Chem*., 2004, **689**, 4540 and references therein.
18 A.S. Yakovenko, S.V. Kolotilov, A.W. Addison, S. Trofimenko, G.P.A. Yap, V. Lopushanskaya and V.V. Pavlishchuk, *Inorg. Chem. Commun*., 2005, **8**, 932.
19 J. W. Egan, B. S. Haggerty, A. L. Rheingold, S. C. Sendlinger and K. H. Theopold, *J. Am. Chem. Soc*., 1990, **112**, 2445.
20 J. L. Detrich, R. Konecny, W. M. Vetter, D. Doren, A. L. Rheingold and K. H. Theopold, *J. Am. Chem. Soc*., 1996, **118**, 1703.
21 J. D. Jewson, L. M. Liable-Sands, G. P. A. Yap, A. L. Rheingold and K. H. Theopold, *Organometallics*, 1999, **18**, 300.
22 S. Hikichi, M. Yoshizawa, Y. Sasakura, H. Komatsuzaki, Y. Moro-oka and M. Akita, *Chem. Eur. J*., 2001, **7**, 5012.
23 D. J. Harding, P. Harding, R. Daengngern, S. Yimklan and H. Adams, *Dalton Trans.*, 2009, 1314.
24 H. Ma, G. Wang, G. T. Yee, J. L. Petersen and M. P. Jensen, *Inorg. Chim. Acta*, 2009, **362**, 4563.
25 H. Ma, S. Chattopadhyay, J. L. Petersen and M. P. Jensen, *Inorg. Chem.*, 2008, **47**, 7966.
26 G. Hogarth, *Progress in Inorg. Chem*., 2005, **53**, 71.
27 K. Nakamoto, in *Infrared and Raman Spectra of Inorganic and Coordination Compounds: Part B, 5th ed*.; John Wiley & Sons: New York, 1997, pp. 91-99.
28 P. J. Desrochers, R. W. Cutts, P. K. Rice, M. L. Golden, J. B. Graham, T. M. Barclay and A. W. Cordes, *Inorg. Chem*., 1999, **38**, 5690.
29 M. Łukasiewicz, Z. Ciunik, and S. Wołowiec, *Polyhedron*, 2000, **19**, 2119.
30 T. Ruman, Z. Ciunik, J. Mazurek and S. Wołowiec, *Eur. J. Inorg. Chem*., 2002, 754.
31 A. W. Addison, T. N. Rao, J. Reedijk, J. Van Rijn and G. C. Verschoor, *J. Chem. Soc., Dalton Trans*., 1984, 1349.
32 F. A. Cotton, G. Wilkinson, C. A. Murillo and M. Bochmann Advanced Inorganic Chemsitry, 6th Ed., John Wiley & Sons: New York, 1999, pp. 1304.
33 D. J. Harding, H. Adams and T. Tuntulani, *Acta Cryst. Sec. C*, 2005, **C61**, m301.
34 H. T. V. Hoa and R. J. Magee *J. Inorg. Nucl. Chem*., 1979, **41**, 351.
35 A. G. El A'mma and R. S. Drago, *Inorg. Chem.*, 1977, **16**, 2975.
36 J. A. Alden, A. M. Bond, R. Colton, R. G. Compton, J. C. Eklund, Y. A. Mah, P. J. Mahon and V. Tedesco, J. Electroanal. Chem., 1998, **447**, 155.
37 M. J. Frisch et al., *GAUSSIAN 03*, revision C02, Gaussian, Inc.: Wallingford CT, 2004.
38 H. Paulsen and A. X. Trautwein, *Top. Curr. Chem.*, 2004, **235**, 197 and references therein.
39 T. E. Bitterwolf, *Inorg. Chim. Acta*, 2008, **361**, 1319.
40 N. Kitajima, K. Fujisawa, C. Fujimoto, Y. Moro-oka, S. Hashimoto, T. Kitagawa, K. Toriumi, K. Tatsumi and A. Nakamura, *J. Am. Chem. Soc*., 1992, **114**, 1277.
41 Bruker, *SMART*, *XSCANS*, *SHEXTL* and *SADABS*, Bruker AXS Inc., Madison, Wisconsin, USA, 2005.
42 G. M. Sheldrick, *SHELXS97* and *SHELXL97*. University of Göttingen, Germany, 1997.

Appendix Five

Oral Presentation at Walailak University

COBALT AND NICKEL TRIS(PYRAZOLYL)BORATE COMPLEXES: A LESSON IN RESEARCH

Assoc. Prof. Dr. David Harding

What are we looking for?

- Redox-active metal complexes: metal complexes which have at least two stable states.

- Metal complexes that can be used as building blocks for larger frameworks.

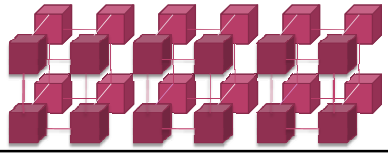

Research Plan

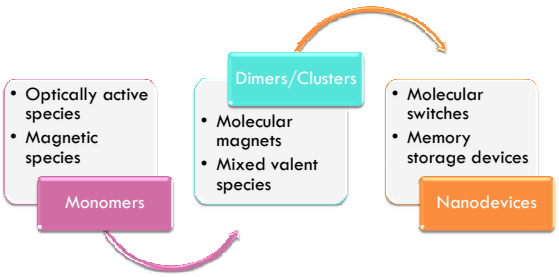

Cycle of Development

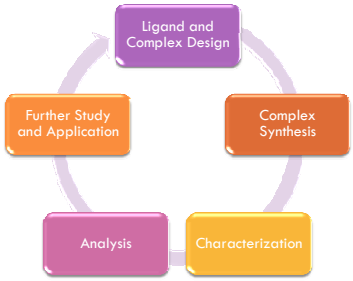

Monomers

- Optical Switches

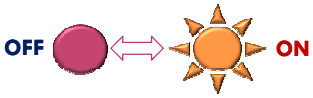

- Magnetic Switches

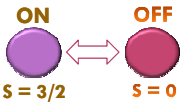

Dimers/Clusters

- Molecular Magnets

- Mixed Valent Species

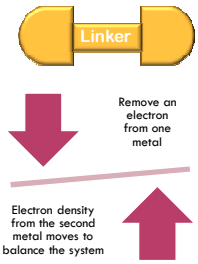

COBALT AND NICKEL TRIS(PYRAZOLYL)BORATE COMPLEXES

Tris(pyrazolyl)borate Ligands

- What is a tris(pyrazolyl)borate (Tp^R) ligand?[1]

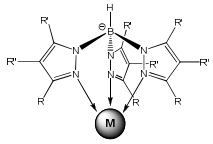

- Monoanionic
- Facially capping
- Six electron donors

1. S. Trofimenko, *Scorpionates: The Coordination Chemistry of Polypyrazolylborate Ligands*, Imperial College Press: London, 1999.

Why Tris(pyrazolyl)borates?

- Tris(pyrazolyl)borates are easily prepared and readily modified.

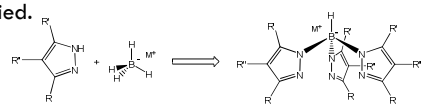

- In this research, tris(3,5-diphenylpyrazolyl)borate (Tp^{Ph2}) is used, a ligand of intermediate steric bulk and electron poor.[2]

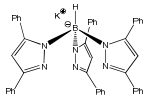

2. N. Kitajima, K. Fujisawa, C. Fujimoto, Y. Moro-oka, S. Hashimoto, T. Kitagawa, K. Toriumi, K. Tatsumi and A. Nakamura, *J. Am. Chem. Soc.*, 1992, **114**, 1277.

Synthesis of $[Tp^{Ph2}CoX]$

- Reaction of KTp^{Ph2} with CoX_2 yields $[Tp^{Ph2}CoX]$.

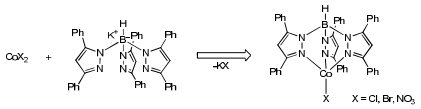

- $[Tp^{Ph2}CoBr]$ is a useful synthon in the preparation of other $[Tp^{Ph2}CoX]$ complexes.

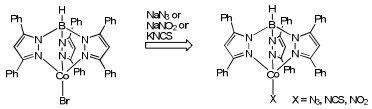

Synthesis of $[Tp^{Ph2}Co(OAc)(Hpz^{Ph2})]$

- The reaction of KTp^{Ph2} with $Co(OAc)_2$ gives $[Tp^{Ph2}Co(OAc)(Hpz^{Ph2})]$.

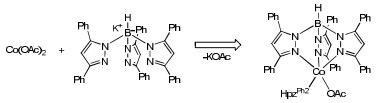

- $[Tp^{Ph2}Co(OAc)(Hpz^{Ph2})]$ is formed as a result of cleavage of the B-N bond of the Tp^{Ph2} ligand.

Structure of $[Tp^{Ph2}Co(OAc)(Hpz^{Ph2})]$

- The cobalt centre is five-coordinate with an intermediate coordination geometry ($\tau = 0.43$).[3]
- The acetate and pyrazole ligands are co-planar.

Bond Lengths	(Å)
Co-O1	1.9712
Co-N1	2.2896
Co-N3	2.0305
Co-N5	2.0347
Co-N7	2.1443

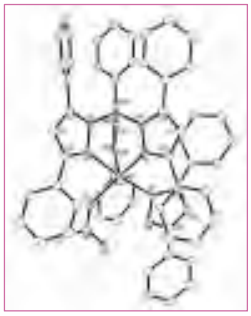

3. A. W. Addison, T. N. Rao, J. Reedijk, J. Van Rijn and G. C. Verschoor, *J. Chem. Soc., Dalton Trans.*, 1984, 1349.

Synthesis of [Tp^{Ph2}Co(β-diketonate)]

- The reaction of [Tp^{Ph2}Co(OAc)(Hpz^{Ph2})] with β-diketones allows preparation of [Tp^{Ph2}Co(β-diketonate)] complexes.

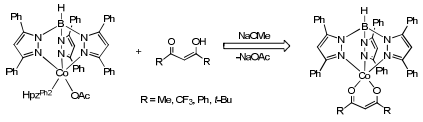

- IR spectroscopy (ν_{CO}) indicates the β-diketonate ligands adopt a chelating coordination mode.

Structures of [Tp^{Ph2}Co(β-diketonate)]

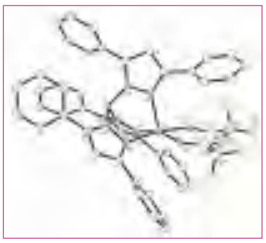

[Tp^{Ph2}Co(hfac)]

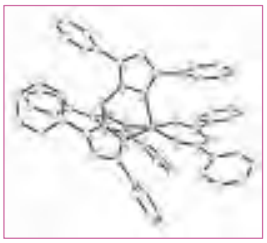

[Tp^{Ph2}Co(dbm)]

Structures of [Tp^{Ph2}Co(β-diketonate)]

- The cobalt centres are five-coordinate with square pyramidal geometries (τ = 0.11 and 0.13).
- The β-diketonate ligands exhibit a 'planar' coordination mode (β = 5.4° and 9.3°).

	hfac (Å)	dbm (Å)
Co-O1	2.0270	1.9802
Co-O2	2.0170	1.9784
Co-N1	2.055	2.1011
Co-N3	2.108	2.0847
Co-N5	2.089	2.1340

UV-Visible Spectrum of [Tp^{Ph2}Co(NO$_2$)]

- The [Tp^{Ph2}Co(NO$_2$)] complex is pink-red in THF and blue in CH_2Cl_2.

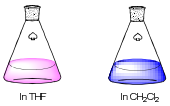

- This may be due to coordination of THF or possibly a change in NO_2 coordination from κ^1 to κ^2.

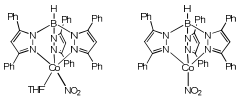

Electrochemistry of [Tp^{Ph2}Co(NO$_2$)]

- The [Tp^{Ph2}Co(NO$_2$)] complex undergoes irreversible one-electron reduction.

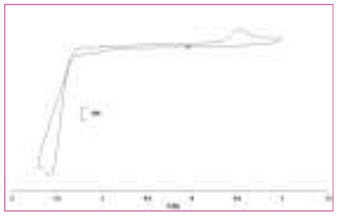

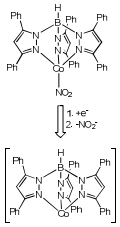

Electrochemistry of [Tp^{Ph2}Co(β-diketonate)] Complexes

- The [Tp^{Ph2}Co(β-diketonate)] complexes undergo irreversible one-electron oxidation.

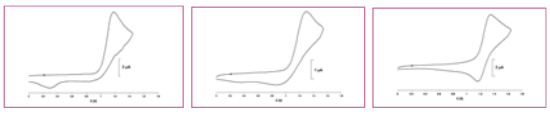

[Tp^{Ph2}Co(acac)] [Tp^{Ph2}Co(dbm)] [Tp^{Ph2}Co(tmhd)]

Complex	[Tp^{Ph2}Co(acac)]	[Tp^{Ph2}Co(dbm)]	[Tp^{Ph2}Co(tmhd)]
E_p / V	1.19	1.27	1.36

Synthesis of [Tp^{Ph2}Co(dtc)]

- The reaction of [Tp^{Ph2}MBr] with Na[dtc] gives novel cobalt dithiocarbamate complexes.

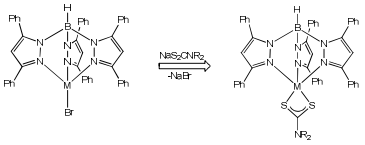

- IR spectroscopy of [Tp^{Ph2}M(dtc)] reveals a κ^3 coordinated Tp^{Ph2} ligand and a chelating dtc ligand.

Crystal structures of [Tp^{Ph2}Co(dtc)]

- The cobalt centres are five-coordinate with an intermediate coordination geometry (τ = 0.4, 0.42).

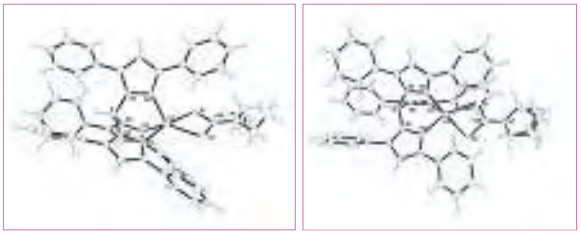

[Tp^{Ph2}Co(S$_2$CNEt$_2$)] [Tp^{Ph2}Co(S$_2$Cpyr)]

Electrochemistry of [Tp^{Ph2}Co(dtc)]

- The cobalt complexes undergo *reversible* one-electron oxidation to Co(III).

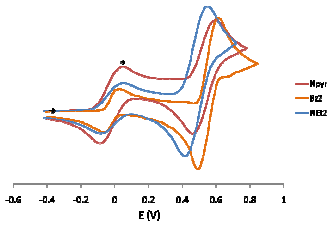

Synthesis of [Tp^{R}Ni(bpym)]$^+$

- The reaction of Tp^{R}NiBr with $AgPF_6$ in the presence of bipyrimidine yields the cations, [Tp^{R}Ni(bpym)]PF_6.

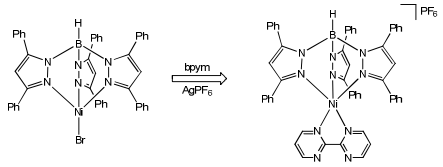

- IR spectroscopy of [Tp^{R}Ni(bpym)]PF_6 reveals a κ^3 coordinated Tp^{R} ligand.

Crystal structure of [Tp^{Ph,Me}Ni(bpym)]$^+$

- The nickel centre is five-coordinate with a square-bipyramidal geometry (τ = 0.07).

[Tp^{Ph,Me}Ni(bpym)]$^+$

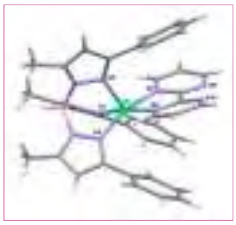

- The bpym ligand is non-planar with π-π interactions between the phenyl rings and the bpym ligand.

Electrochemistry of [Tp^{R}Ni(bpym)]$^+$

- Cyclic voltammetric studies reveal irreversible reduction to Ni^{I} with the degree of reversibility depending on the nature of the Tp^{R} ligand.

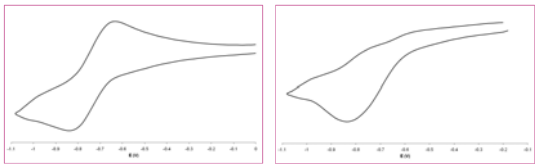

Complex	[Tp^{Ph2}Ni(bpym)]$^+$	[Tp^{Ph,Me}Ni(bpym)]$^+$
E_p / V	-0.73	-0.82

Attempted Dimer Preparation

- Attempts were made to prepare asymmetric dimers by reacting the bipyrimidine complex with $[M(dkte)_2]$.

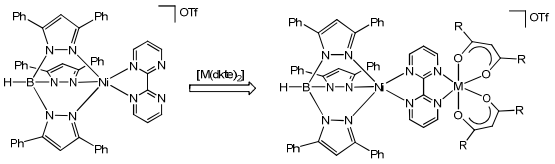

Crystal structure of $[Tp^{Ph2}Ni(dbm)]$

- X-ray crystallographic analysis of the products indicates that $[Tp^{Ph2}Ni(dbm)]$ has been formed rather than the anticipated dimer.

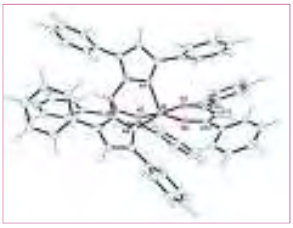

$[Tp^{Ph2}Ni(dbm)]$

Why no Dimers?

- A spacefill diagram suggests that there isn't enough space to fit a large coordination complex.

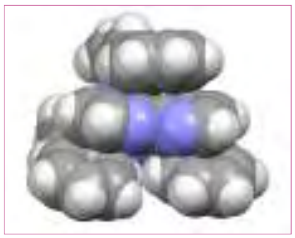

THE LESSON

Rule One: Never Give Up

- Setting up the lab here at Walailak took 4 years.
  - In the first year we had only 2 stirrers and a small amount of glassware.
  - After the third year we designed a new lab and increased our stock of chemicals and glassware.
  - After the fourth year we moved into the new lab and obtained two new vacuum pumps.
- In the first year of my research nothing worked, nevertheless I persevered - good things come to those who wait.

Rule Two: Plan Ahead

- Good research starts with good planning.
  - Sit down at the start of each month and assess what you've done and what needs to be done.

    'Plans are useless but planning is essential'
    President D. Eisenhower
  - Make time for your research, if you don't nothing will happen.
  - Aim high in your plans.

    'Aim at heaven and you will get earth thrown in. Aim at earth and you get neither'
    C. S. Lewis

Rule Three: Do It

- Having made a plan and set aside time in your schedule, the next thing is to do the research!
  - Try to stick to the plan and make sure you achieve the goals on the set dates.
  - If the research takes an unexpected turn - be flexible and see where it goes.

    '*All creative people want to do the unexpected*'
    H. Lamarr
  - Research produces lots of data – keep it organized.

Rule Four: Publish Your Research

- Once the research has been done write up what you've learned.
  - Try to write a little but often this is better than trying to find 2 or 3 free days.
  - Make sure that you carefully read the requirements of the journal you're going to submit to.
  - Once you've finished - Submit!

    '*Courage is resistance to fear, mastery of fear, not absence of fear.*'
    M. Twain

Acknowledgements

- We acknowledge the Thailand Research Fund, the National Research Office of Thailand and Walailak University for funding this research
- The Molecular Technology Research Unit is thanked for additional funding
- The Development and Promotion of Science and Technology is thanked for a scholarship to S. Yimklan
- Summer training students: S. Chooset and J. Kivnang

Acknowledgements

- Finally, thank you to Asst. Prof. Dr. Phimphaka Harding – Her help has been invaluable.

'*Anyone who has never made a mistake has never tried anything new.*'
A. Einstein

Appendix Six

Oral Presentation at Suranaree University of Techonology

REDOX-ACTIVE COBALT TRIS(PYRAZOLYL)BORATE AND β-DIKETONATE COMPLEXES

Assoc. Prof. Dr. David Harding

What are we looking for?

- Redox active metal complexes: metal complexes which have at least two stable states.

- Metal complexes that can be used as building blocks for larger frameworks.

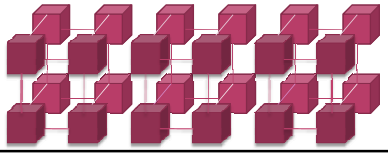

Research Plan

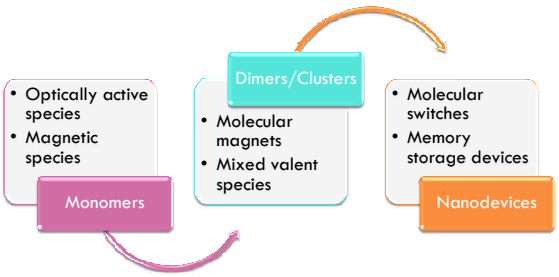

Monomers

- Optical Switches

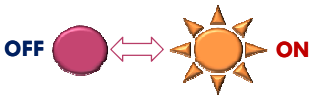

- Magnetic Switches

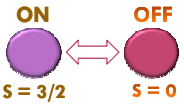

Dimers/Clusters

- Molecular Magnets

- Mixed Valent Species

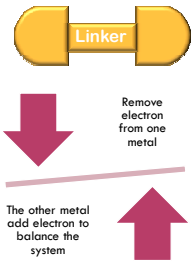

COBALT TRIS(PYRAZOLYL)BORATE COMPLEXES

Tris(pyrazolyl)borate Ligands

- What is a tris(pyrazolyl)borate (Tp^R) ligand?[1]

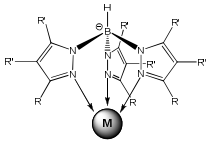

  - Monoanionic
  - Facially capping
  - Six electron donors

1. S. Trofimenko, *Scorpionates: The Coordination Chemistry of Polypyrazolylborate Ligands*, Imperial College Press: London, 1999.

Why Tris(pyrazolyl)borates?

- Tris(pyrazolyl)borates are easily prepared and readily modified.

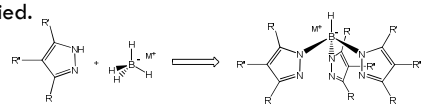

- In this research, tris(3,5-diphenylpyrazolyl)borate (Tp^{Ph2}) is used, a ligand of intermediate steric bulk and electron poor.[2]

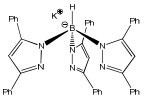

2. N. Kitajima, K. Fujisawa, C. Fujimoto, Y. Moro-oka, S. Hashimoto, T. Kitagawa, K. Toriumi, K. Tatsumi and A. Nakamura, *J. Am. Chem. Soc.*, 1992, **114**, 1277.

Synthesis of $[Tp^{Ph2}CoX]$

- Reaction of KTp^{Ph2} with CoX_2 yields $[Tp^{Ph2}CoX]$.

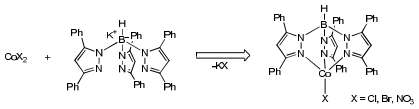

- $[Tp^{Ph2}CoBr]$ is a useful synthon in the preparation of other $[Tp^{Ph2}CoX]$ complexes.

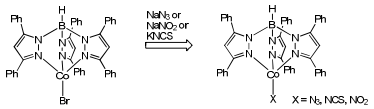

Synthesis of $[Tp^{Ph2}Co(OAc)(Hpz^{Ph2})]$

- The reaction of KTp^{Ph2} with $Co(OAc)_2$ gives $[Tp^{Ph2}Co(OAc)(Hpz^{Ph2})]$.

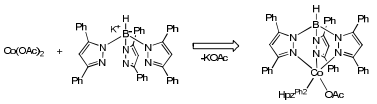

- $[Tp^{Ph2}Co(OAc)(Hpz^{Ph2})]$ is formed as a result of cleavage of the B-N bond of the Tp^{Ph2} ligand.

Structure of $[Tp^{Ph2}Co(OAc)(Hpz^{Ph2})]$

- The cobalt centre is five-coordinate with an intermediate coordination geometry ($\tau = 0.43$).[3]
- The acetate and pyrazole ligands are co-planar.

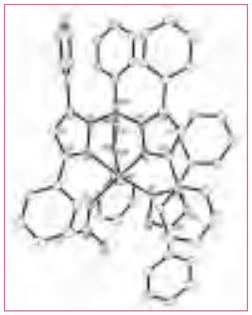

Bond Lengths	(Å)
Co-O1	1.9712
Co-N1	2.2896
Co-N3	2.0305
Co-N5	2.0347
Co-N7	2.1443

3. A. W. Addison, T. N. Rao, J. Reedijk, J. Van Rijn and G. C. Verschoor, *J. Chem. Soc., Dalton Trans.*, 1984, 1349.

Synthesis of $[Tp^{Ph2}Co(\beta\text{-diketonate})]$

- The reaction of $[Tp^{Ph2}Co(OAc)(Hpz^{Ph2})]$ with β-diketones allows preparation of $[Tp^{Ph2}Co(\beta\text{-diketonate})]$ complexes.

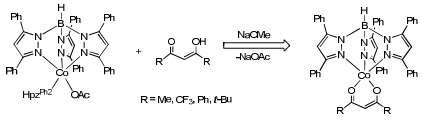

- IR spectroscopy (ν_{CO}) indicates the β-diketonate ligands adopt a chelating coordination mode.

Structures of [Tp^{Ph2}Co(β-diketonate)]

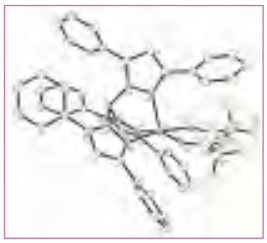

[Tp^{Ph2}Co(hfac)]

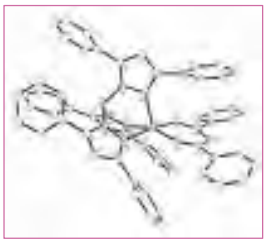

[Tp^{Ph2}Co(dbm)]

Structures of [Tp^{Ph2}Co(β-diketonate)]

- The cobalt centres are five-coordinate with square pyramidal geometries (τ = 0.11 and 0.13).
- The β-diketonate ligands exhibit a 'planar' coordination mode (β = 5.4° and 9.3°).

	hfac (Å)	dbm (Å)
Co-O1	2.0270	1.9802
Co-O2	2.0170	1.9784
Co-N1	2.055	2.1011
Co-N3	2.108	2.0847
Co-N5	2.089	2.1340

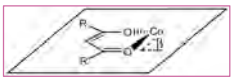

Crystal Packing in [Tp^{Ph2}Co(hfac)]

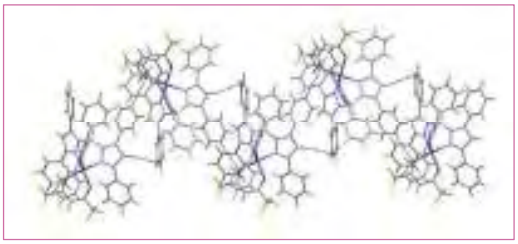

H2…Cg1	2.811 Å	O2…H22	2.637 Å

UV-Visible Spectrum of [Tp^{Ph2}Co(NO$_2$)]

- The [Tp^{Ph2}Co(NO$_2$)] complex is pink-red in THF and blue in CH_2Cl_2.

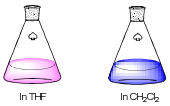

- This may be due to coordination of THF or possibly a change in NO$_2$ coordination from κ^1 to κ^2.

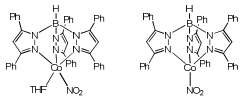

Electrochemistry of [Tp^{Ph2}Co(NO$_2$)]

- The [Tp^{Ph2}Co(NO$_2$)] complex undergoes irreversible one-electron reduction.

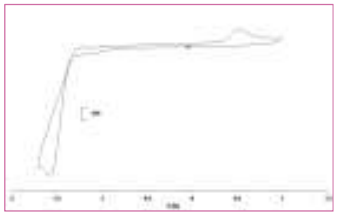

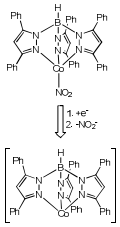

Electrochemistry of [Tp^{Ph2}Co(β-diketonate)] Complexes

- The [Tp^{Ph2}Co(β-diketonate)] complexes undergo irreversible one-electron oxidation.

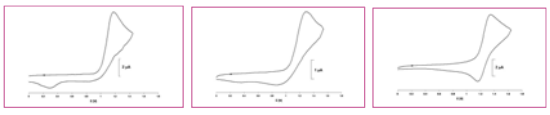

[Tp^{Ph2}Co(acac)] [Tp^{Ph2}Co(dbm)] [Tp^{Ph2}Co(tmhd)]

Complex	[Tp^{Ph2}Co(acac)]	[Tp^{Ph2}Co(dbm)]	[Tp^{Ph2}Co(tmhd)]
E_p / V	1.19	1.27	1.36

Synthesis of [Tp^{Ph2}Co(dtc)]

- The reaction of [Tp^{Ph2}CoBr] with Na[dtc] gives novel cobalt dithiocarbamate complexes.

- IR spectroscopy of [Tp^{Ph2}Co(dtc)] reveals a κ^3 coordinated Tp^{Ph2} ligand.

Crystal structures of [Tp^{Ph2}Co(dtc)]

- The cobalt centres are five-coordinate with an intermediate coordination geometry (τ = 0.4, 0.42).

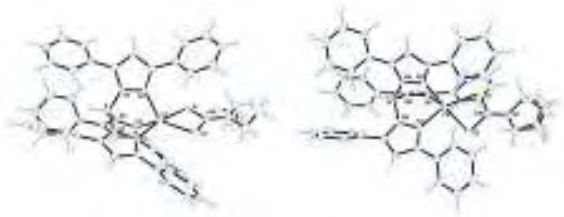

[Tp^{Ph2}Co(S$_2$CNEt$_2$)] [Tp^{Ph2}Co(S$_2$Cpyr)]

Electrochemistry of [Tp^{Ph2}Co(dtc)]

- The cobalt complexes undergo *reversible* one-electron oxidation to Co(III).

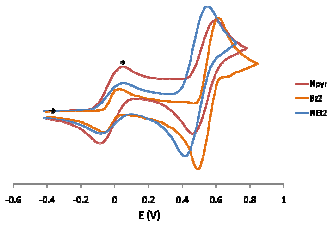

COBALT β-DIKETONATE COMPLEXES

What is a Metal β-Diketonate?

- Metal β-diketonate complexes, [M(β-diketonate)$_2$] (M = Ni, Co, Fe, Cu *etc.*)
- Stable in air.
- Easy to make.
- Dissolve in organic solvents.
- Applications in catalysis, magnetic, electronic and optical devices.
- *Cis* and *trans* isomers are frequently encountered.

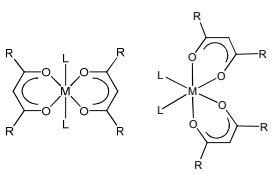

What ligands do we use in this work?

- [M(β-diketonate)$_2$(H$_2$O)$_2$] when M = Ni and Co, β-diketonate ligands = dbm, tmhd and hfac.

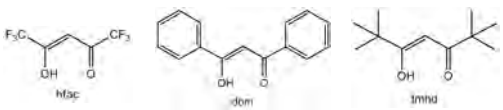

- (4-X-phenyl)-pyridin-2-ylmethylene-amine (ppa^X).

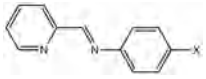

Synthesis of Metal β-Diketonates

- Reaction of β-diketonates with a metal acetate gives $[M(\beta\text{-diketonate})_2(H_2O)_2]$.

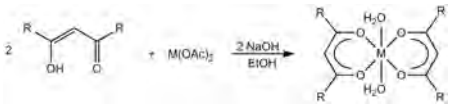

Synthesis of ppa^x ligands

- X = H, Me, Et, OMe, F, Cl, Br and I.
- Molecular sieves are necessary to absorb water to allow isolation of the ppa^X ligands.

4. S. Dehghanpour and A. Mahmoudi, *Main Group Chemistry*, 2007, 6, 121.
5. S. Dehghanpour, N. Bouslimani, R. Welter and F. Mojahed, *Polyhedron*, 2007, 26, 154.

Synthesis of [Co(β-diketonate)$_2$(ppa^x)] Complexes

- Simple addition of the ppa^X ligand to a solution of the cobalt β-diketonate yields the target compounds.

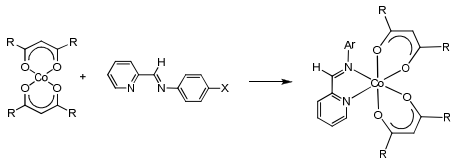

Characterization of Co Complexes

Co Complexes

- IR spectroscopy: $\nu_{C=O}$ = 1586-1596 cm^{-1} for *dbm* and *tmhd* complexes and 1646-1649 cm^{-1} for *hfac* complexes.
- UV-Vis spectroscopy:

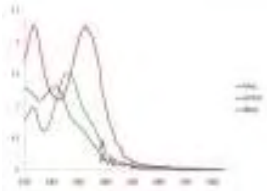

UV-Vis spectra of [Co(β-diketonate)$_2$(ppa^{OMe})].

X-ray Structures of Co Complexes

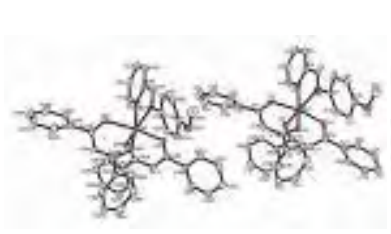

[Co(dbm)$_2$(ppa^{OMe})]

[Co(dbm)$_2$(ppa^{Cl})]

X-ray Structures of Co Complexes

- The *dbm* ligands exhibit both 'planar' and 'bent' coordination modes.

	Ni-ppa^{Cl}	Ni-ppa^{Me}	Ni-ppa^{OMe}	Co-ppa^{OMe}
M-N1	2.091(2)	2.090(4)	2.0812(14)	2.1408(14)
M-N2	2.189(2)	2.180(4)	2.1096(14)	2.1951(14)
M-O1	2.0091(16)	2.013(3)	2.0349(12)	2.0769(12)
M-O2	2.0205(17)	2.005(3)	2.0135(12)	2.0260(12)
M-O3	2.0165(16)	2.027(3)	2.0479(12)	2.0988(11)
M-O4	2.0128(16)	2.010(4)	2.0163(12)	2.0450(12)
β	2.98, 17.06	1.51, 16.57	31.94, 24.72	15.62, 21.94

Crystal Packing in [Co(β-diketonate)$_2$(ppa^X)] Complexes

[Co(dbm)$_2$(ppa^{Cl})] [Co(dbm)$_2$(ppa^{OMe})]

- The complexes are packed in chiral columns.
- CH…O interactions exist between the ppa^X and dbm ligands.
- For X = Cl, Me π…π and CH…π interactions are also observed.

Electron Transfer Studies of Co Complexes

- The Co complexes show unexpected behaviour upon oxidation.
- In theory Co(III) is more stable than Ni(III).

Why do we observe an irreversible oxidation for the dbm and tmhd complexes?

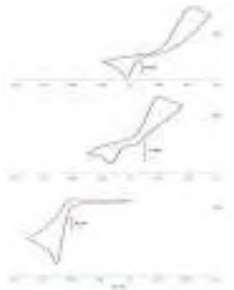

CVs of (a) [Co(dbm)$_2$(ppa^{Cl})], (b) [Co(tmhd)$_2$(ppa^{Cl})], (c) [Co(hfac)$_2$(ppa^{Cl})].

Spin Change upon Oxidation

- The unusual redox behaviour appears to be the result of a spin change upon oxidation – an example of a '*redox induced spin crossover*'.

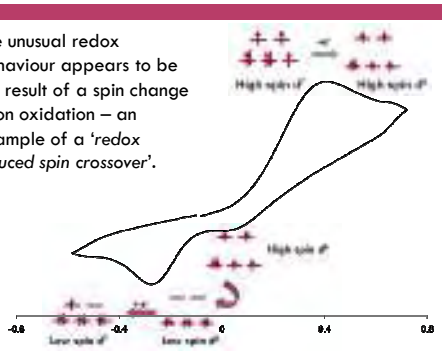

Electron Transfer Studies of Co Complexes

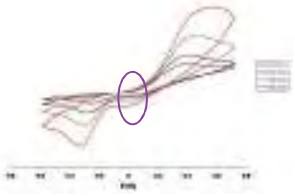

CVs of [Co(tmhd)$_2$(ppa^{Cl})] at different scan rates.

- At higher scan rates the reduction peak for the high spin Co(III) species becomes more visible.
- The stability of the high spin Co(III) species also depends on the nature of the substituent on the β-diketonate ligand.

Isolation of Co(III) Complexes

- The oxidation potentials from the CVs indicate that it may be possible to oxidize the Co(II) complexes chemically.

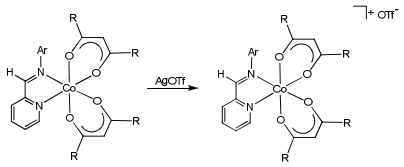

Characterization of Cationic Complexes

- IR spectroscopy: $\nu_{C=O}$ moves to lower wavenumbers compared with the neutral complexes.
- The complexes are NMR active indicative of low spin d^6.

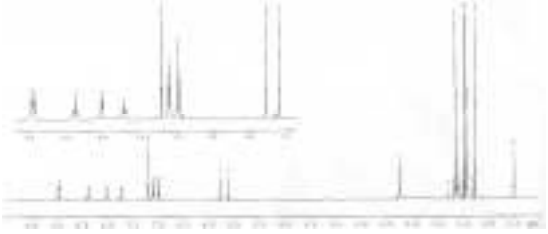

CVs of the Redox Pair

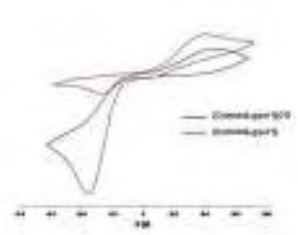

CV of $[Co(tmhd)_2(ppa^{Cl})]$ (–) and $[Co(tmhd)_2(ppa^{Cl})]^+$ (–)

- The oxidation and reduction potentials of the neutral and cationic species are identical.

Conclusions

- The reaction of CoX_2 with KTp^{Ph2} yields $[Tp^{Ph2}CoX]$ complexes which are useful synthons for more complex systems.
- The structure of the $[Tp^{Ph2}Co(\beta\text{-diketonate})]$ and $[Tp^{Ph2}Co(dtc)]$ complexes have intermediate five-coordinate cobalt centres.
- The electrochemistry reveals reversible or irreversible one-electron oxidation to Co(III) for $[Tp^{Ph2}Co(dtc)]$ and $[Tp^{Ph2}Co(\beta\text{-diketonate})]$, respectively.

Conclusions

- The reaction of ppa^X with $[Co(\beta\text{-diketonate})_2]$ yields the octahedral $[Co(\beta\text{-diketonate})_2(ppa^X)]$ complexes.
- The structures of the $[Co(\beta\text{-diketonate})_2(ppa^X)]$ complexes reveal *pseudo*-octahderal cobalt centres with 'bent' and 'planar' dbm ligands.
- Electrochemical studies of $[Co(\beta\text{-diketonate})_2(ppa^X)]$ reveal an unprecedented redox-induced spin crossover.

Acknowledgements

- We acknowledge the Thailand Research Fund, the National Research Office of Thailand and Walailak University for funding this research
- The Molecular Technology Research Unit is thanked for additional funding
- The Development and Promotion of Science and Technology is thanked for a scholarship to S. Yimklan
- Summer training students: Nitisasrt Soponrat, Kittaya Tinpun and Sirirat Samuadnuan

Walailak University

- Walailak University is located in Nakhon Si Thammarat Southern Thailand.

Appendix Seven

Oral Presentation at the Pure and Applied Chemistry International Conference (PACCON) 2010

Cationic Tris(pyrazolyl)borate Bipyrimidine Complexes: Potential Molecular Building Blocks

By Assoc. Prof. Dr. David J. Harding

Materials Technology Research Unit

Tris(pyrazolyl)borate Ligands

- What is a tris(pyrazolyl)borate (Tp^R) ligand?

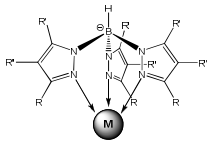

- Monoanionic
- Facially capping
- Six-electron donor

Why Tris(pyrazolyl)borates?

- Tris(pyrazolyl)borates are easily prepared and readily modified.

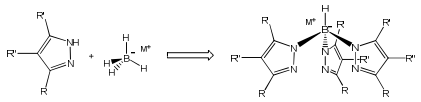

- In this research, Tp^{Ph2} and $Tp^{Ph,Me}$ ligands of intermediate steric and electron poor are used.

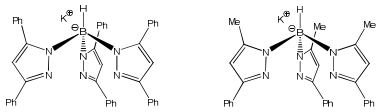

Synthesis of $[Tp^RNi(bpym)]PF_6$

- Reaction of Tp^RNiBr (R = Ph_2; Ph,Me) with bipyrimidine and subsequent addition of KPF_6 gives $[Tp^RNi(bpym)]PF_6$.

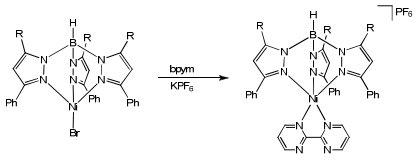

UV-Vis Spectroscopy

- $[Tp^RNi(bpym)]^+$ are dark green solids which are green in solution.

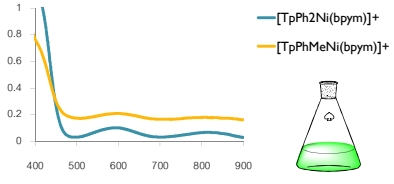

$[Tp^{Ph2}Ni(bpym)]^+$	$[Tp^{PhMe}Ni(bpym)]^+$
340 (2,200)	408 (354)
593 (51)	598 (102)
819 (34)	812 (89)

^1H NMR Spectroscopy

- NMR spectroscopy reveals identical shifts for all the pyrazolyl protons consistent with rapid rotation of the Tp^R ligands.

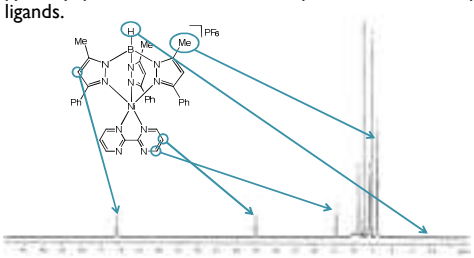

- All protons are shifted due to the presence of the paramagnetic Ni centre.

Structure of $[Tp^{Ph,Me}Ni(bpym)]PF_6$

- The nickel centre is five-coordinate with a square pyramidal geometry (τ = *ca.* 0.1).

Bond Lengths	(Å)
Ni-N1	2.051 (3)
Ni-N3	2.048 (2)
Ni-N5	2.018 (2)
Ni-N7	2.070 (2)
Ni-N8	2.066 (2)
τ	0.12 and 0.07

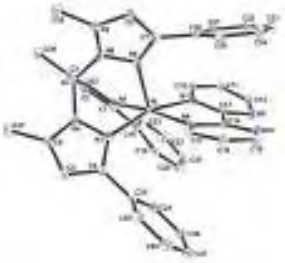

Crystal Packing in $[Tp^{Ph,Me}Ni(bpym)]^+$

- Several CH $\cdots \pi$ and an N $\cdots$ CH interactions form chains which are in turn connected to other chains.

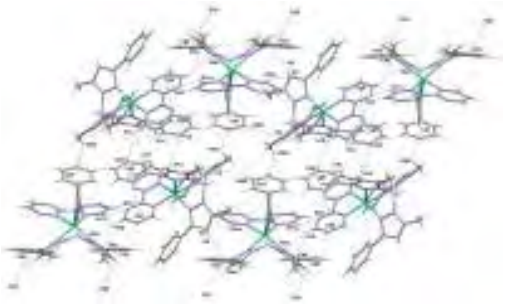

Electrochemistry of $[Tp^{R}Ni(bpym)]^+$

- Cyclic voltammetry shows irreversible reduction with the degree of reversibility dependent on the size of the Tp^R ligand.

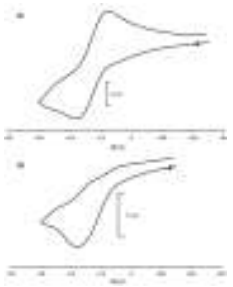

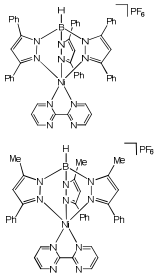

Molecular Building Blocks

- In preparing $[Tp^{R}Ni(bpym)]^+$ we aim to use it as a molecular building block.

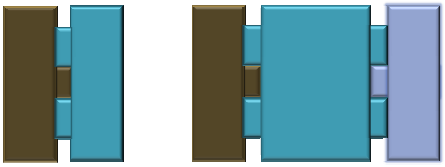

Dimer Trimer

Attempted Dimer Preparation

- Attempts were made to prepare asymmetric dimers by reacting the bipyrimidine complex with $[M(dkte)_2]$.

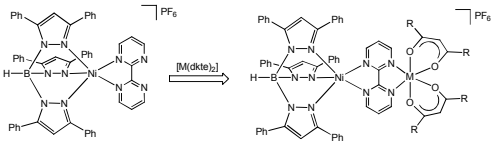

Crystal structure of $[Tp^{Ph2}Ni(dbm)]$

- X-ray crystallographic analysis of the products indicates that $[Tp^{Ph2}Ni(dbm)]$ has been formed rather than the anticipated dimer.

Bond Lengths	(Å)
Ni-N1	2.041 (2)
Ni-N3	2.061 (2)
Ni-N5	2.089 (2)
Ni-O1	1.976 (1)
Ni-O2	1.976 (1)
τ	0.13

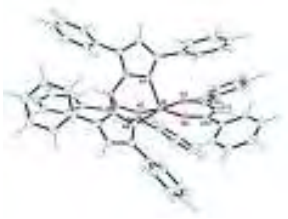

Why no Dimers?

- A spacefill diagram suggests that there isn't enough space to fit a large coordination complex.

- Square planar or tetrahedral coordinators may be better.

Acknowledgements

- We acknowledge the Thailand Research Fund, the National Research Office of Thailand and Walailak University for funding this research.
- The Molecular Technology Research Unit is also thanked.
- J. Kivnang and the summer training program at Walailak University.

Walailak University

- Walailak University is located in Nakhon Si Thammarat Southern Thailand.

Appendix Eight

Poster Presentation at the Annual Thailand Research Fund, Phetchaburi, Thailand, 2008

Synthesis and Electrochemical Studies of Cobalt and Nickel Cyanometallates

D. J. Harding* and P. Harding

Molecular Technology Research Unit, School of Science, Walailak University, Nakhon Si Thammarat, 80161, Thailand

Corresponding author e-mail: hdavid@wu.ac.th *URL: http://resource.wu.ac.th/inorganic_synthesis*

Introduction

Cyanometallates are an increasingly important class of compounds as they are widely used in the preparation of so-called single molecule magnets (SMMs).[1] Of particular relevance to the current work are the tris(pyrazolyl)borate (Tp^R) cyanometallates in which one half of the metal coordination sphere is blocked thereby allowing designed synthesis of metal clusters.[2,3] Herein we present the synthesis and characterization of a series of cobalt and nickel cyanometallates supported by first- and second-generation Tp^R ligands.

Synthetic Method

The reaction of $[Tp^RM(OAc)]$ (R = Ph_2 or Me_3) with two equivalents $[NEt_4]CN$ results in an almost instant colour change from purple to orange (Co) and green to yellow (Ni). Subsequent addition of Et_2O yields the novel cyanometallates $[Tp^RM(CN)_2][NEt_4]$ (M = Co, R = Ph_2 **1** or Me_3 **2**; M = Ni, R = Ph_2 **3** or Me_3 **4**) as orange solids (Scheme 1).

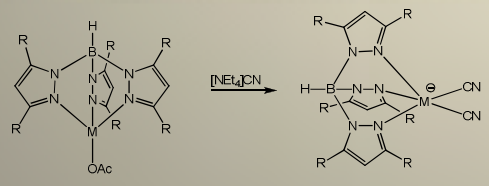

Scheme 1 *Preparation of $[Tp^RM(CN)_2]NEt_4$*

Results and Discussion

IR spectroscopy shows a single cyanide band for all compounds between 2092 and 2128 cm^{-1}. Complexes **1** and **3** are more electron poor than complexes **2** and **4** suggesting that the Tp^{Ph2} ligand is a poorer *net* donor than the Tp^{Me3}. The B-H stretches are in a range typical for κ^3-coordinated Tp ligands with the Tp^{Ph2} ligand *ca*. 100 cm^{-1} higher than the Tp^{Me3} ligand (2504-2603 cm^{-1}). In addition, magnetic susceptability studies indicate that the cobalt complexes have a single unpaired electron while the nickel compounds are diamagnetic.

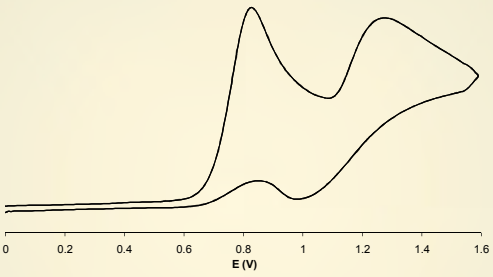

a)

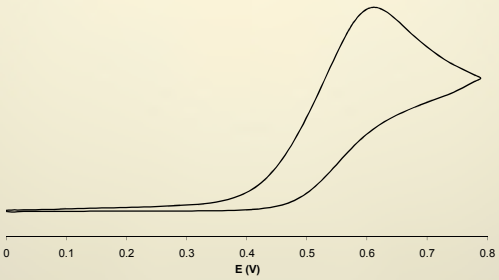

b)

Figure 1 *a) Cyclic voltammograms of (a) $[Tp^{Ph2}Ni(CN)_2]^-$ **3** and (b) $[Tp^{Me3}Ni(CN)_2]^-$ **4**.*

Electrochemical studies of the nickel compounds **3** and **4** show irreversible oxidation to Ni^{III} as shown in Figure 1. The two oxidations are observed at 0.80 and 0.61 V for complexes **3** and **4** respectively, indicating that the Tp^{Me3} ligand is considerably more electron donating that Tp^{Ph2}. In addition, there is a further quasi-reversible oxidation at 1.24 V which is coupled to the first oxidation suggesting that the decomposition species is also redox-active.

Conclusions and Further Work

In conclusion, we have successfully synthesized new tris(pyrazolyl)borate cyanometallates in moderate to good yield. Electrochemical studies reveal that the nickel complexes are redox-active oxidising irreversibly to Ni^{III}.

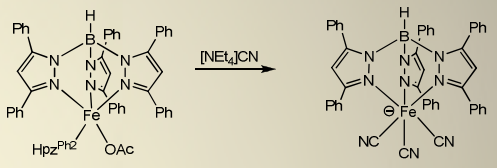

Scheme 2 *Synthesis of $[Tp^{Ph2}Fe(CN)_3]NEt_4$*

Further work in this area will focus on the preparation of iron(III) cyanometallates (Scheme 2). All the cyanometallates prepared will then be combined with other precursors to synthesize metallic clusters.

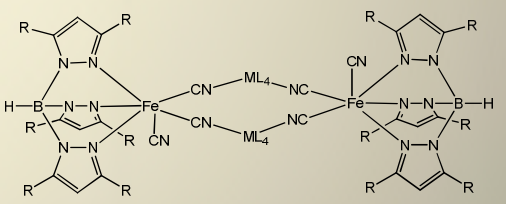

References

1. R. Sessoli, H.-L. Tsai, A.R. Schake, S. Wang, J.B. Vincent, K. Folting, D. Gatteschi, G. Christou and D.N. Hendrickson. *J. Am. Chem. Soc.* 1993, **115**, 1804.
2. D. Li, S. Parkin, G. Wang, G. T. Yee, R. Clérac, W. Wernsdorfer and S. M. Holmes, *J. Am. Chem. Soc.*, 2006, **128**, 4214.
3. D. Li, R. Clérac, S. Parkin, G. Wang, G. T. Yee and S. M. Holmes, *Inorg. Chem.*, 2006**, 45**, 5251.

Acknowledgements

We thank the Thailand Research Fund (Grant No.: RMU5080029) for funding this research.

Appendix Nine

Poster Presentation at the Annual Thailand Research Fund, Phetchaburi, Thailand, 2009

Cobalt and Nickel Tris(pyrazolyl)borate Dithiocarbamates: Stabilization of M^{III}

D. J. Harding* and P. Harding

Molecular Technology Research Unit, School of Science, Walailak University, Nakhon Si Thammarat, 80161, Thailand

Corresponding author e-mail: hdavid@wu.ac.th *URL: http://sites.google.com/site/mdelwu*

Introduction

Tris(pyrazolyl)borates remain useful ligands in the synthesis of half-sandwich transition metal complexes. In this area we have been using the much neglected tris(3,5-diphenylpyrazolyl)borate ligand, Tp^{Ph2} to prepare novel redox-active complexes. In this work we report the successful synthesis of redox-active cobalt and nickel tris(pyrazolyl)borate complexes in which the metal oxidzes reversibly to M^{III}.

Objectives

- To prepare redox-active cobalt and nickel tris-(pyrazolyl)borate complexes.
- Investigate the magnetic properties of these compounds and select the most promising for larger polynuclear systems.

Synthetic Method

The addition of NaS_2CNR_2 (R = Et, Bz) and NaS_2Cpyr (pyr = pyrrolidene) to a suspension of $[Tp^{Ph2}MBr]$ (M = Co, Ni) yields the dithiocarbamate (dtc) complexes, $[Tp^{Ph2}M(S_2CNR_2)]$ (M = Co, R = Et **1**, Bz **2**; M = Ni, R = Et **3**, Bz **4**) and $[Tp^{Ph2}M(S_2Cpyr)]$ (M = Co **5**, Ni **6**) in good yields as purple-brown (Co) or green (Ni) solids (Scheme 1).

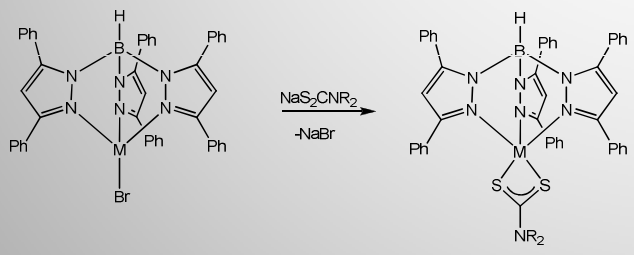

Scheme 1. Preparation of [TpPh2M(dtc)].

Results and Discussion

IR spectroscopy reveals B-H stretches between 2610 and 2623 cm^{-1} indicative of κ^3 coordinated Tp^{Ph2} ligands (Table 1). The UV-Vis spectroscopic spectra are consistent with a five coordinate metal in all cases.

Electrochemical studies reveal that both the Co and Ni complexes undergo *reversible* oxidation to Co^{3+} and Ni^{3+} respectively. The cobalt complexes are *ca*. 80 mV more easily oxidized than the corresponding nickel compounds.

Table 1. Physical, spectroscopic and electrochemical data for $[Tp^{Ph2}M(dtc)]$.

Complex	Colour	Yield (%)	IR ν_{BH} (cm^{-1})	$E^{o'}$ (V)
1	Purple-brown	63	2610	0.49
2	Purple-brown	69	2615	0.56
5	Purple	64	2613	0.54
3	Dark green	85	2624	0.57
4	Dark green	84	2610	0.64
6	Green	77	2626	0.62

The complexes are oxidized in the order Et < pyr < Bz over a range of 70 mV suggesting that the substituent groups have a significant influence on the oxidation potential. Surprisingly, the $[Tp^{Ph2}Co(S_2CNR_2)]$ complexes are more easily oxidized than the $[Tp^{Ph2}Co(\beta\text{-diketonate})]$ complexes by on average 750 mV.

Crystals suitable for X-ray diffraction of **1**, **5** and **6** were grown from CH_2Cl_2/hexanes. The structures of **1** is shown in Figure 1. The crystals structures all show five coordinate metal centres with intermediate coordination geometries being slightly closer to square pyramidal. This contrasts with the related $[Tp^{Ph,Me}Ni(S_2CNEt_2)]$ complex which exhibits a square planar geometry. A significant difference between the cobalt and nickel complexes is that while the Tp^{Ph2} ligand is symmetrically coordinated in **6** one of the pyrazole arms of the Tp^{Ph2} ligand is elongated by between *ca*. 0.06-0.08 Å in **1** and **5**.

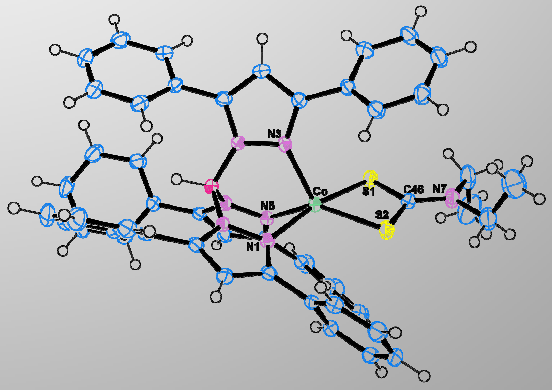

Figure 1. Molecular structure of $[Tp^{Ph2}Co(S_2CNEt_2)]$.

Acknowledgements

We acknowledge the Thailand Research Fund for funding this research (Grant no.: RMU5080029).